

**AN INVESTIGATION OF SOLAR POWERED ABSORPTION  
COOLING SYSTEMS FOR SOUTH AFRICA**

by

**Tatenda Joseph Bvumbe**

“Dissertation submitted in fulfillment of the Master of Science in Engineering in Mechanical Engineering,

School of Engineering, University of KwaZulu-Natal”

Durban

September 2012

Supervisor

DR FREDDIE L INAMBAO

“As the candidate’s Supervisor I agree/~~do not agree~~ to the submission of this thesis. The supervisor must sign all copies after deleting which is not applicable.

.....

NAME OF SUPERVISOR

.....

SIGNATURE

## COLLEGE OF AGRICULTURE, ENGINEERING AND SCIENCE

### DECLARATION 1 - PLAGIARISM

I, **Tatenda Joseph Bvumbe**, declare that

1. The research reported in this thesis, except where otherwise indicated, is my original research.
2. This thesis has not been submitted for any degree or examination at any other university.
3. This thesis does not contain other persons' data, pictures, graphs or other information, unless specifically acknowledged as being sourced from other persons.
4. This thesis does not contain other persons' writing, unless specifically acknowledged as being sourced from other researchers. Where other written sources have been quoted, then:
  - a. Their words have been re-written but the general information attributed to them has been referenced
  - b. Where their exact words have been used, then their writing has been placed in italics and inside quotation marks, and referenced.
5. This thesis does not contain text, graphics or tables copied and pasted from the Internet, unless specifically acknowledged, and the source being detailed in the thesis and in the References sections.

Signed

.....

## COLLEGE OF AGRICULTURE, ENGINEERING AND SCIENCE

### DECLARATION 2 - PUBLICATIONS

DETAILS OF CONTRIBUTION TO PUBLICATIONS that form part and/or include research presented in this thesis (include publications in preparation, submitted, *in press* and published and give details of the contributions of each author to the experimental work and writing of each publication)

Publication 1: **Bvumbe T. J and Inambao F. L:** Solar Powered Absorption cooling Systems for Southern Africa, Domestic Use of Energy Conference, Cape Peninsula University of Technology, Cape Town April 10-13, 2011, also published in **Energize** May 2011

Publication 2: **Bvumbe T. J and Inambao F.L:** Experimental Evaluation of a Solar Powered Absorption System (submitted and under review)

Publication 3: **Bvumbe T. J and Inambao F.L:** Performance of an Autonomous Solar Powered Cooling System, Journal of Energy of Southern Africa, (submitted and under review)

Publication 4:**Bvumbe T.J and Inambao F.L:** Simulation of a Solar Powered Lithium Bromide-Water Absorption Cooling System with Evacuated Tube Collectors, R & Journal of the South African Institute of Mechanical Engineering(submitted and under review)

**In all these papers, I Tatenda J Bvumbe was the main and corresponding author, whilst Dr Freddie L Inambao was the co-author and my research supervisor.**

Signed:

.....

## ACKNOWLEDGEMENTS

Firstly I would like to thank God, Almighty for giving the strength to start, and go on to complete this work. For without Him we are nothing, I will never cease to give thanks. To my parents **Norman and Rosemary Bvumbe**, words will never be enough to express my gratitude for all you have done in my life, your invaluable support and encouragement, once I was a boy now I am a man, and day and night you remain my inspiration. I am also greatly indebted to my supervisor **Dr Freddie L Inambao** for his guidance and his tireless efforts in securing funding for this work. I would also like to thank **Mr. Frank Jeche and wife** for the accommodation in Midrand, **Mr. Frank Major** for making my visit to Voltas Technologies as burden free as possible, **Mr. Hartmut Martin** for his assistance in particular with the Vodafone Site Solution Innovations Center data and help in understanding the general operating characteristic of said system. I would also like to acknowledge the financial assistance of the Center for Engineering Postgraduate Studies for funding me during my stay at UKZN in particular **Professor Nelson M Ijumba**. I would also like to express my heartfelt thanks to all my colleagues in the Green Energy Solutions Research Group for making helpful suggestions throughout the duration of this, my roommates **Tafadzwa Bvumbe and Mike Mutsvandiani** for their support and friendship. Last but not least I would like to thank **Wadzanai Janet Muzenda**, you came in my life when I needed new stimulus, your love has brought new hope, new dreams, you are truly an inspiration.

## ABSTRACT

Increased standards of living and indoor comfort demands have led to an increase in the demand for air-conditioning in buildings in South Africa. Conventional vapor compression systems use refrigerants that damage the ozone layer and contribute significantly to the global warming effect. Therefore, there is an urgent need to implement environmentally cleaner ways of satisfying this air-conditioning demand and absorption cooling systems have shown great potential to do so.

This project is concerned with finding the technical and economic effectiveness of solar powered absorption cooling systems for South African climatic conditions. Solar cooling systems are made up of a solar collector array, water storage tank, absorption chiller and cooling tower for heat rejection. In this study, two complete systems, one utilizing an open wet cooling tower and another using a dry cooler were studied and their technical and economical performance analyzed. One system was installed at Netcare Moot Hospital in Pretoria and comprised of a solar collector array made up of 52 evacuated tube collectors, two 6000litre hot water storage tanks, 35kW LiBr-water absorption chiller, and a wet cooling tower. This system was coupled to an existing vapor compression chiller so that cooling is provided even when no solar energy is available. The installation controlled and remotely monitored through the internet and parameters logged through a Carel Building Management System. The other system is at Vodacom World in Midrand, Johannesburg and is an autonomous solar heating and cooling system aimed at maintaining the building environment at comfort conditions throughout the year. It is made up of a 116m<sup>2</sup> evacuated tube collector array, a 6500litre hot water storage tank, 35kW LiBr-Water absorption chiller, 1m<sup>3</sup> of cold water storage, a dry cooler for the chiller, and two underground rock storages to pre-cool the supply air to the building and the dry cooler respectively. Long term system performance studies were carried out by varying the system control strategy for the chiller, hot water storage tank, existing vapor compression chiller (in the case of the Moot Hospital installation), hot water storage tank, dry cooler (for the Vodacom installation) and the system Coefficient of Performances were calculated and life cycle cost analysis carried out. Due to the fact that solar availability and cooling demand are approximately in phase, solar powered absorption cooling presents a great opportunity for reducing peak electrical cooling energy

demand. It was also discovered that the economic effectiveness of the system increases with the absorption chiller capacity, and it's more advisable to operate the solar absorption cooling system with a vapor compression chiller as a backup for facilities that require uninterrupted cooling. The solar autonomous system is oversized for most of the year since it is designed to cover the peak cooling loads.

*Keywords:* Solar-powered absorption cooling; LiBr-water; System performance; Economic analysis; Dynamic Thermal Building Simulation; Energy Efficiency.

## CONTENTS

1	INTRODUCTION .....	1
1.1	Background .....	1
1.2	State of Solar Thermal Systems .....	1
1.3	Solar Cooling Systems .....	2
1.4	Overview of Absorption Cooling Systems .....	2
1.5	Motivation for the Study .....	4
1.6	Thesis Layout .....	5
2	LITERATURE REVIEW .....	7
2.1	Overview .....	7
2.2	Review of Solar Powered cooling systems .....	7
3	SOLAR COOLING SYSTEMS.....	14
3.1	Overview .....	14
3.2	Sorption Systems .....	14
3.3	Desiccant Systems .....	15
3.4	Adsorption Systems .....	16
3.5	Absorption Cooling Systems .....	17
3.5.1	LiBr-Water Absorption Cycle.....	18
3.6	Absorption Chiller Modeling .....	19
3.7	Cooling Towers.....	23
3.8	Cooling Tower Model.....	24
3.9	Components of Solar Absorption Systems .....	27
3.9.1	Solar Thermal Collectors .....	28
3.9.2	Distribution of Flow in Collectors .....	33
3.10	Controls.....	35
3.11	Water Storage Tanks.....	37
3.11.1	Thermal Stratification .....	38
3.11.2	System sizing .....	40
3.11.3	Storage Tank Modeling.....	40
3.12	Pebble Bed Storage.....	43
4	DESIGN OF ABSORTION COOLING SYSTEMS .....	46



4.1	Overview.....	46
4.2	Design of Solar Absorption Cooling Systems .....	46
4.2.1	Solar Cooling System without storage.....	47
4.2.2	Solar Cooling System with Hot Storage .....	47
4.2.3	Solar Cooling System with Cold Storage.....	47
4.3	Solar Cooling System with both Hot and Cold Storage.....	48
4.3.1	TRNSYS Simulation Software .....	50
4.4	Economic Analysis .....	50
5	CASE STUDIES: SYSTEMS DESCRIPTION.....	53
5.1	Case Studies: Systems Description.....	53
5.2	Absorption Chiller .....	53
5.3	Moot Hospital .....	55
5.3.1	Solar Collector Array.....	57
5.3.2	Thermal Energy Storage .....	58
5.3.3	Control Strategy .....	58
5.4	Vodafone Site Solutions Innovation Center (Vodafone SSIC).....	64
5.4.1	Solar Collector Array.....	65
5.4.2	Heat Exchanger .....	66
5.4.3	Thermal Energy Storage Tanks.....	66
5.4.4	Air Handling Unit .....	66
5.4.5	Thermally Active Slab .....	67
5.4.6	Rock storage for the building air supply.....	67
5.4.7	Rock storage for the supply air to the dry cooler .....	68
5.4.8	Dry Cooler .....	69
5.4.9	Vodafone Control System.....	69
5.5	Data Monitoring System .....	74
5.6	Circulation Pumps.....	75
6	SYSTEM SIMULATIONS USING TRNSYS .....	76
6.1	Overview.....	76
6.2	TRNSYS interface .....	76
6.3	Netcare Moot Hospital System .....	76
6.3.1	Solar Thermal Collector Performance .....	77
6.3.2	Absorption Chiller Performance .....	78

6.4	Vodafone SSIC System.....	81
6.5	Collector Output.....	82
6.6	Absorption Chiller Performance .....	83
6.7	Effect of the rock storages .....	85
7	CASE STUDIES: SYSTEM PERFORMANCE ANALYSIS .....	87
7.1	Overview.....	87
7.2	Moot Hospital .....	87
7.2.1	Solar Collector Performance.....	88
7.2.2	Thermal Energy Storage Tank Performance.....	88
7.2.3	Absorption Chiller Performance .....	89
7.3	Vodafone Site Solutions Innovation Center.....	94
7.3.1	Building Loads.....	94
7.3.2	Solar Array Performance .....	97
7.3.3	Absorption Chiller Performance .....	99
7.3.4	Air Handling Unit (AHU).....	100
7.3.5	Thermally Activated Slab (TAS) .....	101
7.3.6	Dehumidification Fins.....	102
7.3.7	Dry Cooler .....	103
7.3.8	Building environment .....	104
7.4	Vodafone SSIC Economic Analysis .....	104
8	COMPARISON OF SIMULATION AND SYSTEM PERFORMANCE RESULTS .....	108
8.1	Overview.....	<b>Error! Bookmark not defined.</b>
8.2	Moot Hospital System.....	108
8.2.1	Solar Thermal Collector Performance .....	108
8.2.2	Absorption Chiller Performance .....	109
8.3	Vodafone Site Solutions Innovation Center (Vodafone SSIC).....	112
8.3.1	Collector Thermal Performance.....	113
8.3.2	Absorption Chiller Performance .....	113
9	CONCLUSIONS AND RECOMMENDATIONS .....	116
9.1	Conclusions and Recommendations .....	116
9.2	Recommendations for Future Work.....	117
10	References.....	<b>Error! Bookmark not defined.</b>

## LIST OF FIGURES

Figure 3.1: Principles of Solar Driven Cooling .....	14
Figure 3.2: Desiccant System Reticulation Cycle.....	15
Figure 3.3: Schematic of the adsorption cycle .....	17
Figure 3.4: Diagram of a single effect LiBr-water absorption system .....	19
Figure 3.5: Schematics of Counter flow and Cross flow cooling towers .....	24
Figure 3.6: Schematic of a Single Cell Counterflow Cooling Tower .....	25
Figure 3.7: Schematic of a typical solar cooling system .....	27
Figure 3.8: Schematic of a flat plate solar collector schematic .....	28
Figure 3.9: Evacuated tube collector .....	31
Figure 3.10: Schematic of a compound parabolic collector .....	33
Figure 3.11: Basic configuration of a stratified thermal storage tank.....	39
Figure 3.12: Stratified Fluid Storage Tank .....	41
Figure 4.1: Solar absorption cooling system.....	46
Figure 5.1: Yazaki WFC-SC10 chiller performance characteristics .....	53
Figure 5.2: Photograph of the Yazaki WFC-SC10 Absorption Chiller at Moot Hospital, Pretoria.....	55
Figure 5.3: Schematic of the Moot Hospital System Courtesy of Voltas Technologies.....	56
Figure 5.4: Photograph of the arrangement of the Solar Collector Array.....	57
Figure 5.5: Photograph of the two hot water storage tanks.....	58
Figure 5.6: Moot Hospital Control Strategy. Courtesy of Voltas Technologies.....	59
Figure 5.7: Solar Pump Control Logic.....	60
Figure 5.8: Hot Water Valves Logic.....	62
Figure 5.9: Chiller Control Logic .....	63
Figure 5.10: Photo of the Solar Collector Array at Vodafone SSIC .....	65
Figure 5.11: Photograph of the thermally active slab under construction .....	67
Figure 5.12: Schematic diagram showing the rock store and the cooling outputs as a result of pre-cooling and the TAS .....	68
Figure 5.13: Vodafone Absorption Chiller Control Logic.....	70
Figure 5.14: Solar Primary Water Pump Control Logic .....	71
Figure 5.15: Secondary Solar Water Pump Control Logic .....	72
Figure 5.16: Photo of the Plant VisorPro screen.....	74
Figure 6.1: Configuration of the Moot Hospital system using TRNSYS .....	77
Figure 6.2: Distributions of the collector useful energy output, incident solar energy and the collector thermal efficiency on December 4 .....	78
Figure 6.3: Temperature distributions of the chiller water streams on December 4 .....	79
Figure 6.4: Chiller heat energy input and cold energy output distributions on December 4 .....	80
Figure 6.5: Distributions of COP on December 4.....	80
Figure 6.6: Configuration of the Vodafone SSIC system using TRNSYS .....	81

Figure 6.7: Distributions of the collector useful energy output, incident solar energy and the collector thermal efficiency January 31 .....	83
Figure 6.8: Temperature distributions of the chiller water streams on January 31 .....	83
Figure 6.9: Chiller energy distributions on January 31 .....	84
Figure 6.10: Distributions of COP and SCOP on January 31 .....	85
Figure 6.11: Distributions of the ambient temperature and the dry cooler supply air temperature on January 31 .....	86
Figure 7.1: Distribution of Temperature and irradiation for Pretoria .....	88
Figure 7.2: Temperature Distributions in the Hot Water Storage Tank.....	89
Figure 7.3: Moot Hospital Cooling Load Distribution.....	90
Figure 7.4: Temperature distributions of the chiller water streams on December 4 2010. ....	91
Figure 7.5: Chiller energy distributions on December 4 2010.....	92
Figure 7.6: Distributions of the Chiller and Solar COP on December 4 2010.....	93
Figure 7.7: Load Profile for the building .....	95
Figure 7.8: Distribution of the cooling load for January 15.....	96
Figure 7.9: Distribution of heating load on July 21 .....	96
Figure 7.10: Distributions of collector energy output, inlet and outlet temperature on January 31, 2012..	97
Figure 7.11: Distribution of collector efficiency on January 31, 2012 .....	98
Figure 7.12: Temperature distributions of the chiller water streams on January 31, 2012 .....	99
Figure 7.13: Distributions of COP and SCOP on January 31 2012 .....	100
Figure 7.14: Distributions of the AHU temperatures of the water streams and cooling energy on January 31, 2012 .....	101
Figure 7.15: Distributions of the TAS water stream temperatures and the cooling energy on January 31, 2012 .....	102
Figure 7.16: Distributions of the inlet and outlet water temperatures and the dehumidification fins cooling energy on January 31, 2012 .....	103
Figure 7.17: Distributions of the inlet and outlet water temperatures and the dehumidification fins cooling energy on January 31, 2012 .....	103
Figure 7.18: Distributions of the ambient and building humidity and temperatures on January 31, 2012	104
Figure 8.1: Collector outlet temperature distributions for December 4 .....	109
Figure 8.2: Comparison of the chiller water stream temperature distributions for December 4.....	110
Figure 8.3: Comparison of the heat medium energy and the cooling energy for December 4 .....	110
Figure 8.4: Comparison of the recorded and simulated COPs on December 4 .....	111
Figure 8.5: Distributions of ambient temperatures on January 31 .....	112
Figure 8.6: Comparison of collector useful energy output on January 31 .....	113
Figure 8.7: Comparison of the chiller water stream temperature distributions for December 4.....	114
Figure 8.8: Distributions of the heat medium and chilled water energy rates on January 31 .....	114
Figure 8.9: The distributions for the simulated and recorded COP on January 31 .....	115

## LIST OF TABLES

Table 5.1: Yazaki WFC-SC10 Absorption Chiller Specifications.....	54
Table 5.2: HUIJ 16/2.1 Solar collector parameters .....	57
Table 5.3: Linuo LN58/1800-20 U-pipe collector parameters.....	65
Table 5.4: Air Handling Unit Specifications .....	66
Table 5.5: Circulation Pumps Specifications.....	75
Table 7.1: Climate Data for Pretoria .....	87
Table 7.2: Summary of Energy Produced by the Chiller in November 2010 .....	90
Table 7.3: Johannesburg Climatic Data .....	94
Table 7.4: Vodafone SSIC System Capital Costs .....	105
Table 7.5: Commercial power tariffs from 1 April 2012 .....	107
Table 8.1: Summary of the simulated and recorded chiller energy rates.....	111

## NOMENCLATURE

### Latin Symbols

$a_1$	First-order coefficient of the collector efficiency [ $\text{W}/\text{m}^2/^\circ\text{C}$ ]
$a_2$	Second-order coefficient of the collector efficiency [ $\text{W}/\text{m}^2/^\circ\text{C}^2$ ]
$A_{\text{abs}}$	Absorber area [ $\text{m}^2$ ]
$A_{\text{col}}$	Solar collector area [ $\text{m}^2$ ]
$A_p$	Projected area of the tube [ $\text{m}^2$ ]
$A_v$	Surface area of water droplets per tower cell exchange volume [ $\text{m}^2/\text{m}^3$ ]
$C_p$	Specific heat capacity of air [ $\text{J}/\text{kg}\cdot\text{K}$ ]
$C_{\text{pw}}$	Constant pressure specific heat of water [ $\text{J}/\text{kg}\cdot\text{K}$ ]
$C_r$	Specific heat of rock [ $\text{J}/\text{kg}\cdot\text{K}$ ]
$C_s$	Saturation specific heat [ $\text{J}/\text{kg}\cdot\text{K}$ ]
CT	Percentage of cooling tower valve open [%]
CV	Capital value [R]
d	Basic interest rate [%]
EX	Annual expenses [R]
f	Inflation rate [%]
$F_R$	Collector heat removal factor
$G_t$	Solar irradiation on the collector [ $\text{W}/\text{m}^2$ ]
h	Enthalpy [ $\text{J}/\text{kg}$ ]
$h_a$	Enthalpy of moist air per mass of dry air [ $\text{J}/\text{kg}$ ]
$h_D$	Mass transfer coefficient [ $\text{Kg}/\text{m}^2\text{s}$ ]

$h_s$	Enthalpy of saturated air [J/kg]
$h_{sol}$	Enthalpy of solution respectively
$h_v$	Volumetric heat transfer coefficient between air and rock [ $J/m^3 \cdot K$ ]
$L$	Length of rock bed in flow direction [m]
$\dot{m}$	The mass flow rate [kg/s]
$m_a$	Air mass flow rate [ $m^3/s$ ]
$m_w$	Water mass flow rate [ $m^3/s$ ]
$N$	Life time of the plant [years]
$P$	Perimeter of bed [m]
$P(t)$	Investment at time $t$ [R]
$PVF(N, f, d)$	The present value factor [-]
$\dot{Q}$	The heat transfer rate [kW]
$Q_{cell}$	Overall tower cell heat transfer rate [kW]
$Q_{ev}$	Energy into the evaporator [kW]
$Q_{gen}$	Energy into the generator [kW]
$r_f$	Recovery factor
$t$	Time [years]
$T$	The maximum temperature during discharging [ $^{\circ}C$ ]
$T_a$	Ambient air temperature [ $^{\circ}C$ ]
$T_{CTS}$	Cooling tower return temperature [ $^{\circ}C$ ]
$T_{bottom}$	Temperature at the bottom of the storage tank [ $^{\circ}C$ ]
$T_{env}$	Temperature of surroundings [ $^{\circ}C$ ]

$T_i$	Collector inlet fluid temperature [ $^{\circ}\text{C}$ ]
$T_i$	Fluid temperature of node $i$ [ $^{\circ}\text{C}$ ]
$T_o$	The minimum temperature during discharging [ $^{\circ}\text{C}$ ]
$T_{\text{out}}$	Collector outlet temperature [ $^{\circ}\text{C}$ ]
$T_p$	Absorber plate temperature [ $^{\circ}\text{C}$ ]
$T_r$	Rock temperature [ $^{\circ}\text{C}$ ]
$T_{\text{ref}}$	Refrigerant temperature, [ $^{\circ}\text{C}$ ]
$T_{\text{sol}}$	Temperature [ $^{\circ}\text{C}$ ]
$T_w$	Water temperature [ $^{\circ}\text{C}$ ]
$T$	The maximum temperature at the end of the charging period [ $^{\circ}\text{C}$ ]
$U$	Loss coefficient from bed to surroundings [ $\text{W}/\text{m}^2$ ]
$U_L$	Collector heat loss coefficient [ $\text{W}/\text{m}^2$ ]
$V$	Volume of the rock bed [ $\text{m}^3$ ]
$V_{\text{cell}}$	Total cell exchange volume [ $\text{m}^3$ ]
$x_w$	Weak solution concentration [% LiBr]
$x_s$	Strong solution concentration [% LiBr]
$x_i$	Concentration at position $i$ in the cycle [% LiBr]
$\Delta T_{\text{on}}$	Set temperature difference for the pump to turn on [ $^{\circ}\text{C}$ ]
$\Delta T_{\text{off}}$	Set temperature difference for the pump to turn off [ $^{\circ}\text{C}$ ]

### Dimensionless Numbers

$Le$  Lewis number

### Greek symbols



$\tau\alpha$	Collector transmittance absorptance product
$\varepsilon_a$	Air side heat transfer effectiveness
$\varepsilon$	Auxiliary heat exchanger effectiveness
$\Delta$	Difference between two values
$\varepsilon$	NTU of rock bed

### **Subscripts**

$a$	Air stream conditions
$w$	Water stream conditions
$in$	Inlet conditions
$out$	Outlet conditions
$s$	Saturation conditions
$s$	Strong solution
$w$	Weak solution
$sol$	Solution
$ref$	Refrigerant
$env$	Environment

### **Acronyms and Abbreviations**

AHU	Air Handling Unit
ASHRAE	American Society of Heating, Refrigeration and Air Conditioning Engineering
COP	Coefficient of Performance
CPC	Compound Parabolic Collector

ETC Evacuated Tube Collector

FPC Flat Plate Collector

HVAC Heating Ventilation and Air Conditioning

IEA International Energy Agency

LCC Life Cycle Costs

NPV Net Present Value

NTU Number of Transfer Units

PV Photovoltaic

SCOP Solar Coefficient of Performance

TMY Typical Meteorological Year

## CHAPTER ONE

---

### 1 INTRODUCTION

#### 1.1 Background

Air-conditioning is the dominating energy consuming service in buildings in many countries and the world demand for cooling and dehumidification of indoor air is growing due to increasing comfort expectations and increasing cooling loads, as well as building architectural characteristics and trends (1). The air-conditioning of buildings is carried out mainly using vapor compression systems. These systems require high amount of energy, result in high electricity peak loads and employ chlorine bearing refrigerants which impact negatively on the environment. In the atmosphere, due to ultra violet radiation the refrigerants break up and release their chlorine atoms which promote the breakdown of the ozone layer. These refrigerants remain in the atmosphere for many years and trap heat more effectively than carbon dioxide leading to increased global temperatures. The high electricity consumption occurs only for a few weeks a year and cannot be covered at a reasonable cost, if one tries to apply a rational tariff system, as the investments needed in infrastructure are unjustified (2). In addition to this, South Africa has been experiencing electricity shortages and ever increasing energy prices. As a result there is an urgent need for air conditioning systems that are driven by renewable energy whilst at the same time having minimum impact on the environment. Solar energy in particular, has the potential to supply a sizable percentage of the cooling energy demand because solar radiation levels in South Africa are among the highest in the world. The annual 24-hour solar radiation average for South Africa is  $220\text{W}/\text{m}^2$ . Most of the interior parts of the country receive average insolation in excess of  $5\text{kWh}/\text{m}^2$  with some parts of the Northern Cape averaging  $6\text{kWh}/\text{m}^2/\text{day}$  (3). In general, solar cooling is an attractive idea because the cooling loads and availability of solar energy are approximately in phase.

#### 1.2 State of Solar Thermal Systems

The International Energy Agency (IEA) under their Solar Heating and Cooling program Tasks 25 and 38 carried out a survey of solar thermal installations in 55 countries worldwide (4). By the end of the year 2010, the solar thermal capacity in operation worldwide was found to be  $195.8\text{GW}_{\text{th}}$ , corresponding to 246.2 million square meters of collectors. Of this  $151.8\text{GW}_{\text{th}}$  were flat plate collectors and evacuated tube collectors. Sadly, of this installed capacity, Sub-Saharan African countries, namely Namibia, South Africa and Zimbabwe account for only  $0.8\text{GW}_{\text{th}}$ . The utilization of solar thermal energy varies from

region to region and can roughly be distinguished by the type of solar thermal collector used, the way of system operation and the main application the energy gained from the sun is used for. Of all the regions of the world, Europe has the most sophisticated market for offering a diverse selection of solar thermal applications and these include solar domestic hot water systems, space heating systems for single and multi-family houses and hotels, district heating plants as well as systems for industrial applications and for air conditioning and cooling. The total collected solar energy for the systems in these 55 recorded countries is 162 125GWh, which represents energy savings equivalent of 17.3 million tons of oil and an annual avoidance of 53.1 million tons of carbon dioxide (4). Close to a thousand solar air-conditioning plants have been installed worldwide, which cover all types of technologies and sizes (1). Recently, mega watt-scale solar heating and cooling installations have gained increased interest and have been realized or are under development e.g. Riyadh, Saudi Arabia, a solar thermal plant, with total capacity of 25MW<sub>th</sub> (36 305m<sup>2</sup>), was commissioned in 2011, Singapore, thermal heating and cooling installation with 2.7MW<sub>th</sub> (3 900m<sup>2</sup>) was installed in 2011.

### 1.3 Solar Cooling Systems

Solar energy can be used in cooling by two main principles i.e. photovoltaic powered vapor compression systems and thermally driven air-conditioning technologies. Today, the first principle – solar electricity driven cooling – is mainly used for solar driven refrigerators for cooling medicine in remote, sunny regions, while the second principle – solar thermally driven cooling – is mainly applied for comfort cooling and air-conditioning in buildings and first pilot installations have been realized for large capacity refrigeration applications (1). The most used thermally driven technologies operate on the absorption and desiccant cooling cycles. For temperature demands of 60 – 80°C, desiccant cooling systems (DCS) are suited for utilization of solar thermal energy. In comparison with solar desiccant cycles and mechanical processes, solar absorption cycles are more reliable, feasible, and quiet (5). Therefore, this project is concerned with determining the energetic and economic feasibility of solar powered absorption systems for South Africa.

### 1.4 Overview of Absorption Cooling Systems

The development of absorption refrigeration has been linked to period of high energy prices (2). Due to an increase in knowledge regarding the amount of environmental degradation caused by vapor compression systems, a resurgence of interest in absorption cooling systems has been recorded. In the USA for example, 41% of primary energy use is experienced in buildings and with 70% of this energy

being met by fossil fuels, buildings are responsible for an estimated 38% of carbon dioxide emissions (6). Other than this, the energy consumption by vapor compression air-conditioning systems is very high. As a result, energy efficient technologies such as absorption cooling have to be promoted to minimize energy consumption whilst maintaining the economic performance of the system.

The most common, globally used type of thermally driven technology to produce chilled water is absorption cooling. The absorption cooling system, which has simpler capacity control, mechanism, easier implementation, high reliability, silent operation and long service life and low maintenance costs is a genuine candidate for efficient and economic use of solar energy for cooling applications. In comparison to vapor compression systems, absorption systems use low temperature thermal energy collected from the sun without need to convert this energy into mechanical energy. The basic physical process in an absorption system consists of at least two chemical components, one of them serving as the refrigerant and the other as the absorbent. For air-conditioning applications, absorption systems commonly use lithium bromide-water (LiBr-water) or ammonia-water ( $\text{NH}_3$ -water) working pairs. The generator of the LiBr-water units may be powered by low cost solar thermal collectors thus making these units most suitable for solar applications. The  $\text{NH}_3$ -water machine requires high generator temperatures in the range 125-170°C (7). This temperature requires the use of medium concentration ratio parabolic collectors, which have increased maintenance requirements, whereas the LiBr-water machines require a temperature in the range 75-120°C, which is easily achieved using flat plate or evacuated tube collectors. The LiBr-water machine has a higher coefficient of performance (COP) and costs less than the  $\text{NH}_3$ -water (8). This is because the  $\text{NH}_3$ -water machine requires a rectifier to prevent any water vapor entering the evaporator and also requires higher pressure hence higher pumping power. The LiBr-water machine has a limited range of operation due to onset of crystallization occurring at the point of the recuperator discharging into the absorber but excellent performance low cost making it a favorable candidate for use in solar cooling systems. Apart from the single-effect machines, double-effect machines are also available. These have a higher COP in the range 1.1-1.2, but require driving temperatures in the range of 140-160°C (5). As a result, these types of systems are only available in large capacities of 100kW and above. Single effect machines have a COP in the range of 0.5-0.8, while electrically driven compression chillers today work at COPs around 3 or higher. Therefore solar fractions have to be higher than about 50% to start saving primary energy (9).

The main obstacle to the development of small scale absorption systems has been the unavailability of small absorption machines (less than 20kW). In the last few years new products such as Sonnenklima,

EAW, Rotartica and Klimatwell have entered the market and all are in the capacity range between 5-15kW (10).

### 1.5 Motivation for the Study

According to the Department of Energy, South Africa seeks to achieve a 15% renewable energy contribution to the energy mix within the decade. Despite this, almost all the research and development work concerning solar energy has concentrated on the provision of Solar Domestic Water Heating and little work has been done regarding solar cooling systems. Based on current technologies and the thermally driven cooling devices available on the market, properly designed solar air conditioning systems can lead to significant primary energy savings. (11). It is this projects' aim to investigate the technical and economical performance of a solar absorption system with all the driving energy being provided by solar energy.

Lack of cost competitiveness of solar cooling systems has resulted in a lack of demonstration projects to serve residential housing needs. This is despite the existence of a large potential market for systems of less than 10kW capacities to serve the domestic air conditioning needs (12). The major challenges to large scale utilization of solar cooling are initial costs, low system performance and limited system operation time due to the nature of solar energy availability, lack of practical knowledge about design and system operation strategies. There are no standardized design guidelines in existence and common practices for design and construction are not available. It is one of this study's objectives to contribute positively to the knowledge for the design and performance characteristics of solar absorption cooling systems for Southern African climatic conditions. The future of solar cooling methods depends on developments beyond the cooling process itself. System optimization is achieved by coming up with different sub-system combinations and determining the cost per unit of cooling energy produced. In addition to this the available surface for surface collector installation and building integration considerations are also important factors in this respect (13). A solar absorption system is a complex dynamic system and it is difficult to predict with certainty the annual energy saving, and therefore, the return on investment (14). This uncertainty is also another obstacle to wider application of solar cooling. In order to come up with an effective system design, the influence of key parameters on overall system performance is investigated by carrying out parametric studies.

In this study, TRNSYS modeling was carried out on two solar powered absorption systems. The two complete solar powered cooling systems comprising of a solar collector array, storage tank, cooling

tower, a 35kW LiBr-water absorption chiller and distribution pumps and controllers were designed, and installed at two sites in Pretoria and Midrand and had their technical and economic performances analyzed. System performance data was collected and compared with the simulations results. The first system was installed at Netcare Moot Hospital in Pretoria and comprised of a solar collector array made up of 52 evacuated tube collectors, two 6000 liter hot water storage tanks, 35kW LiBr-water absorption chiller, and a wet cooling tower. This system was coupled to an existing vapor compression chiller so that cooling is provided even when no solar energy is available. The installation was controlled and remotely monitored through the internet and parameters logged through a Carel Building Management System. The other system is at Vodacom World in Midrand, Johannesburg and is an autonomous solar heating and cooling system aimed at maintaining the building environment at comfort conditions throughout the year. It is made up of a 116m<sup>2</sup> vacuum tube collector array, a 6.5m<sup>3</sup> hot water storage tank, 35kW LiBr-Water absorption chiller, 1m<sup>3</sup> of cold water storage, a dry cooler for the chiller, and two underground rock storages to pre-cool the supply air to the building and the dry cooler, respectively. The Vodacom system is the first six star green building with all its energy needs supplied by solar energy.

## 1.6 Thesis Layout

The first chapter introduces the study and gives the background of the research question to be answered. The world is experiencing an ever rising amount of building energy use especially during the hot summer months. This is putting unbearable pressure on the electricity grid during peak cooling hours. This project is an attempt at addressing those challenges through use of solar energy powered cooling systems using the case of South Africa. In this chapter an overview of the solar cooling situation is given and the major absorption cooling systems introduced.

The second chapter contains the literature review, giving an overview of the studies that have been done around the world concerning solar powered absorption systems. The contribution of these studies to promote the adoption of solar cooling systems and how it has influenced the design of these systems is also presented.

In the third chapter various solar cooling systems are discussed. The chapter starts by presenting desiccant, adsorption and absorption cooling systems and analyzing how they work. Absorption systems being the most widely used and also the focus of this work are looked at in more depth. The components that are usually found in a typical solar absorption system are described in detail and the equations that represent their performance are also given.

Chapter 4 describes the different solar powered absorption cooling system configurations. This involves variations in thermal storage devices, auxiliary cooker and whether the system is integrated or autonomous. These configurations depend on a lot of factors like size, location, etc and their effect on system performance is explained in detail.

In Chapter 5, two cases studies, namely the Netcare Moot Hospital system and the Vodacom World system are described. There are some differences between these systems the major ones being that the Moot system was installed to replaced some percentage of cooling energy that was being supplied by an already existing vapor compression chiller whilst the Vodacom system is an autonomous system for a new all solar powered building. Also, the Moot system is cooled by a wet cooling tower whereas with the Vodacom system, the heat rejection is achieved through use of a dry cooler and a rock store.

In Chapter 6, TRNSYS simulations are carried out for both systems and their results presented. A complete system performance analysis will be carried out for each system and the main performance indicators calculated.

Chapter 7 presents the system performance results obtained during the operation of the systems. The Moot system was commissioned in October 2009 and was in operation up until November 2011 when it was decommissioned whereas the Vodafone Ste Solutions Innovation Center system was commissioned in November 2011 and is still operational. An economic analysis has been carried out for the Vodafone system and the annuity calculated and the cost per unit of cold produced found.

Chapter 8 contains the comparison of simulation results and the recorded system performance data and the discrepancies are explained. The main discrepancies are due to the weather data and the differences between the data sets used are explained in depth.

In Chapter 9, the main conclusions of this study are summarized and the achievements are discussed. The results are analyzed and necessary improvements recommended. Suggestions for improving technical effectiveness and economic competitiveness are given. Ways of improving Research and Development efforts in this field has been discussed.



## CHAPTER TWO

---

### 2 LITERATURE REVIEW

#### 2.1 Overview

There is little South African Literature on solar cooling systems. The first solar absorption system in South Africa and indeed the whole of Southern Africa was the one designed, installed and commissioned at Moot Hospital in Pretoria by Voltas Technologies in October 2009 (15). Data was collected and analyzed and the system performance results are presented in this study. The lack of literature is in sharp contrast to the international energy arena where numerous systems have been, designed, built and analyzed. The last few years have seen a lot of research being carried out on systems energetic analysis and optimization. The International Energy Agency (IEA), for example, started an ongoing program, Solar Heating and Cooling (SHC) in 1977 which is an international collaborative effort of experts of IEA member countries and the European Union with the aim of improving conditions for the market launching of solar –assisted HVAC systems (1). The collaborative work of the IEA SHC spans over three decades and has generated valuable results and products. These programs promoted a reduction of primary energy consumption and electricity peak loads due to air-conditioning, developing a friendly way for the environment, to heat and cool the buildings (16). In this chapter a review of recent solar powered absorption cooling simulations, designs and installations is presented.

#### 2.2 Review of Solar Powered cooling systems

Ghaddar et al, (14) performed an analytical study of solar utilization in space cooling of a small residential application using solar LiBr-water absorption cooling in Beirut, Lebanon. They carried out a parametric study under Beirut’s climatic conditions to determine the monthly and yearly solar fraction of total solar energy use in the particular building. It was found that for every 3.5kW of refrigeration, 23.3m<sup>2</sup> of collector area was required and when utilized with a water storage tank ranging from 1000liters to 1500liters, the system could efficiently operate solely on solar energy for 7hours a day. The acceptable operating range of the absorption system was found to be when it was supplied with hot water from the solar system between 65°C and 85°C corresponding to a required generator load between 12 and 14.5kW. After carrying out an economic analysis they concluded that the solar cooling system was marginally competitive only when combined with domestic water heating.

Ming Qu et al, (17) at Carnegie Mellon University designed, installed and studied a 16kW double effect LiBr-water chiller, with 52m<sup>2</sup> of linear parabolic trough collectors. This system also happens to be the smallest high temperature cooling system in the world. It was found that the system could potentially supply 39% of the cooling load of the building space in Pittsburgh, if it includes a properly sized storage tank. Calise et al, (13) carried out transient analysis of heating and cooling systems in various configurations. They analyzed the case studies results on a monthly basis, concentrating on the energy and monetary flows of the standard and optimized configurations. The simulation results showed that the solar collector pump flow rates and storage tank volume have to be properly sized if satisfactory economic performance and energy efficiency is to be obtained. The results were found to be encouraging as for the potential of energy savings but appeared still far from economic profitability. The economical profitability of the systems could only be improved by significant public funding.

Ali et al, (18) carried out a performance study of an integrated cooling plant having both free cooling and solar powered LiBr-water absorption chiller. This system has been in operation since August 2002, in Oberhausen, Germany. A floor space of 270m<sup>2</sup> is air conditioned by the plant, which includes a 35.17kW absorption chiller, vacuum tube collectors with total aperture area of 108m<sup>2</sup>, hot water storage capacity of 6.8m<sup>3</sup> and 134kW cooling tower. The results show that COP varies between 0.37 and 0.81. Tsoutsos et al, (2) designed a solar absorption cooling system for a hospital in Greece. Four alternative scenarios were analyzed with different heating and cooling solar fractions. The scenario that optimized the financial and environmental benefits consisted of 500m<sup>2</sup> of solar collector surface driving a 70kW absorption chiller, with 15m<sup>3</sup> hot water storage tank complimented by 50kW electricity driven compression chiller. The system had a solar fraction of 74.73% and a payback period of eleven and a half years without funding subsidies and this could be reduced to 6.9 years with a 40% subsidy. They concluded that the financial investment for these systems was high and further work needed to be carried out to reduce this cost. It was discovered that use of the solar energy powered system resulted in significant primary energy savings.

Casals, (12) carried out detailed TRSYNS dynamical simulations of some commercial solar heating and cooling installations implemented in Spain and concluded that solar absorption cooling possessed genuine potential of reducing the cooling energy demand on the electricity grid. He concluded that delays in determining solar energy costs and technical limitations are resulting in loss for potential market share for the technology. Vidal et al, (19) carried out a simulation and optimization of a solar energy driven air conditioning system for a house in Chile. The results showed that a solar absorption system with 110m<sup>2</sup> of

flat plate collectors, a 7m<sup>3</sup> storage tank could provide up to 70% of the cooling demand of a 149m<sup>2</sup> house in Santiago.

Mittal et al, (20) modeled and simulated a solar absorption cooling system using a flat plate collector, a 10.5kW LiBr-water absorption machine, using weather data for Haryana, India. The effects of hot water inlet temperatures on the COP were investigated and it was found out that high hot water inlet temperature increases the COP of the system and decreases the surface area of the components. Marc et al, (21) implemented a solar absorption system in Reunion without a back-up system to cool school class rooms. Experimental analysis showed that it is very difficult to design a solar energy absorption cooling system without back-up and to define the appropriate refrigeration capacity of the chiller. Chaouchi and Gabsi, (22), working with weather data for Gabse, Tunisia showed that the best performance in terms of COP was obtained when working with low generator temperature and high pressure. Also, values of COP remain weak and depend on the power of the fluid pump.

Florides et al, (23) modeled and simulated an absorption cooling system using TRNSYS simulation program and the Typical Meteorological Year (TMY) for Nicosia, Cyprus. A system optimization was carried out in order to select the appropriate type of collector, the optimum storage tank volume, and the optimum collector slope and area. It was found out that the optimum system should consist of 15m<sup>2</sup> compound parabolic collectors with a tilt of 30° and a 600liters storage tank. It was concluded that the utilization of solar powered absorption chillers even with limited economic benefits should be encouraged given the amount of pollution resulting from use of fossil fuels. Zhai and Wang, (24), carried out a review of absorption and adsorption solar cooling systems in China and concluded that because of high initial costs and high solar specific collector area the large scale residential application of solar cooling technologies was unfeasible, however that it was highly desirable to design solar powered integrated energy systems for public buildings. In public buildings there is enough roof areas to install solar collectors and as a result integrated energy systems are capable of supplying cooling and heating and can even enhance natural ventilation. It was further concluded that solar energy systems used only for cooling purposes are not economically viable because capital costs are very high.

Agyenim et al, (11) developed a LiBr-water experimental solar cooling system and tested it during the summer months of 2007 at Cardiff University, UK. The system was made up of 12m<sup>2</sup> evacuated tube collectors, a 4.5kW LiBr-water absorption chiller, a 1000liters cold storage tank and a 6kW fan coil. A system performance evaluation was carried out and it was found out that the average COP was 0.58.

They proved the feasibility of the concept of cold storage and concluded that this type of arrangement had potential use for domestic cooling systems.

Kalogirou and Florides, (25) and Eicker and Pietruschka, (9) have carried out studies and shown that dynamic system simulations are necessary to determine the correct solar thermal system size and that depending on the location, available solar radiation and size and type of solar collector, solar absorption cooling has the potential to efficiently and economically supply part or all of a chosen buildings cooling load. These studies have also shown that to achieve a given a certain solar fraction, a range of varying collector surfaces and storage tank sizes are required depending on building cooling load profile, chosen system technology and control strategy. These studies show that control strategy has a strong influence on solar thermal system design and performance (9).

Balaras et al, (26) surveyed and analyzed over 50 solar-powered cooling projects in different climatic zones as part of the Solar Air-conditioning in Europe (SACE) project. This project aimed to assess the state of the art and to provide a clear picture of the potential, future needs and the overall perspectives of this technology. They carried out a parametric study to examine the current cost situation for solar assisted air conditioning. For southern European and Mediterranean areas, it was found that solar air-conditioning systems can lead to primary energy savings in the range of 40-50%. It was also concluded that the cost of solar powered air conditioning in buildings and market integration promotion can be achieved through increased research and development.

Balghouthi et al, (27) carried out studies on a solar powered cooling system made up of, parabolic trough solar collectors, a 16kW LiBr-water double effect absorption chiller, cooling tower, back-up heater, two tanks for storage and a set of fan-coils in the building to be conditioned. In 2008 and 2009, water was used as the heat transfer fluid (HTF) and the system was run without thermal energy storage. This system operation was changed in 2010 with the HTF now being thermal oil and two tanks one being for temperature stabilization and the other as back up tank for night storage. The COP ranged from 0.8-0.91 during system operation. Even though the nominal capacity of the chiller was 16kW, the maximum output obtained was 12kW. It was found out that the back-up night storage improves the solar fraction of the system from 0.54 to 0.77. The avoided carbon dioxide emissions during a cooling season were approximately 3000kg corresponding to an equivalent energy saving of 1154 litres of gasoline.

Al-Alili et al, (28) modeled and optimized a solar powered air conditioning system in TRNSYS using Typical Meteorological Data 2, TMY2 data for Abu Dhabi. The system used evacuated tube collectors to

drive a 10kW, NH<sub>3</sub>-water absorption chiller. They optimized the system performance and its total cost separately using single objective optimization algorithms. The results of the optimization showed that the global minimum heater consumption was 1845 kWh. It was also found out that a cost savings and heater consumption reduction of up to 24.5% can be achieved compared to the baseline system.

Jia et al, (29) proposed a novel solar-powered absorption air conditioning system driven by a bubble pump with energy storage, which utilizes a working fluid storage technique. The solar collection system was simulated and analyzed based on the weather conditions of South China. Quieter system operation is achieved through solution circulations using a bubble pump instead of a mechanical pump. The system had a solar collector area of 19.15m<sup>2</sup>, initial charging mass of 379.5kg and the mass fraction was 54.16% and temperature of the solution was 34.5°C, and with this system configuration it was found that the respective COPs of the air conditioning system and the entire system (including the solar panel) were 0.7771 and 0.4372.

Moorthy, (30) carried out performance analysis on a system made up of 84 heat pipe evacuated tube collectors with a total absorber surface area of 235m<sup>2</sup>, a 105kW double effect LiBr-water chiller and two 8m<sup>3</sup> hot and chilled water storage tanks. It was concluded that solar energy is able to produce sufficient energy to power the solar air conditioning system. The solar collector efficiency varied from 26 to 51% during day time and stored energy can be used for several hours during night time. The system COP varied from 0.7 to 1.2 throughout the system operation time and overall system efficiency varied from 27-48%.

Ortiz et al, (31) created numerical model of a solar-thermal assisted HVAC in a 700m<sup>2</sup> educational building and used it to predict the performance and optimize the control parameters. They found out that the solar assisted system could provide over 90% of the total heating requirements after the adoption of particular energy conservation strategies. The external cooling energy required was reduced by between 33% and 43% due to the use of the solar cooling system. They concluded that if the system is not properly designed, high pressure losses in the distribution pipes and consequently increase pumping power requirements can reduce or even negate completely the energy saved. Results also showed that the building could be operated without any external contribution, by heating the building in the coldest hours of the day and using any excess heat to produce chilled water to be stored and used when required. They concluded that maximum performance can be achieved by operation of a solar powered cooling system within a larger district energy system.

Palacin et al, (32) carried out experimental validation of a dynamic TRNSYS simulation model of an existing solar cooling installation located in Zaragoza, Spain. The system has a  $85\text{m}^2$  solar collector array, with only  $37.5\text{m}^2$  used to supply heat to the solar air-conditioning system in the summer. The system also has a 4.5kW air cooled, single effect LiBr-water absorption chiller, hot water tank and an auxiliary boiler. They observed a great influence of the outdoor air on the chiller COP. After removing the dry cooling tower, an open geothermal cycle was designed and installed as a new heat rejection system. It was then observed that the COP dependence on the outdoor temperature was removed and a constant COP was obtained.

Assilzadeh et al, (33) carried out simulation and modeling of a solar absorption system in Malaysia and found out that continuous operation and increase in system reliability could be achieved through use of a  $0.8\text{m}^3$  hot water tank. They concluded that the optimum system for Malaysia's climate for a 3.5kW system consists of  $35\text{m}^2$  evacuated tube collectors tilted at  $20^\circ$ . They used TRNSYS to perform the system optimization. It was also observed that air collectors are not costs effective for solar cooling applications because heat exchange surface areas required are very large.

Darkwa et al, (34) carried out an evaluation of a typical integrated solar absorption system to determine its overall performance. Their study was intended to evaluate the performance of the system located in China, so as to find out the operational and technical barriers facing large scale systems. The results were analyzed and the solar collectors were found to have an operational efficiency of 61%. The chiller achieved a COP of 0.69. They concluded that the integrated solar powered absorption system has proven potential as a viable cooling technology for buildings. To maintain the hot water supply temperature for a system relying solely on solar energy, it is necessary to add secondary heat sources.

Rosiek and Batlles, (35) analyzed the solar absorption cooling system installed at the Solar Energy Research Center (CIESOL), at the University of Almeria. The system is made up of a Yazaki WFC SC20, 70kW single effect absorption chiller,  $64\text{m}^2$  flat plate solar collector arrays, a 170kW cooling tower and two storage tanks with a capacity of 5000l each. When the available solar energy is insufficient to run the chiller, heat is provided by a 100kW auxiliary heat source. During summer the system solar field could sufficiently supply all the heating energy required. The value for the COP was 0.6 and the cooling capacity was 40kW.

Bermejo et al, (36) tested the solar cooling plant at the Engineering School of Seville during the period 2008-2009. The system is composed of a 174kW double effect absorption chiller. The heat input is

provided by a 354m<sup>2</sup> linear concentrating Fresnel collector and a direct fired natural gas burner. The results showed that the chiller operated with a COP between 1.1 and 1.25. The solar energy input represented 75% of the generator heat input. They also observed that if the solar cooling plant runs on a cloudy day, the gas consumption increases significantly, representing the 60% of the net energy injected into the generator.

Southern African countries are lagging behind in terms of utilization of solar energy with the two systems discussed in this project being the only known solar powered absorption cooling system installations. This is particularly disappointing given the abundant solar resources at region's disposal. It is this project's objective to thoroughly investigate the techno-economic performance of these systems and recommend how best they can be implemented for Southern African conditions, South African weather conditions in particular.

## CHAPTER THREE

---

### 3 SOLAR COOLING SYSTEMS

#### 3.1 Overview

There are two main ways of solar energy utilization i.e. direct conversion into electricity and exploitation of the heat energy produced by the sun (37). The utilization of solar energy for cooling can be achieved by two main principles i.e. electrical and thermal sorption.

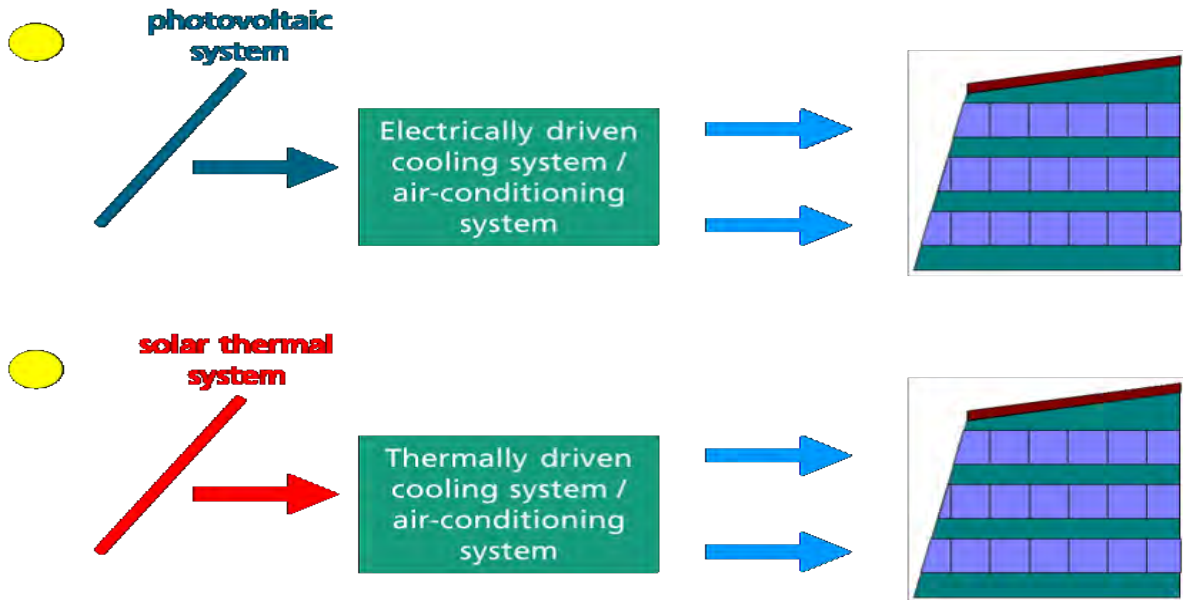


**Figure 3.1: Principles of Solar Driven Cooling (38)**

Solar photovoltaic (PV) driven systems are characterized by high initial costs and low system efficiency. These systems may be any of three main types" i.e. photovoltaic (PV) Peltier systems, PV vapor compression mainly utilized for refrigerators for cooling medicines in remote areas and PV evaporator cooling. The high costs of solar cells and their low efficiency make utilizing PV powered cooling systems very expensive. This project focuses on solar cooling using thermo-mechanical means.

#### 3.2 Sorption Systems

Solar sorption refrigeration technologies are the prevailing option for the utilization of solar energy in air-conditioning (37). These use the heating effect of the sun rather than solar electricity to produce refrigeration. In these systems the refrigeration effect is produced by the chemical or physical attraction between a pair of substances. Adsorption or absorption systems are mainly closed cycle whereas the



desiccant system is mainly open. In desiccant systems, sorbents are used for the dehumidification of incoming air, which in that sense is not a refrigeration process, though it is certainly part of air conditioning. In adsorption solids are used to remove substance from gaseous and liquid solutions. The substance is separated from one phase and accumulates in another.

### 3.3 Desiccant Systems

Desiccant systems are essentially open absorption cycles, utilizing water as refrigerant in direct contact with air with a solid or liquid operating as the desiccant. The desiccant is used to facilitate the exchange of sensible and latent heat of the conditioned stream. After providing the cooling effect the desiccant is discarded from the system and new refrigerant supplied hence the term „open“. The process air is treated in a dehumidifier and goes through several additional stages before being supplied to the conditioned space. The solar heat source achieves sorbent regeneration by heating the ambient or exhaust air to the required temperature (39). A typical desiccant system is shown in Figure 3.2. In this system the moisture (latent load) in the process air is removed by a desiccant wheel (DW) then the temperature (sensible load) of the dried process air is reduced to the desired comfort conditions by sensible coolers (e.g., heat exchangers (HX), evaporative coolers (EC)). The latent and sensible loads are handled separately and more efficiently in components designed to remove that load. The desiccant in the dehumidifier is regenerated (reactivated) by application of heat to release the moisture, which is exhausted to the outdoors (40).

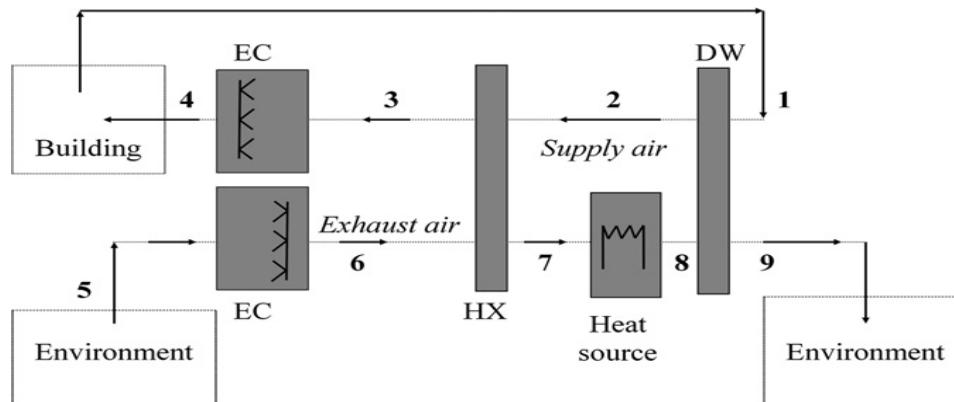


**Figure 3.2: Desiccant System Reticulation Cycle (DW: desiccant wheel, HX: air-to-air heat exchanger, EC: evaporative cooler)**

Corrosion caused by inorganic salts and carryover of liquid desiccant in air is a major problem in desiccant systems. This problem makes solid desiccant, more attractive than liquid systems (41).

### 3.4 Adsorption Systems

The main difference between absorption and adsorption cooling systems lies in the nature of the sorbent, which in the latter is a solid material and in the duration of cooling cycle, which is significantly longer for adsorption. The adsorption cooling cycle generally consists of a generator, a condenser, a pressure-relief valve and an evaporator as shown in Figure 3.3. At the beginning (Stage-1), the system is at a low pressure and temperature. The adsorbent bed is ideally always saturated with vapor at this stage. The adsorbent bed is heated and refrigerant start to desorb from the adsorbent bed at Stage-2, which raises the system pressure. Desorbed refrigerant condenses in the second vessel and rejects heat as a result of condensation. Finally, the hot adsorbent bed (Stage-3) is cooled back to ambient temperature at stage 4 causing the refrigerant to reabsorb on the bed (42). Adsorption systems are classified into two categories: intermittent and continuous. Intermittent systems are daily cycles hence they are more suitable for solar application. (37). Adsorption cycles are usually operated without any moving parts through the use of fixed adsorbent beds. This results in silent operation, high reliability and long system life but also results in intermittent cycle operation and thus decreasing system COP. Two adsorbent beds have to be used out of phase to ensure constant evaporator vapor flow rate and consequently continuous cooling. (43).

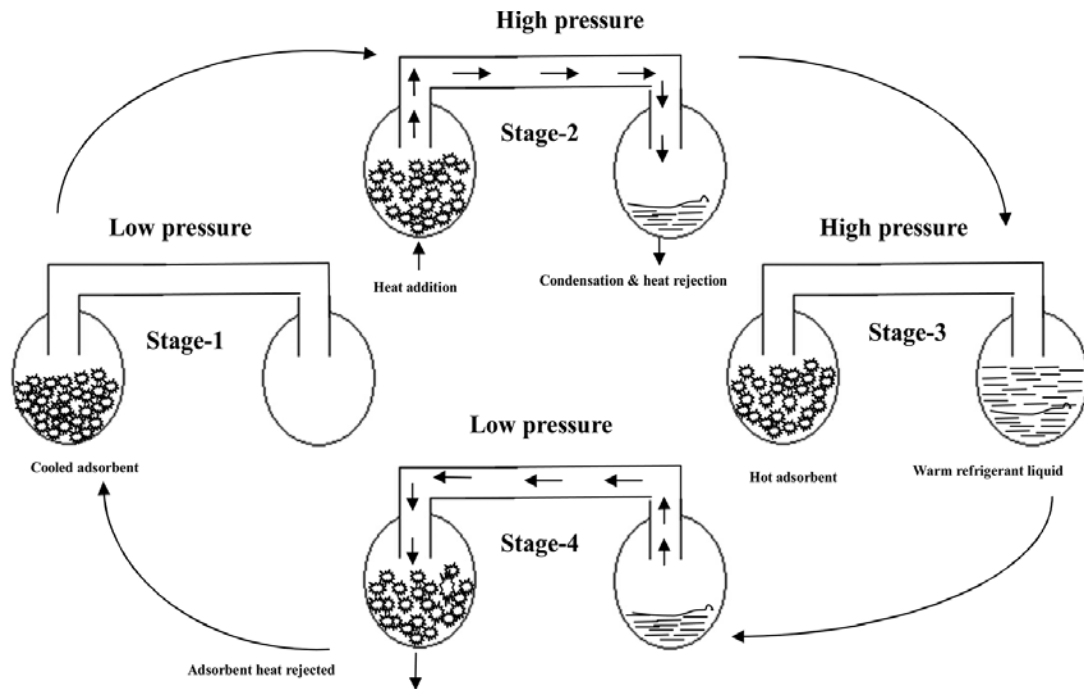


**Figure 3.3: Schematic of the adsorption cycle (42)**

Adsorbents like zeolite, silica gel, activated carbon are physical adsorbents having highly porous structures with surface-volume ratios in the order of several hundred that can selectively collect and retain refrigerants. When saturated they can be regenerated simply by being heated (44). Regeneration temperatures of 170°C are required for the zeolite/water systems, while active carbon/methanol systems, and silica gel/water systems, can utilize heat at temperatures below 100°C. The most commonly used pairing for air conditioning systems is silica gel–water (37). The COP of the silica gel–water chiller is relatively low at about 0.4-0.5, and as a result the Solar COP of the solar driven adsorption air conditioning system is only about 0.16-0.2 (41). Compared to absorption chiller, adsorption chillers are more expensive and they have lower commercial availability

### 3.5 Absorption Cooling Systems

The main difference between vapor compression systems and absorption systems is in the way that pressurization and refrigeration circulation are achieved. Unlike the vapor compression system that uses a mechanical compressor to circulate the refrigerant, the absorption cycle uses an absorbent to circulate the refrigerant. They are thermally activated thus high input power is not required. The temperature requirements are in the low to moderate range thus making absorption cooling a good candidate for renewable energy applications. Two types of absorption cooling machines (chillers) are available on the

market, the single effect and double effect. Single effect machines are mainly used for building cooling loads where water is required at 6-7°C, and can operate with hot water temperatures from 75°C when water is pressurized, and have COPs of around 0.7 (26). These low driving temperatures allow single effect machines to be operated using flat plate collectors. On the other hand, double effect machines have two stages of generation to separate the refrigerant and absorbent. The temperature needed to drive a double effect machine is higher than that required by the single effect machine and is in the range of 155°C to 205°C. The COP of double effect machines are in the range from 0.9 to 1.2 [10]. Although double effect machines have higher COP values, they are more expensive and can only be utilized when a high temperature heat source is available. As a result this project will make use of a single effect absorption chiller. The most common working fluid pairs are LiBr-water and NH<sub>3</sub>-Water. The generator temperatures required by a LiBr-Water chiller are lower at 75°C to 120°C compared to 125°C to 175°C for the NH<sub>3</sub>-Water chillers. LiBr-Water units are most appropriate for solar applications since low cost flat plate collectors can be used whereas the NH<sub>3</sub>-Water units require use of medium concentration ratio parabolic collectors, which have increased maintenance requirements. Also LiBr-Water units have a higher COP (0.6-0.8) compared to 0.6 to 0.7 for the NH<sub>3</sub>-Water (7). The NH<sub>3</sub> –Water system is more complicated because it also contains a rectifier that ensures that no water vapor enters the evaporator where it could freeze. As a result of this a LiBr-Water single effect unit will be used in this project. The only disadvantage of the LiBr-water unit is that its evaporator cannot operate below 5°C since the refrigerant is water vapor.

### 3.5.1 LiBr-Water Absorption Cycle

The LiBr-water absorption cycle shown in Figure 3.4 has the working pair fluid of LiBr (absorbent) and water (refrigerant). Heat is supplied to the generator to vaporize the water and separate the lithium bromide from the solution; the water vapor is cooled in the condenser and then passed to the evaporator whilst the LiBr is conveyed to the absorber as a solution with low refrigerant content. The weak solution entering the generator is preheated by passing the strong solution through a heat exchanger. In the evaporator at low temperature and low pressure, the water evaporates and absorbs heat thereby providing cooling to the space to be cooled. In the absorber there is absorption of the evaporated refrigerant by the absorbent forming the refrigerant absorbent solution. The strong solution is then pumped to the generator to start the whole cycle again. The heat of absorption and condensation is removed by cooling water from

a cooling tower. The cooling water flows through the absorber first because the absorber temperature affects the cycle efficiency more than the condensing temperature (45).

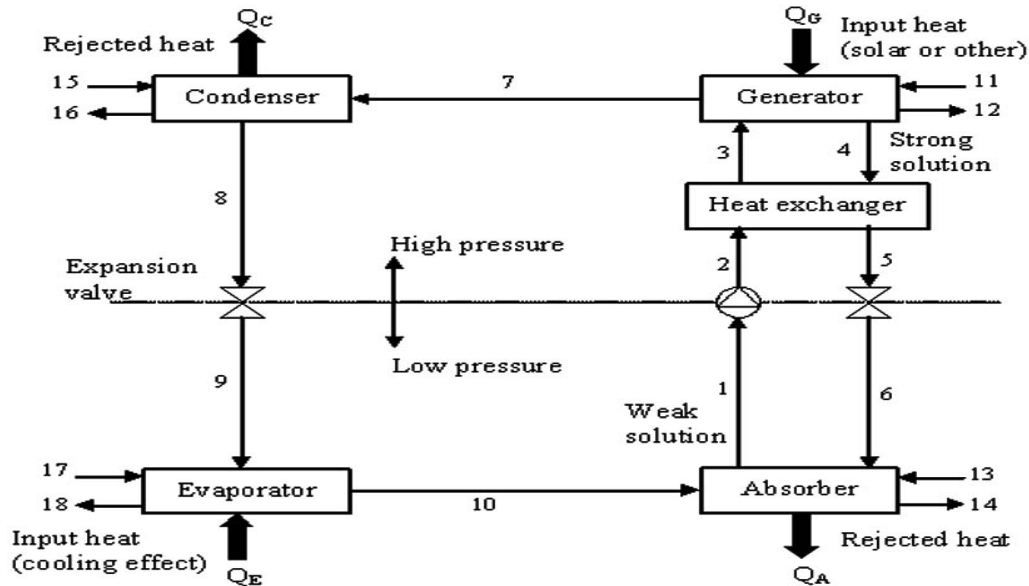


**Figure 3.4: Schematic diagram of a single effect LiBr-water absorption system (10)**

The Coefficient of Performance, (COP) is given by:

$$COP = \frac{Q_{ev}}{Q_{gen}} \quad (3.1)$$

Where:

$Q_{ev}$  Energy into the evaporator

$Q_{gen}$  Energy into the generator

### 3.6 Absorption Chiller Modeling

To accurately predict the performance of a thermal system that makes use of an absorption chiller, there is need to come up with a mathematical model that describes the operation of its components. Mathematical models of various complexities have been developed for different purposes such as single simulation of absorption system, evaluation of potential working fluids, optimization and design (46). The model used here is a steady state one suggested by Grossman and Michelson, 1985 as cited by (47). The structure of the model is as follows:

- i. A main mass balance is applied to the entire cycle, expressing the conservation of the refrigerant and absorbent.
- ii. Each component of the chiller is modeled by a set of equations representing the energy balances of the internal and external stream, and heat transfer equations.
- iii. The thermo physical properties of the working fluids are needed to complete the model.

The following assumptions are made in the development of the model:

- i. There are steady state conditions at each component.
- ii. Pressure drops and heat losses in components and tubes are negligible.
- iii. Solution pump work is neglected both in COP calculation and in determination of weak solution properties.
- iv. There is no heat transfer in the expansion valves.
- v. The refrigerant leaves the condenser and evaporator as saturated liquid and saturated vapor respectively.
- vi. The weak solution leaving the absorber and the strong solution leaving the generator are assumed to be in a saturated state.

In order to carry out the cycle analysis, mass and energy balance must be performed at each component and this is done in the following equations where:

$x_w$	Weak solution concentration
$x_s$	Strong solution concentration,
$x_i$	Concentration at position $i$ in the cycle
$\dot{m}$	The mass flow rate,
$\dot{Q}$	The heat transfer rate,
$\varepsilon$	The efficiency of solution heat exchanger
$h$	Enthalpy

*For the weak solution:*

$$x_1 + x_2 + x_7 = x_w \quad (3.2)$$

*For the strong solution:*

$$x_4 + x_5 + x_6 = x_s \quad (3.3)$$

*At the absorber:*

$$\dot{m}_6 + \dot{m}_{10} = \dot{m}_1 \quad (3.4)$$

$$\dot{m}_1 x_1 = \dot{m}_6 x_6 \quad (3.5)$$

The energy balance is given as:

$$\dot{Q}_a = \dot{m}_6 h_6 + \dot{m}_{10} h_{10} - \dot{m}_1 h_1 \quad (3.6)$$

*At the generator:*

$$\dot{m}_3 = \dot{m}_7 + \dot{m}_4 \quad (3.7)$$

This represents the total mass balance.

$$m_1 x_1 = m_4 x_4 \quad (3.8)$$

This represents the LiBr balance and the energy balance is given as:

$$\dot{Q}_g = \dot{m}_7 h_7 + \dot{m}_4 h_4 - \dot{m}_3 h_3 \quad (3.9)$$

*At the condenser:*

$$m_7 = m_8 = m_{ref} \quad (3.10)$$

This is the total mass balance and the energy balance is given as:

$$\dot{Q}_c = \dot{m}_{ref}(h_7 - h_8) \quad (3.11)$$

*At the evaporator:*

$$\dot{m}_9 + \dot{m}_{10} = \dot{m}_{ref} \quad (3.12)$$

This represents the total mass balance and the energy balance is given as:

$$\dot{Q}_e = \dot{m}_{ref}(h_{10} - h_9) \quad (3.13)$$

*At solution heat exchanger:*

$$\dot{m}_4 + \dot{m}_2 = \dot{m}_3 + \dot{m}_5 \quad (3.14)$$

Equation 3.1 represents the total mass balance and the energy balance is given as:

$$\dot{m}_2 h_2 + \dot{m}_4 h_4 = \dot{m}_3 h_3 + \dot{m}_5 h_5 \quad (3.15)$$

The heat exchanger efficiency is given as:

$$\varepsilon = \frac{h_4 - h_5}{h_4 - h_2} \quad (3.16)$$

*At the expansion valves:*

$$\dot{m}_8 = \dot{m}_9 = \dot{m}_{ref} \quad (3.17)$$

$$\dot{m}_5 = \dot{m}_6 \quad (3.18)$$

Equation 3.18 represents the total mass and the energy balances are given as:

$$h_8 = h_9 \quad (3.19)$$

$$h_5 = h_6 \quad (3.20)$$



The equilibrium temperature and enthalpy of LiBr-H<sub>2</sub>O solution can be obtained by the following equations (7):

$$T_{sol} = T_{ref} \sum_{i=0}^3 a_i x_i + \sum_{i=0}^3 b_i x_i \quad (3.21)$$

And

$$h_{sol} = \sum_{i=0}^4 c_i x_i + T_{sol} \sum_{i=0}^4 d_i x_i + T_{sol}^2 \sum_{i=0}^4 e_i x_i \quad (3.22)$$

Where:

$T_{ref}$  Refrigerant temperature,

$T_{sol}$  Temperature

$h_{sol}$  Enthalpy of solution respectively

The constant coefficients of  $a_i, b_i, \dots, e_i$  were presented by (7).

### 3.7 Cooling Towers

In a solar absorption cooling system there is need to remove the excess heat generated in the absorber and condenser sections of the chiller. The most effective way of doing this is through the use of a cooling tower. Cooling towers use either evaporation of water to remove process heat and cool the working fluid to near the wet bulb temperature or rely solely on air to cool the working fluid to near the dry-bulb air temperature. Water-cooled chillers are normally more energy efficient than air-cooled chillers due to heat rejection to tower water at or near wet-bulb temperatures. Air cooled towers can cool water to within 11°C of the dry bulb temperature whereas wet cooling towers can economically cool water to within 3 to 6°C of the wet bulb temperature (48). As a result, the chiller in this project will be use a wet cooling tower. The cooling tower is connected in series, first the absorber then the condenser, this allows for easy operation since a single pump can be used without the control problem associated with a parallel design (46).

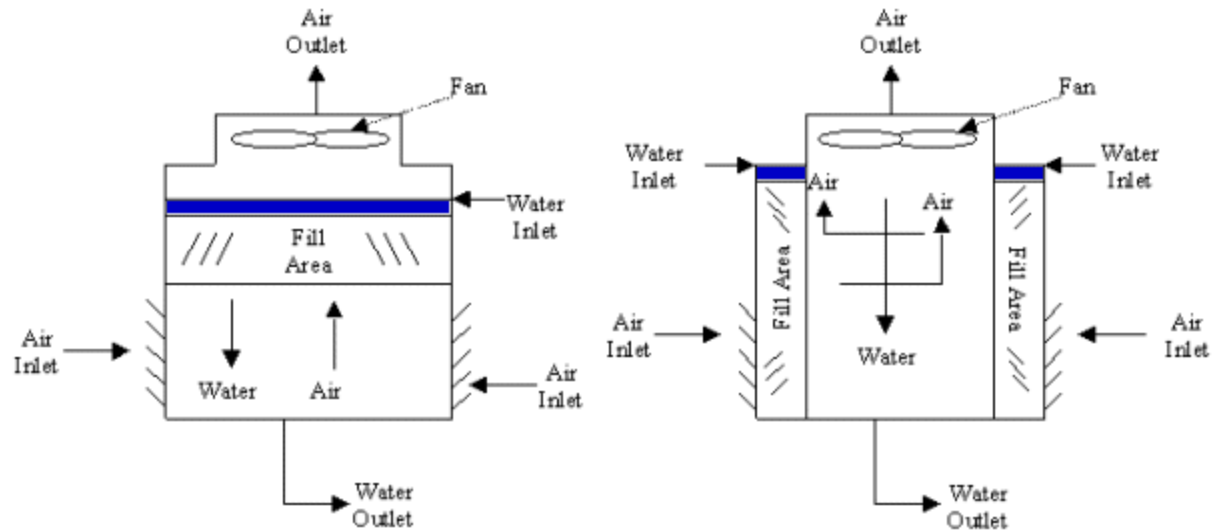


**Figure 3.5: Schematics of Counter flow and Cross flow cooling towers (48)**

In a cooling tower, a hot water stream is in direct contact with an air stream and cooled as a result of sensible heat transfers due to temperature differences with the air and mass transfers resulting from the evaporation to the air. Cooling towers are direct (open circuit) or indirect (closed circuit), the difference being that in the direct type the air is indirect contact with water whereas in the indirect it is not. There are two types of cooling towers: counter flow and cross flow. In a counter flow tower air travels upwards through the fill or tube bundles, whereas water moves downwards. In a cross flow cooling tower, the water still moves downwards like in a counter flow cooling tower but the air moves in the horizontal direction. In mechanical-draft cooling towers, air is forced the tower by use of mechanical fans. This is in contrast to natural-draft towers where the draft is provided by buoyancy of the exhaust air.

### 3.8 Cooling Tower Model

There is no mathematical model that is capable of simulating every detail of the simultaneous heat and mass transfer process within the tower (49). Consequently, simplifying assumptions have to be made for the analysis. These assumptions according to Milosavljevic and Heikkila (48) are as follows:

- i. The water film is thin and mixed, hence the temperature can be assumed constant through the thickness of the water film
- ii. An analogy between heat and mass transfer is assumed and Lewis,  $L_e$  number for humid air is assumed to be unity.

- iii. The mass flow rate of water per unit of cross-sectional area of tower is constant.
- iv. Specific heat of air stream mixture at constant pressure is the same as that of the dry air.
- v. Water lost by drift is negligible.
- vi. Negligible heat transfer from tower to water or to air stream. Negligible heat transfer through the tower walls to the environment.

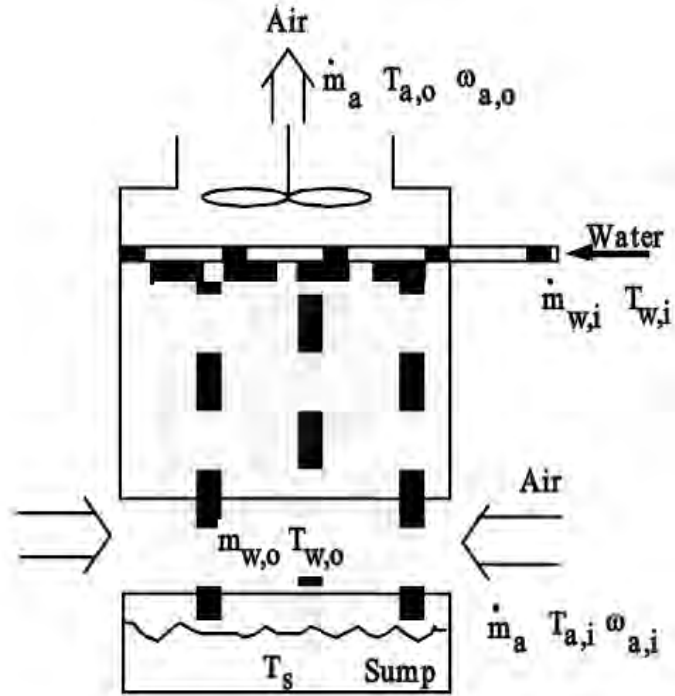


**Figure 3.6: Schematic of a Single Cell Counterflow Cooling Tower (50)**

For a known effectiveness, the heat rejection for an individual tower cell is given by:

$$Q_{cell} = \varepsilon_a m_a (h_{a,w,i} - h_{a,i}) \quad (3.23)$$

Where:

$Q_{cell}$  Overall tower cell heat transfer rate

$\varepsilon_a$  Air side heat transfer effectiveness

$m_a$  Air mass flow rate

$h_a$  Enthalpy of moist air per mass of dry air

Using the assumption that the Lewis number is equals to one, the effectiveness is given by (48):

$$\varepsilon_a = \frac{1 - \exp[-Ntu(1 - m)]}{1 - m \exp[-Ntu(1 - m)]} \quad (3.24)$$

Where:

$Ntu$  = Mass number of transfer units and is given by:

$$Ntu = \frac{h_D A_v V_{cell}}{m_a} \quad (3.25)$$

Where:

$h_D$  Mass transfer coefficient

$A_v$  Surface area of water droplets per tower cell exchange volume

$V_{cell}$  Total cell exchange volume

$$m = \frac{m_a C_s}{m_{w,i} C_{pw}} \quad (3.26)$$

Where:

$m_w$  Water mass flow rate

$C_{pw}$  Constant pressure specific heat of water

$C_s$  Saturation specific heat

This is the average slope of the saturation enthalpy with respect to the temperature curve and is given by:

$$C_s = \frac{h_{s,w,i} - h_{s,w,o}}{T_{w,i} - T_{w,o}} \quad (3.27)$$

Where:

$h_s$  Enthalpy of saturated air

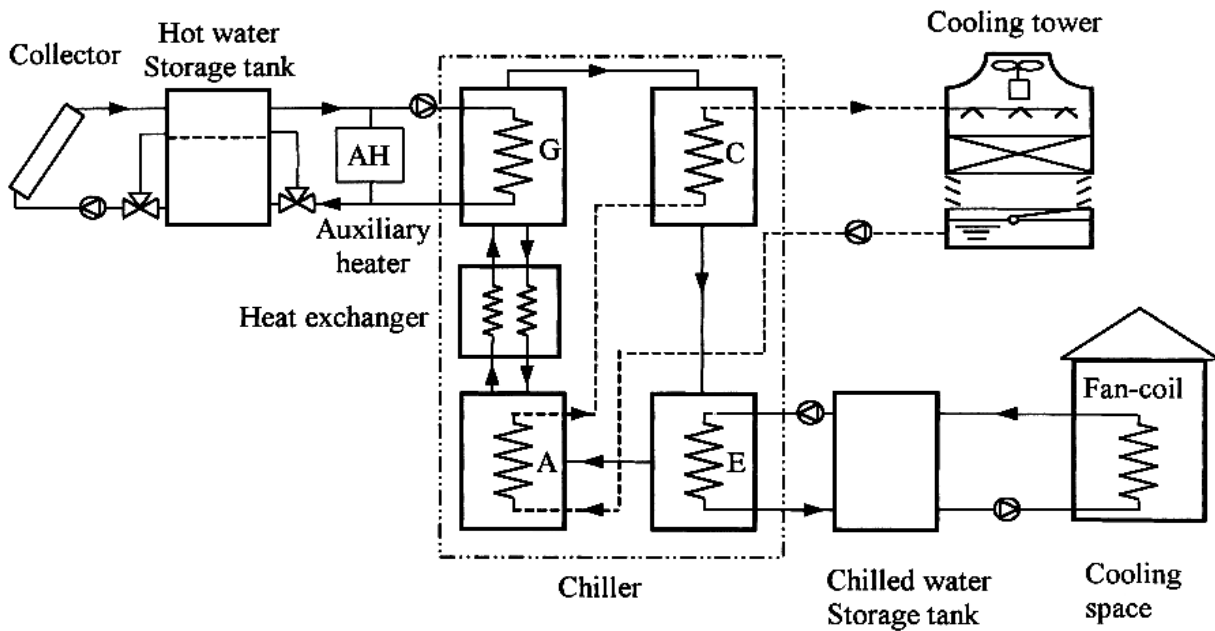
$T_w$  Water temperature

Subscripts:

- a* Air stream conditions
- w* Water stream conditions
- in* Inlet conditions
- out* Outlet conditions

### 3.9 Components of Solar Absorption Systems

Solar cooling systems are generally composed of solar thermal collectors, a form of heat storage, a thermally driven cooling device, the distribution system, and a back-up system (26). The only difference that is there between solar cooling facilities is in terms of component arrangement and configuration.



A – absorber; G – generator; C – condenser; E – evaporator

Figure 3.7: Schematic of a typical solar cooling system (30)

### 3.9.1 Solar Thermal Collectors

A thermal solar collector is a special kind of heat exchanger that transforms radiant energy into heat. It is made up of a receiver that absorbs the solar radiation and then transfers the thermal energy to a working fluid. The analysis of thermal solar collectors presents unique problems of low and variable energy fluxes and relatively large importance of radiation (51). For efficient solar collection, a solar collector should have high absorptance and low heat loss coefficient to ensure a high percentage of the incident solar irradiation is converted into useful energy. Flat plate collectors, evacuated tube collectors and compound parabolic collectors are all suitable for use in air conditioning systems (33).

#### 3.9.1.1 Flat Plate Collectors (FPC)

The simplest form of a flat plate collector (FPC) is a metallic absorber plate exposed to solar radiation with a thermal fluid circulating within. The thermal losses for this arrangement are high due to the effects of the wind is convection losses. To improve the performance of this type of collector, a transparent cover or glazing is introduced so that it isolates the absorber plates from the wind and causes the greenhouse effect inside the collector, recuperating part of the solar radiation reflected by the absorber (52).

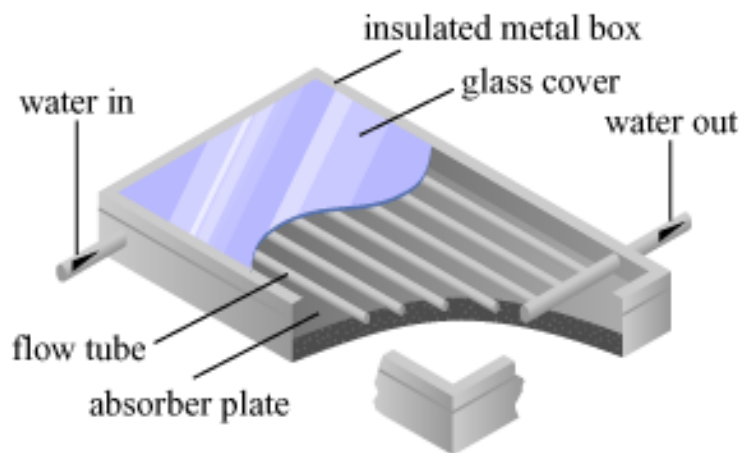


Figure 3.8: Schematic of flat plate solar collector schematic (53)

A flat plate collector is made up of an absorber plate of solar energy, a transparent cover (glazing) that is transparent to solar radiation and opaque to long wave, a heat transfer fluid (air, antifreeze or water) to remove heat from the absorber, and back and edge insulation to reduce heat losses by conduction. They utilize both beam and diffuse solar radiation, do not require tracking of the sun and require little maintenance. The glazing reduces radiation losses from the collector as it is transparent to short wave radiation from the sun but opaque to long-wave thermal radiation emitted by the absorber plate. It also reduces convection losses because of the stagnant air layer between the absorber plate and the cover. The heat insulating backing reduces conduction losses. Flat plate collectors outlet temperatures range between 70-90°C and up to 100°C for selectively coated absorbers (54; 55).

To conveniently describe solar collector operation, the energy balances on each component are required. The design and performance analysis of solar collectors presents unique and unconventional problems in heat transfer, optics and material science and is concerned with obtaining least cost energy. It may be desirable to design a collector with efficiency lower than the one that is technologically possible if the cost is significantly reduced (51). By applying the conservation of energy principle on the absorber, glass cover and working fluid we come up with a set of governing differential equations. The governing equations are then solved as a system.

The useful energy collected by a collector can be obtained from the Hottel, Whillier-Bliss equation (51) as:

$$Q_u = A_{col} F_R [G_t \tau \alpha - U_L (T_i - T_a)] \quad (3.28)$$

Where:

$\tau \alpha$  Absorptance-transmittance product of the solar collector

$U_L$  Collector heat loss coefficient

$T_p$  Absorber plate temperature

$T_a$  Ambient air temperature

$G_t$  Solar irradiance over time,  $t$

$A_{col}$  Solar collector area

$F_R$  Collector heat removal factor

$T_i$  Collector inlet fluid temperature

The efficiency is equal to:

$$\eta = F_R \left[ \tau\alpha - U_L \frac{(T_i - T_a)}{G_t} \right] \quad (3.29)$$

If the heat loss ( $U_L$ ) is considered as the sum of two terms, a constant factor ( $a_1$ ) and a second term dependent on the difference between fluid and ambient temperature [ $a_2(T_i - T_a)$ ], it can be expressed as:

$$U_L = a_1 - a_2(T_i - T_a) \quad (3.30)$$

The efficiency equation can also be computed as:

$$\eta = \eta_o - a_1 T_m^* - a_2 G_t (T_m^*)^2 \quad (3.31)$$

Where  $T_m^*$  is the reduced temperature difference given as:

$$T_m^* = \frac{(T_i - T_a)}{G_t} \quad (3.32)$$

Where:

$\eta_o$  Optical collector efficiency [%]

$T_o$  Collector outlet temperature [°C]

$a_1$  Linear heat loss coefficient,  $\text{Wm}^{-2}\text{K}^{-1}$

$a_2$  Quadratic heat loss coefficient,  $\text{Wm}^{-2}\text{K}^{-2}$

### 3.9.1.2 Evacuated Tube Collectors (ETCs)

When higher temperatures are desired, one needs to reduce the heat loss coefficient and this can be achieved through use of evacuated tube collectors. They minimize convective heat loss by placing the absorbing surface in a vacuum and consequently they produce higher outlet temperature in the range of 80°C to 130°C (54). There are many evacuated tube collector designs on the market and all of them use selective coatings on absorbers because with a non selective absorber, radiation losses would dominate



and eliminating conduction losses alone would not be very effective. Evacuated tube collectors (ETCs) use liquid vapor phase change materials to transfer heat at high efficiency. The problem with the design of ETCs is that it is difficult to extract heat from a long thin absorber contained in a vacuum tube (56).

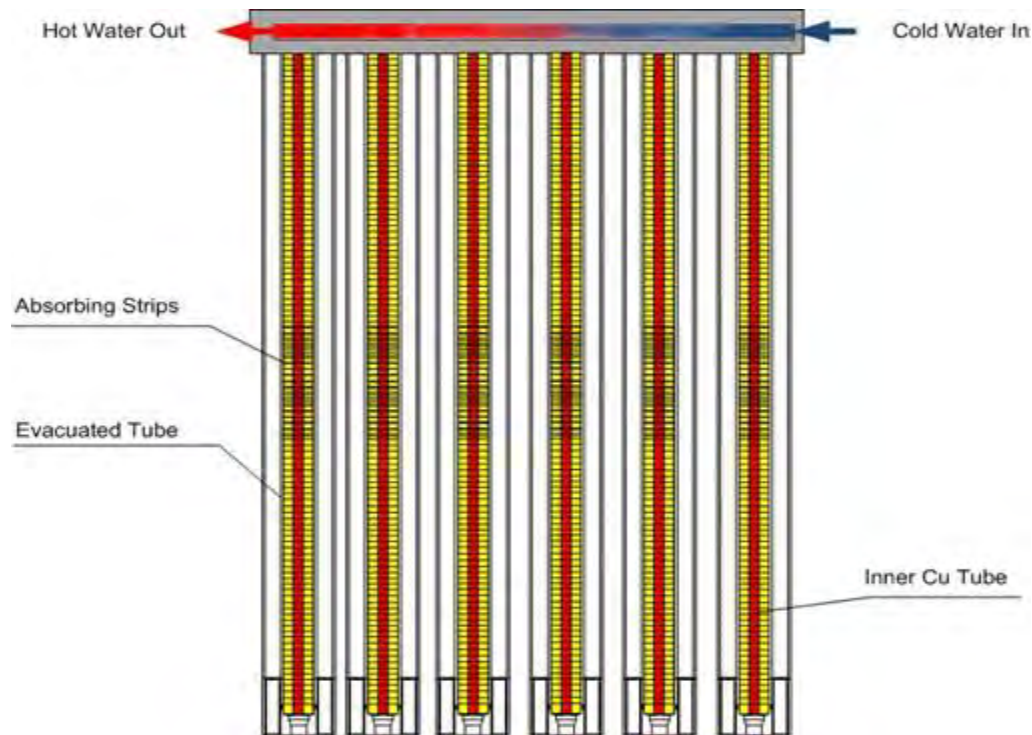


**Figure 3.9: Evacuated tube collector (57)**

A heat pipe provides the most elegant way of extracting heat from an evacuated tube (58). The need for glass to metal seals can be avoided by the Dewar or thermos-bottle design. This design is the only one that has demonstrated long life under transient outdoor conditions (56). The selective absorber coating is applied to the outside (vacuum side) of the inner tube to extract heat from the absorber surface. The collector places a feeder concentrically inside the absorber. The heat transfer fluid enters through the feeder which is open at the other end and allows the fluid to return to the annulus between feeder and absorber plate. The performance penalty due to the thermal short circuiting between incoming and outgoing fluid seems to be acceptable in this case (58). Alternatively, a copper sheet is placed inside the absorber touching the glass to obtain good heat transfer from the glass to copper sheet as shown in Figure 3.9. Hail stones damage is a serious problem for ETC designs that contain glass-to-metal seals and also there is need for a mechanism to prevent thermal shock. ETCs are excellent for operating temperatures up to 120-150°C range. They are non-tracking and many of them use some kind of reflector enhancement (58).

The losses to the environment,  $Q_L$  in this type of collector occur primarily through radiation and are described by:

$$Q_L = U_L(T_i - T_a) \quad (3.33)$$

Where:

$U_L$  Heat loss coefficient

$T_i$  Collector water inlet temperature

$T_a$  Ambient temperature

The expression that gives the useful energy gain is then:

$$Q_u = \frac{A_p}{A_{abs}} [G_t \tau \alpha - U_L(T_i - T_a)] \quad (3.34)$$

Where:

$A_p$  Projected area of the tube

$A_{abs}$  Absorber area

$\tau \alpha$  Collector transmittance absorptance product

$G_t$  Solar irradiation on the collector

### 3.9.1.3 Compound Parabolic Collectors (CPCs)

As shown in Figure 3.10, compound parabolic collectors are a special type of collector fabricated in the shape of two meeting parabolas. Heat losses are approximately proportional to absorber area. By concentrating the incident radiation on an aperture onto a smaller absorber, one can reduce the heat loss per collector aperture area (58). CPCs are non-imaging concentrators. They have the capability of reflecting to the absorber all of the incident radiation within wide limits. All the radiation that enters the aperture within the collector acceptance angle reaches the absorber surface because of multiple internal reflections (54). The area reflecting the solar radiation is considerably larger than the absorption area thus enhancing outlet collector temperatures and lowering heat losses to ambient by the use of vacuum

technique (52). In a CPC, the absorber can be flat, cylindrical, bifacial etc. CPCs with low concentrations and non-evacuated receivers may be economical for temperatures around the boiling point of water (58).

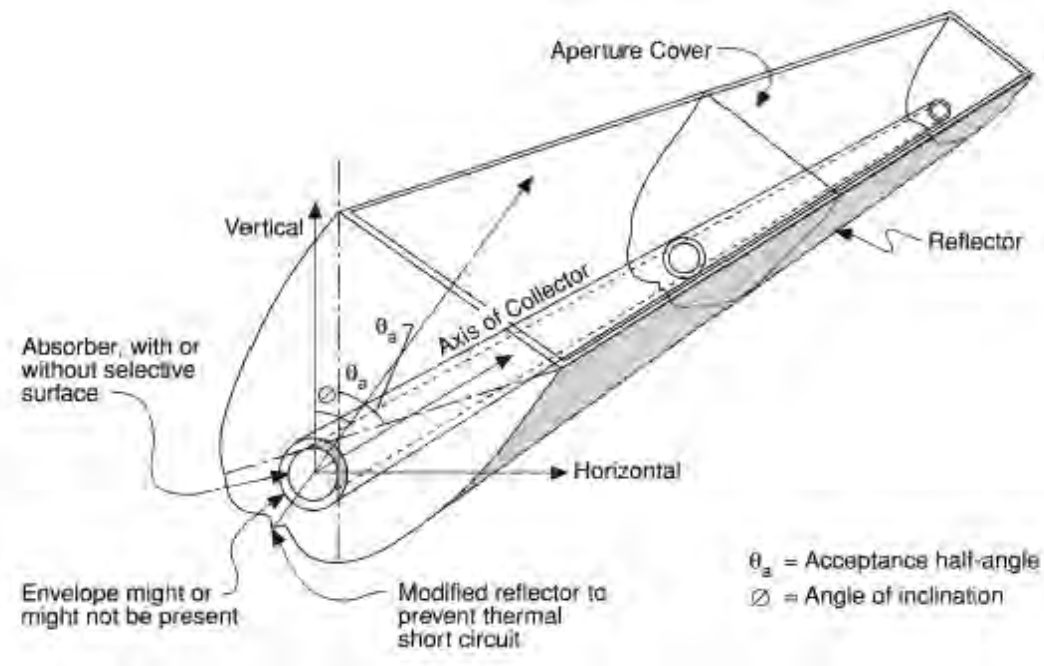


**Figure 3.10: Schematic of a compound parabolic collector (58)**

### 3.9.2 Distribution of Flow in Collectors

In practice usually, a combination of collectors in series, parallel or mixed configuration has to be used. Performance depends on the flow rate through the risers and on the inlet temperature to each individual module (sub collector). For collectors in parallel the flow splits up whereas in a series connection the flow rate is the same in each sub collector. If this difference in flow rate does not make a significant change in collector efficiency factor, the performance will remain almost constant (51). Prakash et al, (1990) as cited in (59) carried out investigations on a collector array under different configurations and concluded that the purely parallel combination is advantageous over others because the pumping costs required were much less. Karwa et al, (59) have shown that for air collectors, using constant pumping power, an array with sub collectors in parallel is about 3-33% better in thermal efficiency than an array with sub collectors in series. The collector performance calculations presented here were done with the assumption that there is uniform flow distribution in all of the risers of a single collector or multiple collectors. Culham and Sauer, (1984) as cited by (59) found out that for water collectors, if the flow rate in the riser tubes of the collector is at least 35% of the nominal value, then the non-uniform flow

distribution has only a marginal effect on the total energy collection. With non uniform flow, the parts of the collector with low flow through the riser will have lower collector heat removal factor ( $F_R$ ) than the rest of the collector. Series connection increases the effective flow rate through the individual collectors and the increased turbulence from the increased fluid velocity increases the heat transfer coefficient and hence collector efficiency. The increased fluid velocity also results in an increased pressure drop and results in the requirement of higher pumping power, high cost pump and increased electricity consumption. Designers need to be wary of reducing installation costs by series connection at the expense of pumping losses (60). An appropriate combination of series and parallel connections will be made for the collector array to be used in this project to optimize collector array efficiency and installation costs.

The number of solar collectors in series can be calculated by the following equations (6):

The efficiency for one collector is given by:

$$\eta = \eta_o - a_1 T_m^* - a_2 G_t (T_m^*)^2 \quad (3.35)$$

Where:

$\eta_o$  Optical collector efficiency [%]

$T_o$  Collector outlet temperature [ $^{\circ}\text{C}$ ]

$a_1$  Linear heat loss coefficient,  $\text{Wm}^{-2}\text{K}^{-1}$

$a_2$  Quadratic heat loss coefficient,  $\text{Wm}^{-2}\text{K}^{-2}$

The useful energy for the whole array is

$$Q_{tot} = C_p \dot{m} (T_o - T_i) \quad (3.36)$$

Where:

$C_p$  Fluid specific heat capacity

$\dot{m}$  Collector fluid flow rate

$T_o$  Collector outlet temperature

$T_i$  Collector inlet fluid temperature

The useful energy for the array can also be given as:

$$Q_{tot} = \eta N A_{col} G_t \quad (3.37)$$

Equating equations (3.37) and (3.36) and substituting the value of  $\eta$  from equation (3.35) and solving, the number of solar collectors in series, N is given as:

$$N = \frac{C_p \dot{m} (T_o - T_i)}{A_{col} (\eta_o G - a_1 T_m^* - a_2 (T_m^*)^2)} \quad (3.38)$$

The highest allowed pressure drop in the collector is the limiting characteristic even so increasing the flow rate only enhances the heat transfer for a limited range.

### 3.10 Controls

The control of a solar cooling system involves the simultaneous control of the system parts in order to fulfill one or more given tasks. The choice of control system is essential for system performance and should focus on increasing cooling efficiency and reduction of electrical energy consumption by pumps, blowers etc. There are four categories to be considered when designing automatic controls for solar cooling systems:

- i. Collection to storage
- ii. Storage to load
- iii. Auxiliary heater (if any) to load
- iv. Miscellaneous (heat dumping, freeze protection, overheating etc.)

The three major control system components are sensors (detect conditions: pressure, temperature etc), controllers (receive information from sensors, process it and send signals for corrective action to be taken) and actuated devices (pumps, valves, alarms etc). Correct setting, operation and location of the sensors is important if the system is to perform efficiently with minimum maintenance costs..

Two types of control schemes are commonly used on solar collectors in building scale applications: on-off (differential) and proportional. On-off is the most widely used scheme (51). As a result, in this project

on-off control was used and its operation is presented here. A decision is made to turn the circulating pumps on or off depending on whether or not useful energy is available from the collector. The pump is turned on when the difference between the collector outlet temperature and the storage tank bottom temperature exceeds a set amount. Once the pump is running and the temperature falls below a set value, the controller stops the pump. Care must be taken when selecting  $\Delta T_{on}$  and  $\Delta T_{off}$ , the temperature difference between the temperature at the bottom of the tank,  $T_{bottom}$  and the collector outlet temperature,  $T_{out}$  at which the pump is turned on and off respectively. If this is too high, collector efficiency will be adversely affected and if it is too low, there will be short cycling of the pump.

The following two conditions (equations 3.39 and 3.40) need to be satisfied for the pump to turn on and off respectively:

$$T_{out} - T_{bottom} \geq \Delta T_{on} \quad (3.39)$$

$$T_{out} - T_{bottom} \geq \Delta T_{off} \quad (3.40)$$

Where:

$\Delta T_{on}$  Set temperature difference for the pump to turn on

$T_{out}$  Collector outlet temperature

$T_{bottom}$  Temperature at the bottom of the storage tank

$\Delta T_{off}$  Set temperature difference for the pump to turn off

Duffie and Beckman (51), suggest that for system stability the following must be satisfied:

For a system operating without an auxiliary heat exchanger:

$$\Delta T_{off} \leq \frac{A_c F_R U_L}{\dot{m} C_p} \Delta T_{on} \quad (3.41)$$

And for system with an auxiliary heat exchanger:

$$\Delta T_{off} \leq \frac{A_c F_R U_L}{\varepsilon (\dot{m} C_p)_{min}} \Delta T_{on} \quad (3.42)$$

Where:

$\varepsilon$  Auxiliary heat exchanger effectiveness

The turn-on criterion must be significantly higher than the turn-off criterion. The pump should not be operated until the value of useful energy collected exceeds the value of pumping (51). In the morning the fluid in the pipes/ducts between the storage tank and the collector will be colder than the temperature at the bottom of the storage tank. When the pump first turns on, cold fluid will enter the collector resulting in low temperature being detected by the outlet sensor, so the controller will turn off the pump until fluid in the collector is heated to the proper temperature for the pump to turn on again. Besides the wear and tear of the pump and motor, this is an efficient way to heat fluid in the collector and inlet ducts to the proper temperature.

The relevant controlled parameters for the absorption chiller are:

- i. Hot water inlet temperature and mass flow: is a result of the control of the solar thermal system (collector and storage tank).
- ii. Cooling water inlet temperature: depends on the cooling tower type and performance.
- iii. Chilled water outlet temperature: depends on the chilled water distribution system and cannot be influenced.

### 3.11 Water Storage Tanks

In order to reduce the time of mismatch between solar energy supply and cooling load demand, energy storage is required. This energy storage is usually a water storage tank between the collector array and the chiller or cold water storage tank between the chiller and the building cooling load or both. Due to the nature of solar energy some form of hot water storage is always required regardless of the presence of cold water storage or not. . Li and Sumathy (61), Martinez, (62) have shown that the use of only hot water storage results in higher system efficiency, simpler operation, lower cost components, and smaller storage size. As a result, this project will make use of hot water storage only. The development of efficient and inexpensive storage devices is as important as developing new sources of energy. A good storage system should have a long storage time and a small volume per unit of stored energy. In the design of a water storage tank, the following considerations have to be met:

- i. Temperature ranges over which storage tank has to operate. The lower temperature limit is determined by the requirements of the process and the upper limit by the process, vapor pressure of the water or the collector heat loss.
- ii. Volume of the tank- this has a significant effect on the operation of the rest of the system. Short term storage units which can meet fluctuations over a period of 2 or 3 days are the most economical (62).
- iii. Heat losses from the storage have to be kept to a minimum.
- iv. The rate of charging and discharging.
- v. Cost of the storage unit. This includes the initial cost of the tank and insulation plus the operating costs.

The First Law efficiency of thermal energy storage systems can be defined as the ratio of energy extracted from the storage to the energy stored in it:

$$\eta = \frac{(T - T_o)}{(T - T_o)} \quad (3.43)$$

Where;

$T$  The maximum temperature during discharging

$T_o$  The minimum temperature during discharging

$T$  The maximum temperature at the end of the charging period

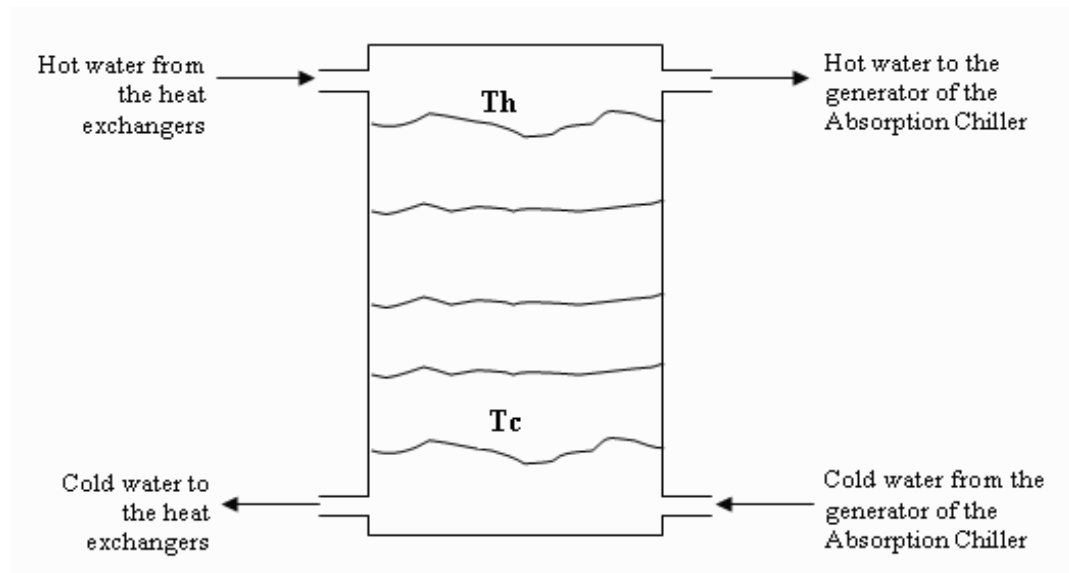
### 3.11.1 Thermal Stratification

Improvement in storage is achieved by thermal stratification. This is the phenomenon where the temperature of the stored fluid increases with elevation as shown in Figure 3.11. Thermal stratified storage tanks are an effective management technique to improve the efficiency of solar thermal systems. Stratification allows an optimal use of the storage with minimized heat losses and can also be used to ensure that collector inlet is as low as possible (63). The layered temperature difference results in increased solar collector efficiency. Perfect stratification is very difficult to achieve in practice due to agitation by water entering from the collector and diffusion from entering water before it reaches the appropriate level. The temperature layers are destroyed by the formation of natural convection currents due to the temperature near the tank walls being lower than that in the inner parts of the tank. Significant improvements in yearly system performance can be achieved if stratification is maintained in the storage



tank [44]. Good thermal insulation is required to maintain stratification over long periods. Advantages of thermal stratification include:

- i. Water at a higher temperature than the overall mixing mean temperature can be drawn from the top of the tank, thereby improving the satisfaction of the load.
- ii. Collection efficiency for the collector is improved since the collector inlet temperature is lower than the mixed mean storage temperature.
- iii. The storage tank can be at a lower mixed mean temperature for a given temperature requirement from the load, hence reducing heat losses from the storage tank.



$T_h$  Temperature of hot water

$T_c$  Temperature of cold water

**Figure 3.11: Basic configuration of a stratified thermal storage tank:  $T_h > T_c$  (52)**

In practice stratification is obtained by a charge via the top of the tank with an inlet temperature much higher than the temperature of the surrounding water and injecting at a low flow rate (63). Diffusers should introduce water to the tank uniformly and a low velocity so that buoyancy forces create and maintain a thermo cline. It is important that the water distribution system in the tank be carefully designed so as to create thermal stratification. Methods of analysis and design of inlet and outlet diffusers are difficult because of the complex nature of the characteristics of the inlet and outlet water (64). The diffusers need to be properly designed so as to maintain uniform velocities and reduce any disturbing factors. If the total opening area in any diffuser branch is half the cross sectional area of the branch pipe,

then a uniform static pressure and thus uniform discharge velocity can be achieved. (64). Use of manifolds can also help achieve storage tank stratification without requiring modifications in system operation.

### 3.11.2 System sizing

Storage tank system sizing involves the following tasks:

- i. *Design load analysis*: this determines the design loads for a storage tank system and involves calculation of the buildings cooling load profile. It also includes determination of the design day conditions, peak cooling load and charging and discharging cycles.
- ii. *Determination for system temperature differentials*: these are determined by the chiller output temperature and the discharge segments of the cycle.
- iii. *Allowances for thermal losses and pumping energy*: the thermal losses have to be calculated and apportioned to both the charge and discharge segments of the cycle.
- iv. *Sizing of the system components for full storage*: in the full storage mode, the entire on-peak load would be serviced directly by the storage without contribution from the chiller.

### 3.11.3 Storage Tank Modeling

The modeling of thermal stratification in storage tanks is an important issue for the design and optimization of storage tanks in solar thermal systems (63). Accurate modeling of water storage tanks requires an accounting of the stratification within such storage tanks; overall system performance is significantly affected by the storage temperature distribution (65). There are two main models that have been developed namely the multimode and plug flow models (66). Kleinbach, (66) showed that the plug flow method tends to over predict the thermal performance. In this project the multi node model will be used.

#### 3.11.3.1 Multinode Model

These are simple and are suitable for implementation into overall energy system simulation programs which allow long term studies (62). A storage tank of diameter,  $D$  and length,  $L$  is modeled and divided

into  $N$  nodes (sections) in the longitudinal direction with energy balances written for each node. This results in a set of  $N$ , differential equations that can be solved to get the time distribution of temperature for each. The degree of stratification depends on tank design, size, location and design of inlets and outlets, flow rates of entering and leaving streams.

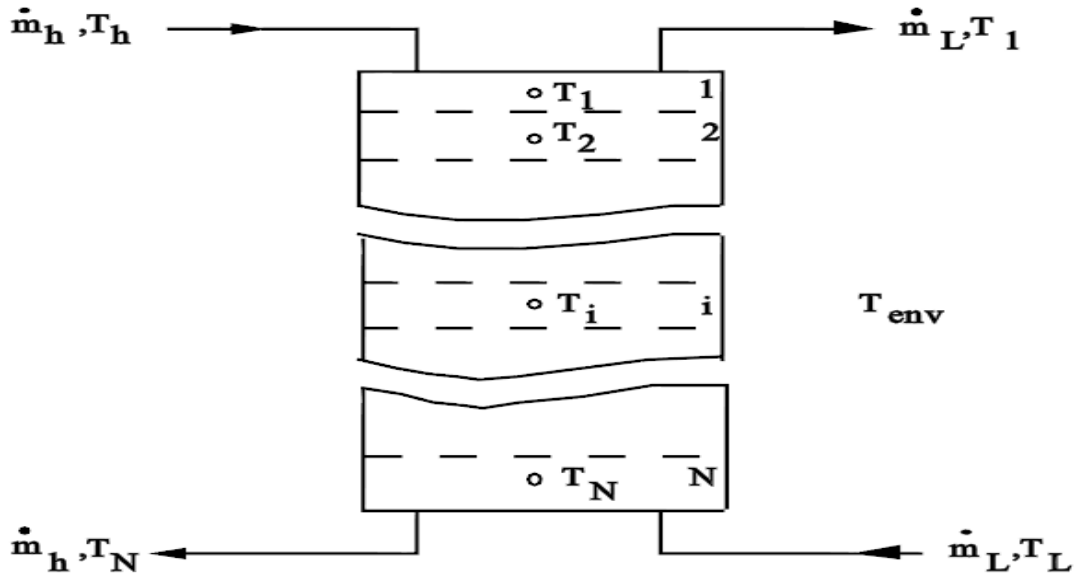


**Figure 3.12: Stratified Fluid Storage Tank (50)**

A collector control function  $F_i^c$  can be defined to determine which node receives water from the collector (51). This is defined as:

$$F_i^c = \begin{cases} 1 & \text{if } i = 1 \text{ and } T_{co} > T_i \\ 1 & \text{if } T_{i-1} > T_{co} > T_i \\ 0 & \text{if } i = 0 \text{ or } i = N + 1 \\ 0 & \text{if otherwise} \end{cases} \quad (3.44)$$

Where:

$T_i$  = Fluid temperature of node  $i$

NB: If the collector is operating only one control function can be non-zero.

The liquid returning from the load can be controlled in a similar manner with a load control function,  $F_i^L$ :

$$F_i^L = \begin{cases} 1 & \text{if } i = N \text{ and } T_{Lr} < T_N \\ 1 & \text{if } T_i \geq T_{Lr} > T_i \\ 0 & \text{if } i = 0 \text{ or } i = N + 1 \\ 0 & \text{if otherwise} \end{cases} \quad (3.45)$$

Return is always to a node closest but lower than the collector/load return temperature. The net flow between nodes is upwards or downwards and depends on values of the collector and load flow rates and the two control functions. We can conveniently define a mixed-flow rate,  $\dot{m}_{m,i}$  that represents the net flow into node  $i$  from node  $i-1$  excluding the effects of flow, if any directly into the node from the load.

This mixed flow rate is given as:

$$\dot{m}_{m,1} = 0 \quad (3.46)$$

$$\dot{m}_{m,i} = \dot{m}_c \sum_{j=1}^{i-1} F_j^c - \dot{m}_L \sum_{j=i+1}^N F_j^L \quad (3.47)$$

$$\dot{m}_{m,N+1} = 0 \quad (3.48)$$

With these control functions energy balance on node  $i$  can be expressed as:

$$\begin{aligned} \dot{m}_i \frac{dT_{s,i}}{dt} = & \left( \frac{UA}{C_p} \right)_i (T_a - T_{s,i}) + F_i^c \dot{m}_c (T_{co} - T_{s,i}) + F_i^L \dot{m}_L (T_{Lr} - T_{s,i}) \\ & + \begin{cases} \dot{m}_{m,i} (T_{s,i-1} - T_{s,i}) & \text{if } \dot{m}_{m,i} > 0 \\ \dot{m}_{m,i+1} (T_{s,i} - T_{s,i+1}) & \text{if } \dot{m}_{m,i+1} < 0 \end{cases} \end{aligned} \quad (3.49)$$

In order to maintain the stability of the system, the chosen number of nodes must not be too many, as the water flowing in the storage tank (either load flow or collector flow) in a given time must not exceed the amount of water occupied in each node (65). Kleinbach (66), has suggested that 15 may be chosen as the maximum number of nodes for the multi-node approach. Also, the number of nodes cannot be too low as it would under predict the output of the system by nearly 10%. The main governing parameters in limiting the maximum number of nodes are the flow rates (collector flow and load flow), volume of storage tank and the time step. The collector flow rate plays a more significant role in deciding the number of nodes compared to load flow. High collector flow rates tend to decline the thermocline, thus affecting system performance. Li and Sumathy (65) showed that system COP is low with increase in tank volume but if tank volume is too small then with increase in collector area system COP decreases sharply beyond a certain point. This is due to:

- i. By using a small volume, the system can't effect solar cooling at night hence effective operation period is reduced.
- ii. A small tank volume results in a higher bulk temperature in the tank, which increases heat loss and reduces collector efficiency.
- iii. A too small volume of tank might not be able to balance the fluctuation of solar radiation, which will result in frequent on/off cycling of the chiller and consequently greater heat loss during the transitional period of stable operation.

The design and optimum sizing of the storage tank should be done, so that the tank can balance the solar radiation and also provide enough thermal energy to drive the chiller when no solar radiation is available. It is recommended to keep the number of nodes between four and fifteen. Three or four nodes may represent a reasonable compromise between conservative design (for which  $n = 1$ ) and the limiting situation of carefully maintained high degrees of stratification (51). A stratified tank with partitioned mode and with 4 nodes is recommended for solar air-conditioning systems and it is preferred that the upper part be restricted to a quarter of the entire volume (65). The partitioning is achieved by placing two baffle plates horizontally in the upper part of the tank. In the morning the tank will operate with the upper part of the tank, while in the afternoon, the whole tank will be used. The two plates are perforated, so that in the whole tank mode, the collector return-flow in between the plates can locate at a position with the temperature close to its own.

### 3.12 Pebble Bed Storage

This uses the heat capacity of a bed of loosely packed particulate material to store energy. An appropriate heat transfer fluid is used to add or remove energy from the bed. In operation, hot air from solar collectors flows through the bed in order to transfer heat energy to the storage material elements. Flow is maintained through the bed in one direction during addition of heat and in the opposite direction during the extraction of heat. Simultaneous heat addition and removal is impossible. Packed beds represent the most suitable storage units for air-based solar systems (55). The high heat transfer coefficient between the air and solid causes quick heat transfer from the air to solid.

Optimum system sizing is based on system parameters and operating conditions. A well-designed packed bed storage system has a high heat transfer coefficient between the air and solid so as to promote thermal stratification, low storage material costs and low bed conductivity when there is no air flow. So, the sizing of a packed bed storage system should be done according to the amount of energy to be stored at the required temperature. The size of the bed should be fixed in such a way that the bed absorbs

maximum amount of energy delivered by the flowing air during the charging phase and mean temperature of the bed at the end of the charging should become nearly equal to the inlet air temperature.

A major advantage of a pebble bed is its high degree of thermal stratification. In solar heating systems, a packed bed does not normally operate with constant inlet temperature. The variable solar radiation, ambient temperature, load requirements and collector inlet temperature result in a variable collector outlet temperature during the day. The pebble bed storage system can be modeled after making the following assumptions i.e. one dimensional plug flow, no axial conduction or dispersion, constant properties, no mass transfer, no heat loss to the environment and no temperature gradients within the solid particles. The differential equations that describe the fluid and rock temperatures are given as (51):

$$\rho_r C_r \frac{\partial T_r}{\partial t} = h_v (T - T_r) \quad (3.50)$$

$$\frac{\partial T}{\partial (X/L)} = \varepsilon(T_r - T) - \left( \frac{UPL}{\dot{m}C_p} \right) (T - T_{env}) \quad (3.51)$$

Where:

$T_r$  Rock temperature

$T$  Air temperature

$T_{env}$  Temperature of surroundings

$t$  Time

$U$  Loss coefficient from bed to surroundings

$P$  Perimeter of bed

$L$  Length of rock bed in flow direction

$\dot{m}$  Air mass flow rate

$C_p$  Specific heat capacity of air

$h_v$  Volumetric heat transfer coefficient between air and rock

$V$  Volume of the rock bed

$C_r$  Specific heat of rock

$\varepsilon$  NTU of rock bed

In equations (3.50):

$$\varepsilon = \frac{h_v V}{\dot{m} C_p} \quad (3.52)$$

## CHAPTER 4

### 4 DESIGN OF ABSORTION COOLING SYSTEMS

#### 4.1 Overview

This chapter presents various possible configurations for solar powered absorption cooling systems. Their operational characteristics and drawbacks are described in detail. The solar absorption cooling system is made up of many components and for one to carry out an adequate system analysis; use of simulation software is required. Solar simulation softwares are discussed and TRNSYS is described in detail. Also, a method of system economic analysis is presented.

#### 4.2 Design of Solar Absorption Cooling Systems

In normal practice, a solar cooling system usually replaces or integrates a conventional one (45). An investor that chooses this kind of system has high expectations for energy savings and economic convenience. As a result, a proper design method has to address these expectations. A solar cooling plant is a combination of different components. Broad varieties of feasible configurations for a solar cooling plant are available and are discussed here. The configurations of the solar cooling systems differ from one another depending on whether hot or cold storage or both are used, the presence of an auxiliary boiler etc. The thermal power needed is supplied by the solar collector array, the thermal energy storage tank or the auxiliary boiler. Also, there should be a mechanism for removing the heat of condensation and absorption from the chiller and this is normally done by a wet or dry cooling tower.

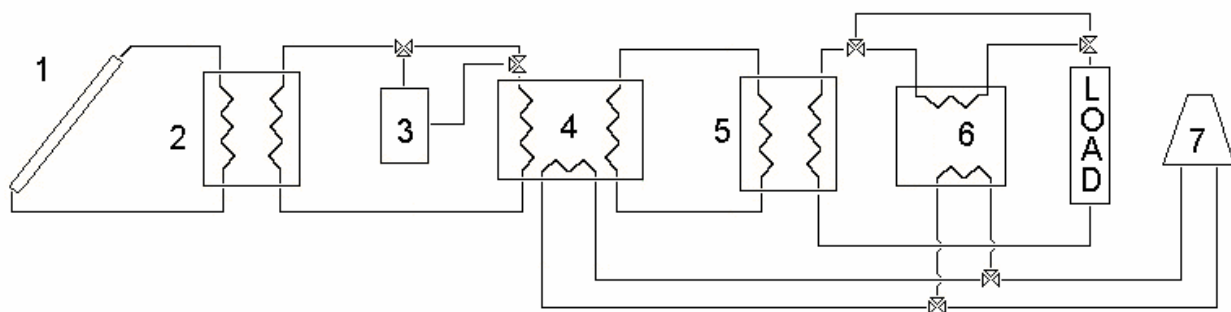


**Figure 4.1: Solar absorption cooling system: 1=collector array; 2=hot storage; 3=auxiliary boiler; 4=absorption chiller; 5=cold storage; 6=compression chiller; 7=cooling tower (45)**



#### 4.2.1 Solar Cooling System without storage

The simplest system is one where the absorption chiller is directly coupled to the collector array. It is made of the collector array, chiller and cooling tower (1+4+7) as indicated in Figure 4.1. This direct coupling, results in higher generator temperatures in the morning, and thus higher heat input to the generator and consequently the cooling process begins much earlier. The collector inlet temperature increases and higher losses are experienced (52). Low heat is available to the generator later in the day and none at night. In this case, the absorption chiller has to be sized to satisfy the peak demand and the solar collector array must be oversized so that it is able to provide the generator driving heat during periods of low radiation. This system is economically and energetically inefficient since for long periods heat is wasted.

#### 4.2.2 Solar Cooling System with Hot Storage

In this configuration a hot storage tank is added and this is placed after the collector array and before the absorption chiller as shown by (1+2+4+7) in Figure 4.1. The hot storage tank takes care of the intermittent behavior of solar energy by storing excess solar heat, which is then utilized if the available solar heat is not sufficient. The storage capacity must be evaluated by matching the thermal power produced by the collectors and the chiller. This arrangement also reduces the need for auxiliary heating device (67). The cooling process begins late because the storage has to be heated to acceptable temperature levels first before it is able to drive the absorption chiller. There are lower collector heat losses due to lower collector inlet temperatures and the collector array area is also reduced. A significant reduction in the collector area can be achieved by the introduction of an auxiliary boiler connected in parallel with collector array (1+2+3+4+7) in Figure 4.1. A percentage of the energy needs of the chiller will be supplied by the auxiliary burner. In this project, due to the high levels of solar heat available, it was deemed unnecessary to utilize an auxiliary burner. The availability of stored heat allows for extended cooling hours since the process is now decoupled from solar radiation availability.

#### 4.2.3 Solar Cooling System with Cold Storage

Another possible configuration is one, in which the cold water produced by the chiller is stored in a cold storage tank as indicated by (1+4+5+7) in Figure 4.1. The cold storage tank allows the storage of excess cooling storage potential and is utilized if the available cold production of the chiller is insufficient to

satisfy the cooling load. This allows a slight a slight reduction in the absorption chiller capacity because the peak of the cooling demand could be satisfied by the cold storage (45). The temperature difference between the storage temperature and the ambient, results in this configuration experiencing lower losses than the one that uses a hot water storage tank. Care must be taken when designing adequate storage volume because high volumes of cold storage will prevent the cooling energy produced from reaching the load effectively (67).

### 4.3 Solar Cooling System with both Hot and Cold Storage

This configuration is mainly used in large facilities where large energy densities have to be stored and the problem of space is not important (68). This configuration represented by (1+2+4+5+7) in Figure 4.1 experiences the greatest amount of heat loss because of all the elements introduced and the consequent loss of useful heat. With proper design, a facility utilizing this configuration can continue producing cold at late hours of the afternoon. Every solar cooling system is either operated autonomously or in conjunction with a traditional vapor compression system. The integration of an absorption chiller to the conventional system i.e. (1+4+5+6+7) in Figure 4.1 has the advantage that any load not covered by solar energy is met by the compression chiller, avoiding the use of a back up burner.

Solar powered absorption cooling has the potential for primary energy savings but the economic convenience is not guaranteed. For a solar cooling system to work efficiently, the solar collection section as well as the thermal storage must be carefully designed. Properly sizing the hot and cold storages optimizes the performance of the solar collector and reduces the absorption chiller capacity. The chiller is the most costly item of the plant. The initial investment might be too high to be repaid within the life cycle of the system (52). A proper design method has to deal with that otherwise the spread of this technology will remain limited. In this project, the design approach was of the simulation- optimization type. Several simulations of the system will be carried out changing the main design variables until an optimum value of the objective function is found. The objective function in this project is to maximize primary energy savings whilst minimizing life cycle costs of the system.

Although the components of solar energy systems are commercially available, the arrangement of the entire system requires special attention in the design, sizing of components and control strategy. The sizing of solar cooling systems is complex and involves unpredictable components such as weather data and predictable ones like the solar collector. The proper sizing of the components of a solar system is a complex problem which includes both predictable (collector and other components performance characteristics) and unpredictable (weather data) components (54). The design process involves making a

number of crucial decisions regarding the operation of the system e.g. whether to incorporate a backup system or have a solar autonomous system, and whether to allow flexibility in the comfort conditions. The first step is to come up with mathematical models i.e. assumptions, equations and data which characterize the performance of all discrete system components. In general the component models will include mass, momentum and energy balance equations, thermo-physical property functions and appropriate heat transfer relationships. These mathematical model relationships and numerical solution method will be implemented into a computer based design tool which will predict the operating cycle and related information of interest like cooling capacity, COP, primary energy consumption, flow rate etc. One can proceed to investigate equipment trade-offs and identify alternative workable designs, allowing secondary factors such as equipment costs or COP to be used in making a final selection of design parameters. If the models have sufficient detail, the number of parameters available to the designer also increases and this allows effects that are normally overlooked to be studied. Computer modeling and simulation of solar thermal systems presents the following advantages:

- i. Elimination of the expenses involved in prototype building..
- ii. Provision of in-depth understanding of the fundamental technical details and relationships important to the performance of the system.
- iii. Arrangement of complex systems in a format that is easily understandable allowing identification of critical processes for which more or better technical information is needed thus helping to define research needs and priorities.
- iv. Optimization of the system components is also achieved through consideration of more alternatives and enables the off-design performance to be investigated prior to actually building the unit.
- v. Estimation of the amount of energy that the system delivers.
- vi. Provision system temperature variables.
- vii. The use of the same weather data allows the effects of system design variable changes to be estimated.

Over the years the following softwares have been developed for the simulation of solar thermal systems: Watson, TRNSYS, Polysun\*Sol and  $f$ -Chart. Drury et al (69) carried out comparative studies of the various solar simulation softwares. TRNSYS was found to be by far the most comprehensive, accurate, capable and flexible design software around. As a matter of fact, the other design tools namely Polysun and T\*Sol present validation results against TRNSYS. As a result, this investigation will be carried out using TRNSYS as a simulation tool.

### 4.3.1 TRNSYS Simulation Software

This is simulation software for the analysis of thermal energy systems developed at the University of Wisconsin, Madison. Users are provided with the source code of the kernel and component models, allowing for rapid prototyping and customization of components and entire systems. In recent years, TRNSYS has become the most reliable modeling and simulation program oriented towards solar applications used by researchers (52). It has an open and modular structure that consists of many subroutines that model system components and also allows one to create components that are not included in the standard package. TRNSYS provides flexibility in solar designs and can be used to analyze combination of different energy systems. TRNSYS maintains weather generators that use real weather data from meteorological stations throughout the world for its calculations. This makes TRNSYS useful for places where solar facilities are to be simulated, designed and constructed but there is no available reliable experimental data, since the weather generators allow easily changing the facility location.

The mathematical models of the components are given in terms of their ordinary differential or algebraic equations. The system components can be in any desired manner thus the TRNSYS simplifies the simulation process to an exercise of identifying all system components. The mathematical descriptions of these components are then carried out and information flow is easily identified. The next step is the construction of a system information flow diagram. This flow diagram is used to construct a deck file that contains information about all system components, output format and the weather data.

### 4.4 Economic Analysis

From an economic point of view, the challenge is to come up with a system that costs as little as possible. The economic problem is reduced to comparing projected future operating costs and a known initial investment due to the fact that solar energy systems have initial costs with very little operating costs. The costs of a solar energy system are broken down into two main categories: investments (costs and delivery costs, construction and installation costs of collectors, storage unit, pumps, and fans and controllers, chillers etc) and operating costs including costs of operation of pumps and fans, interest on loans if system was constructed using borrowed funds, insurance etc. Careful design can minimize the cost of operating the pumps. System performance is much more sensitive to collector area variation than any

other parameter (51) and as a result the economic problem is reduced to solar system size determination, with all other parameters approximately fixed in relationship to the collector array area.

To measure economic performance we use the total cost of the cooling system. We will make use of the annuity method. In this method, the time value of money is accounted for by calculating the net present value (NPV) which is a series of incoming and outgoing cash flows that are discounted to the time that they were either incurred or received. This is done using the rate of inflation and the basic interest rate (70). The capital value (CV) is given as:

$$CV = \sum P(t) \frac{(1+f)^t}{(1+d)^t} \quad (4.1)$$

Where:

$CV$  Capital value  
 $P(t)$  Investment at time  $t$   
 $t$  Time  
 $d$  Basic interest rate  
 $f$  Inflation rate

If we multiply the future operating costs of the system by the present value factor(PVF) we discount these costs to the present value. The PVF is given by the following equation:

$$PVF(N, f, d) = \frac{1+f}{d-f} \left[ 1 - \left( \frac{(1+f)}{(1+d)} \right)^N \right] \quad (4.2)$$

Where:

$PVF(N, f, d)$  The present value factor  
 $N$  Life time of the plant

Since solar air conditioning systems don't generate any annual income (70), by simply summing the discounted investment costs and operating expenses we get the NPV. It is here defined with a positive sign to obtain annuity values:

$$NPV = CV + EX.PVF(N, f, d) \quad (4.3)$$

Where:

$EX$  Annual expenses

Included in the annual costs are maintenance costs and the costs for energy and water.

To obtain the annuity, we multiply the NPV by a recovery factor, which is a function of the discount rate and the life time of the plant.

$$a = NPV \cdot r_f(N, d) \quad (4.4)$$

Where:

$r_f$  Recovery factor and is given as:

$$r_f = \frac{d(1 + d)^N}{(1 + d)^N - 1} \quad (4.5)$$

The cost per kWh of cooling energy produced is the ratio of the annuity divided by the annual cooling energy produced (70). The economic analysis will be carried out for the Vodacom System; there is no accurate cost data available for the Moot Hospital System.

## CHAPTER FIVE

### 5 CASE STUDIES: SYSTEMS DESCRIPTION

#### 5.1 Case Studies: Systems Description

A typical solar powered absorption cooling system is made up of the absorption chiller and four additional sub-systems: heat medium production, cold medium production, heat rejection, and load (71). The following sections describe the various system components selected for the solar absorption cooling system. In this chapter, the two case studies i.e. Netcare Moot Hospital and Vodacom World solar powered cooling systems are described in detail. This includes a comprehensive description of each sub-system and all its components. The control strategies for these sub-systems and components of the solar cooling systems are also described.

#### 5.2 Absorption Chiller

The Yazaki WFC-SC10, 35kW chiller with a LiBr-water working pair was used for both the Netcare Moot Hospital and The Vodacom World installations. The chiller's performance characteristics are given in Fig 5.1 below.

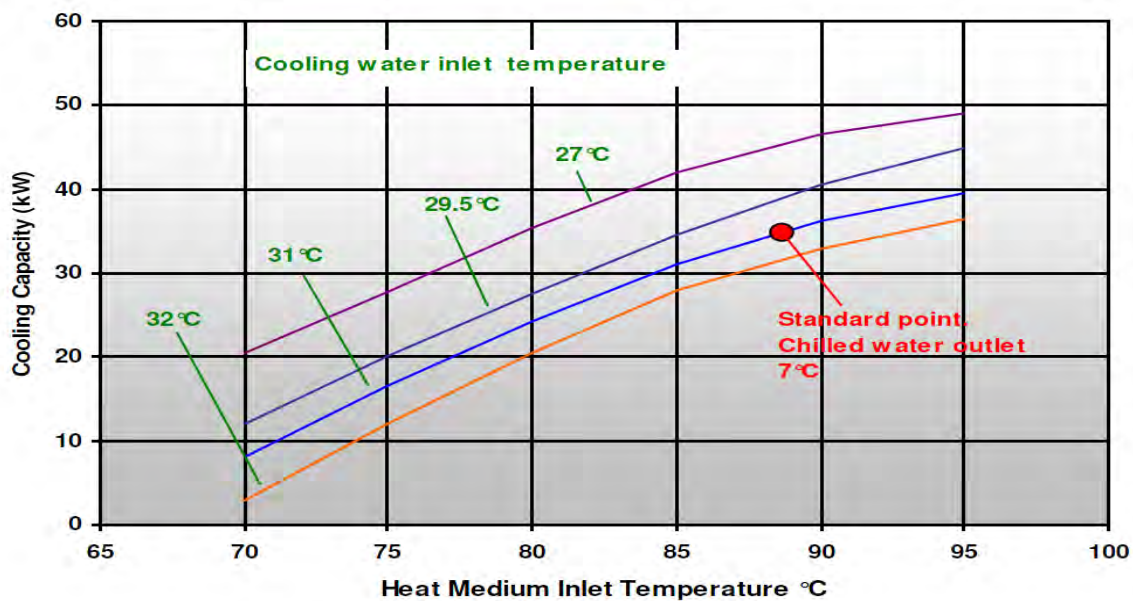


Figure 5.1: Yazaki WFC-SC10 chiller performance characteristics (72)

The chiller used in these case studies has a nominal capacity of 35kW, with the specifications given in Table 5.1. The absorption cycle is driven by hot water at 70-95°C. Cooling of the condenser and absorber is achieved through use of a cooling tower. Crystallization is prevented in the generator by utilizing a solution pump and gravity drain-back system. The chilled and hot water outlet temperature control is carried out by a microprocessor that controls a 3-way valve and a separately supplied hot water temperature supply pump. If the hot water supply temperature exceeds 95°C the chiller will shut down and require manual reset.

**Table 5.1: Yazaki WFC-SC10 Absorption Chiller Specifications**

<b>Generator:</b>	
Inlet Temperature	88°C
Outlet Temperature	83°C
Flow Rate	1.52l/s
<b>Condenser and Absorber:</b>	
Inlet Temperature	31°C
Outlet Temperature	35°C
Flow Rate	5.11/s
<b>Evaporator:</b>	
Inlet Temperature	12.5°C
Outlet Temperature	7°C
Flow Rate	2.4l/s
<b>Electrical Energy Consumption</b>	210W



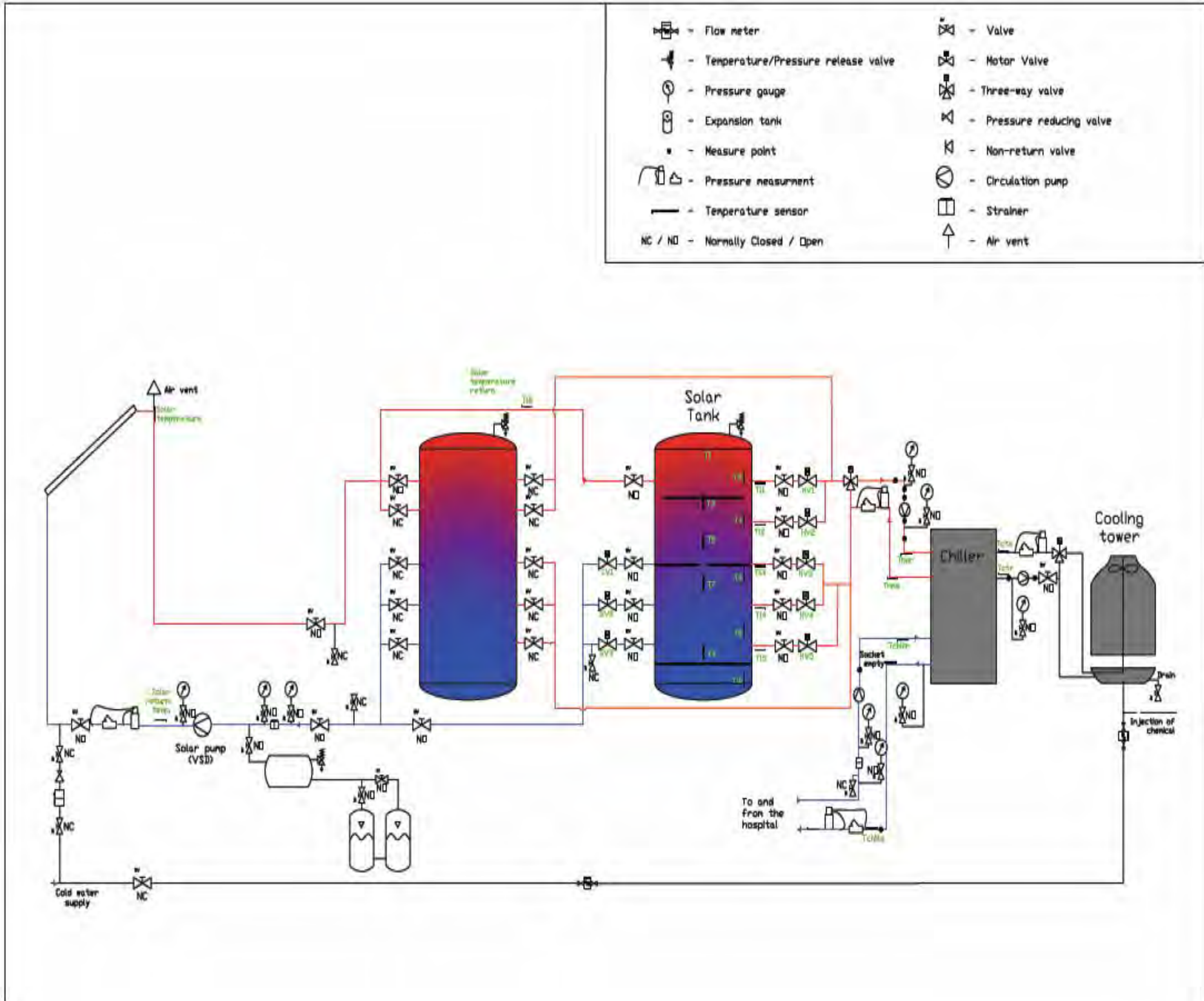


**Figure 5.2: Photograph of the Yazaki WFC-SC10 Absorption Chiller at Netcare Moot Hospital, Pretoria: on left are the two storage tanks and the chiller is on the right**

### **5.3 Moot Hospital**

The first case study is the system installed on the roof of Netcare Moot Hospital in Pretoria. This initiative was as a result of a partnership between Netcare and Voltas Technologies. Netcare provided the roof space and the opportunity to install and operate the solar powered absorption system in parallel with the existing conventional air-conditioning plant in October 2009. The main purpose of this system was to demonstrate the economics and operating characteristics of solar absorption cooling systems for South African weather conditions and define a new way of cooling buildings in southern Africa. The system consists of 52 evacuated tube collectors (ETCs), two hot water storage tanks with a volume of 6000litres each, 35kW Yazaki absorption chiller shown in Figure 5.2, open cooling tower, Carel BMS system to monitor and record the systems performance data. The complete system layout is shown in Figure 5.3.

Figure 5.3: Schematic of the Moot Hospital System Courtesy of Voltas Technologies



### 5.3.1 Solar Collector Array

The solar collector array is responsible for the collection of solar energy and the production of the hot water that drives the absorption chiller. It is made up of 52 HUI 16/2.1 evacuated tube collectors manufactured by Himin Solar Energy Group Co., Ltd arranged in a well balanced parallel flow. They are connected in rows of 8 collectors in series with a tilt angle of 30° facing North as shown in Figure 5.4.



**Figure 5.4: Photograph of the arrangement of the Solar Collector Array**

The parameters for the HUI 16/2.1 evacuated tube collectors (ETCs) are shown in Table 5.2 below.

**Table 5.2: HUI 16/2.1 Solar collector parameters**

Parameter	Value
Intercept efficiency	0.779
First order efficiency coefficient	2.103W/m <sup>2</sup> .K
Second order efficiency coefficient	0.0107W/m <sup>2</sup> .K <sup>2</sup>
Aperture Area	1.764m <sup>2</sup>

### 5.3.2 Thermal Energy Storage

The system was installed with two hot water storage tanks with a volume of 6000 litres each to store the excess energy collected during periods of high solar irradiation. It was initially envisaged that one of the tanks would contain phase change material for use as thermal energy storage but due to financial constraints this idea was abandoned and only one of the 6000litre tanks was activated in the end. In addition to the hot water storage tanks, there is also a 1500litre cold water storage tank that stores the excess chilled water that is produced by the system. This tank is also used to store the chilled water that is produced by the existing vapor compression chiller. The system has three pumps namely; the heat medium pump, chilled water pump and the cooling tower pump. All the pumps are started when the solar powered absorption chiller requires them to do so. The pumps all have variable speed drive (VSD) control.



**Figure 5.5: Photograph of the two hot water storage tanks**

### 5.3.3 Control Strategy

The control strategy of any solar powered absorption cooling system plays an important role in determining the amount of electricity that is saved and the amount of cooling energy that is made available. An adequate control scheme will maximize temperatures entering the hot water storage tank and the absorption chiller generator, leading to a better performance of the system [57]. The main

components that are controlled are the solar valves and pumps, the hot water valves, the chillers (absorption and existing compression), cooling tower fan and cooling tower valve as shown in Figure 5.6.

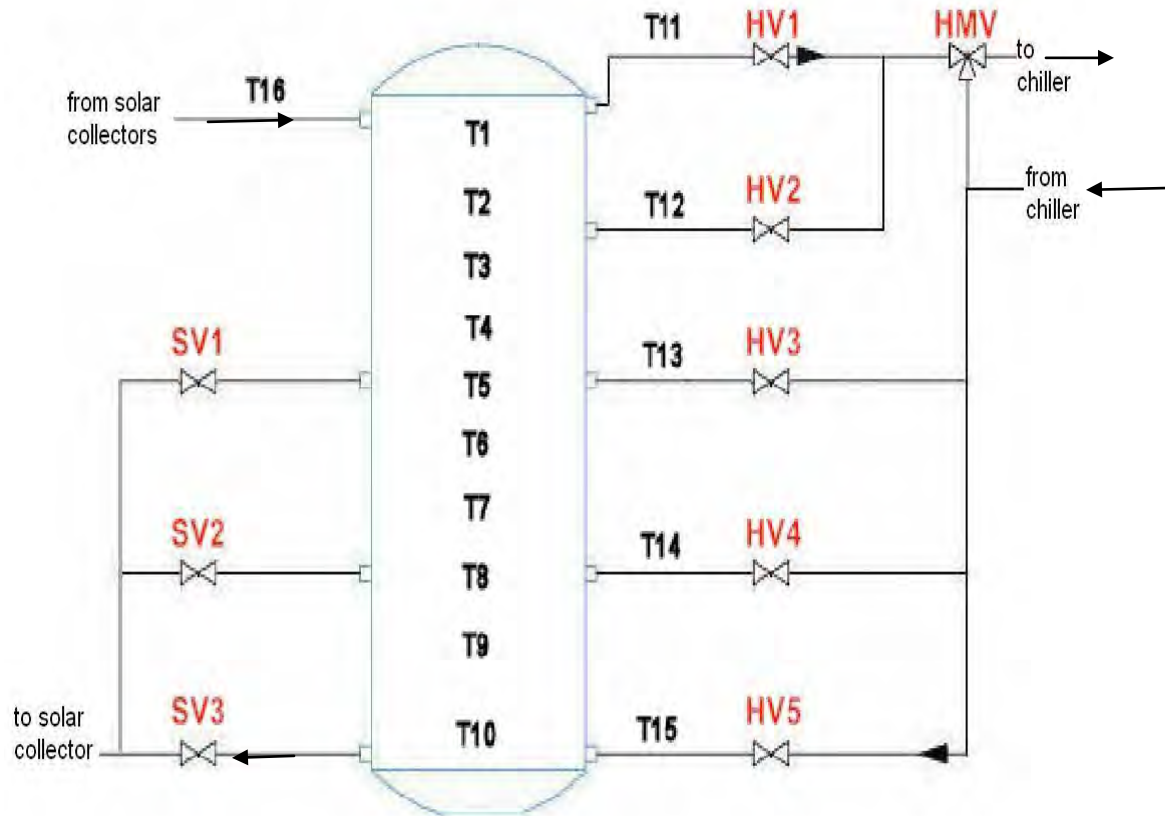


**Figure 5.6: Moot Hospital Control Strategy. Courtesy of Voltas Technologies**

In Figure 5.6 the abbreviations used are:

*T1 - T16* Water temperatures in, coming in and out of the hot water storage tank.

*SV1 – SV3* Valves (solar valves) that release water going to the solar collectors

*HV1-HV5* Valves (hot water valves) that receive hot water coming from the chiller to the storage tank

*HMV* The hot water 3-way valve that controls the hot water temperature going to the chiller

### 5.3.3.1 Solar Valves and Pump

If the solar return temperature,  $T_{16}$  in Figure 5.6, is greater or equal to  $85^{\circ}\text{C}$ , then the solar pump will be turned on and runs until the average tank temperature,  $T_{av}$  exceeds  $93^{\circ}\text{C}$ , then it is turned off. The pump is only turned back on again if the average tank temperature becomes less than  $90^{\circ}\text{C}$  as depicted in Figure 5.7.

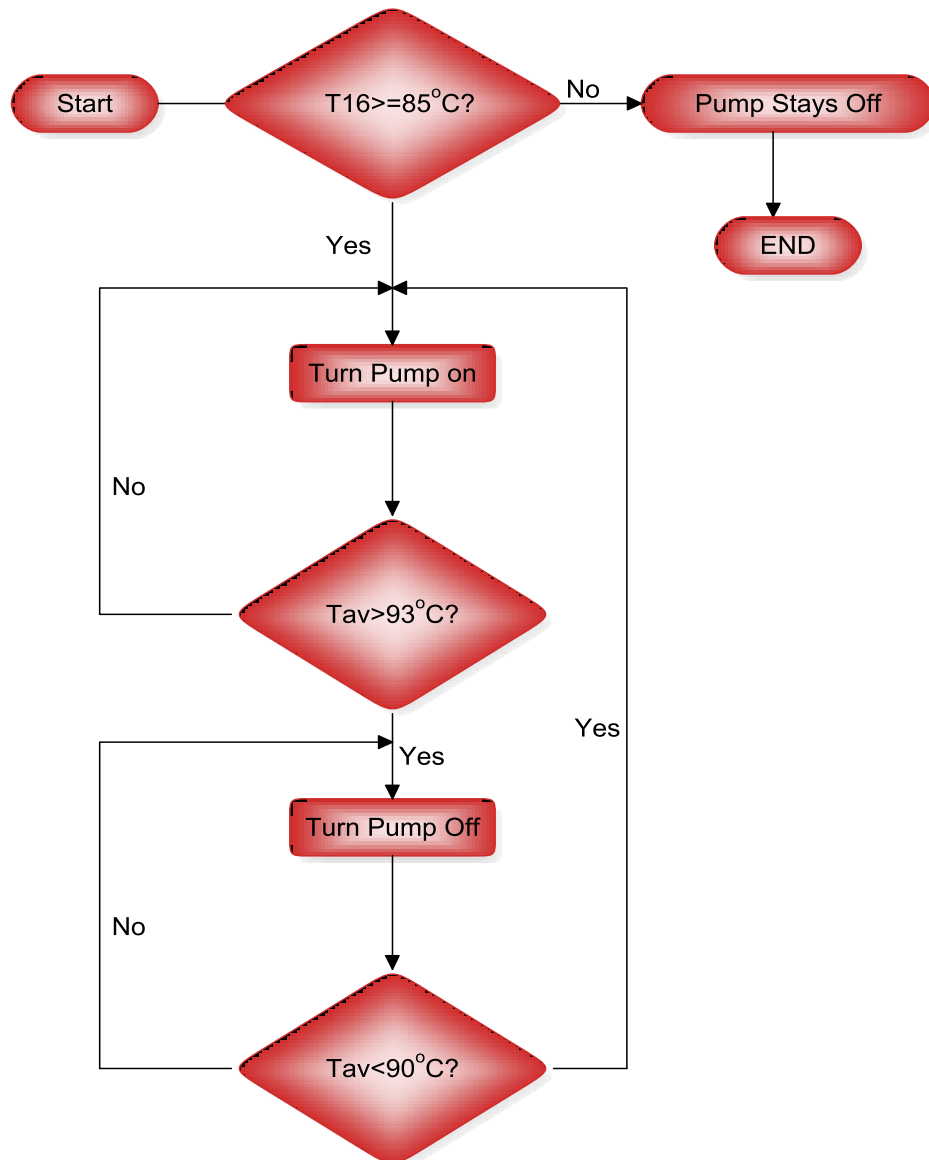


Figure 5.7: Solar Pump Control Logic

The solar valves are controlled in the following manner: The temperature of the water at the solar valves is compared to the solar return temperature and the temperature differentials determine which valve will be opened. The equations for the control logic are presented below.

$$\text{If } \Delta T_1 = (T_{16} - T_{SV1}) > 3^\circ\text{C} \quad (5.1)$$

Then *SV1* opens

$$\text{If } \Delta T_2 = (T_{16} - T_{SV2}) > 3^\circ\text{C} \text{ and } \Delta T_4 = (T_{SV1} - T_{SV2}) > 0^\circ\text{C} \quad (5.2)$$

Then *SV2* opens

$$\text{If } \Delta T_3 = (T_{16} - T_{SV3}) > 3^\circ\text{C} \text{ and } \Delta T_5 = (T_{SV2} - T_{SV3}) > 0^\circ\text{C} \quad (5.3)$$

Then *SV3* opens

### 5.3.3.2 Hot Water Valves

If  $T_1 > 95$  or  $T_2 > 95$ , then the mixing valve (HMV) closes to stop the high water temperature from entering the chiller. The control logic for the rest of the hot water valves is shown in Figure 5.8 and represented by the following equations:

$$\text{If } T_{hmr} \geq T_{13} \quad (5.4)$$

Then *HV3* opens

$$\text{If } T_{hmr} < T_{13} \text{ and } T_{hmr} \geq T_{14} \quad (5.5)$$

Then *HV4* opens

$$\text{If } T_{hmr} < T_{13} \text{ and } T_{hmr} < T_{14} \quad (5.6)$$

Then *HV5* opens

Where:



$T_{hmr}$  Hot Water Return Temperature from the chiller

$HV3, HV4$  and  $HV5$ , are hot water valves

Appropriate temperatures  $T13$  and  $T14$  are indicated in Figure 5.8

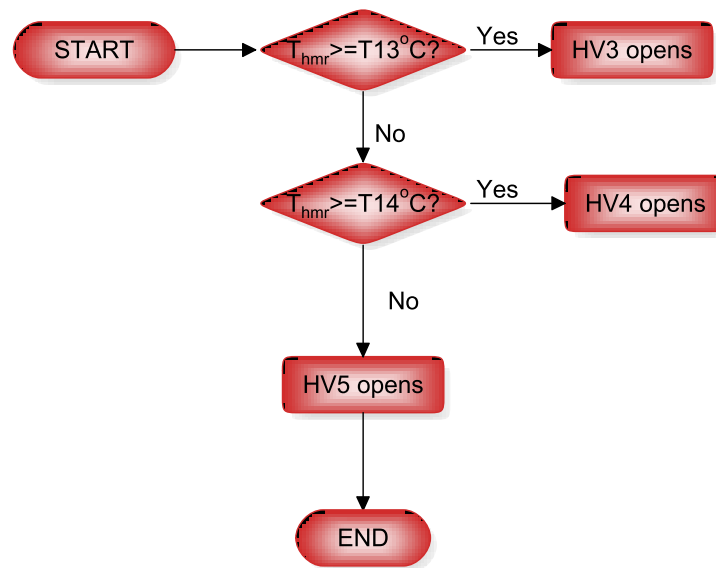


**Figure 5.8: Hot Water Valves Logic**

### 5.3.3.3 Chiller Control

The two chillers i.e. the solar powered absorption and existing compression chiller have time and temperature control systems. The solar chiller has priority over the compression chiller from 9:00-17:00 as shown in Figure 5.9. If the temperatures,  $T1$  or  $T2$  are greater or equal to  $85^{\circ}\text{C}$  the solar chiller will be switched on and operates in conjunction with two compressors of the vapor compression chiller. The two chillers run together in this mode until the chilled water supply temperature falls below  $8^{\circ}\text{C}$ , then one of the compression chiller compressors is switched off. This compressor is only turned back on if the chilled water temperature rises above  $8.3^{\circ}\text{C}$ . The compression chiller is turned off completely allowing for autonomous solar chiller operation when the chiller supply temperature falls below  $6.5^{\circ}\text{C}$ . One of the compression chiller compressors is only switched on when the chilled supply temperature exceeds  $6.8^{\circ}\text{C}$ . The electric chiller has priority between 17:00-7:00. If during this time,  $T1$  is greater than  $93^{\circ}\text{C}$  the solar chiller runs and is only turned off when  $T1$  falls below  $88^{\circ}\text{C}$ .



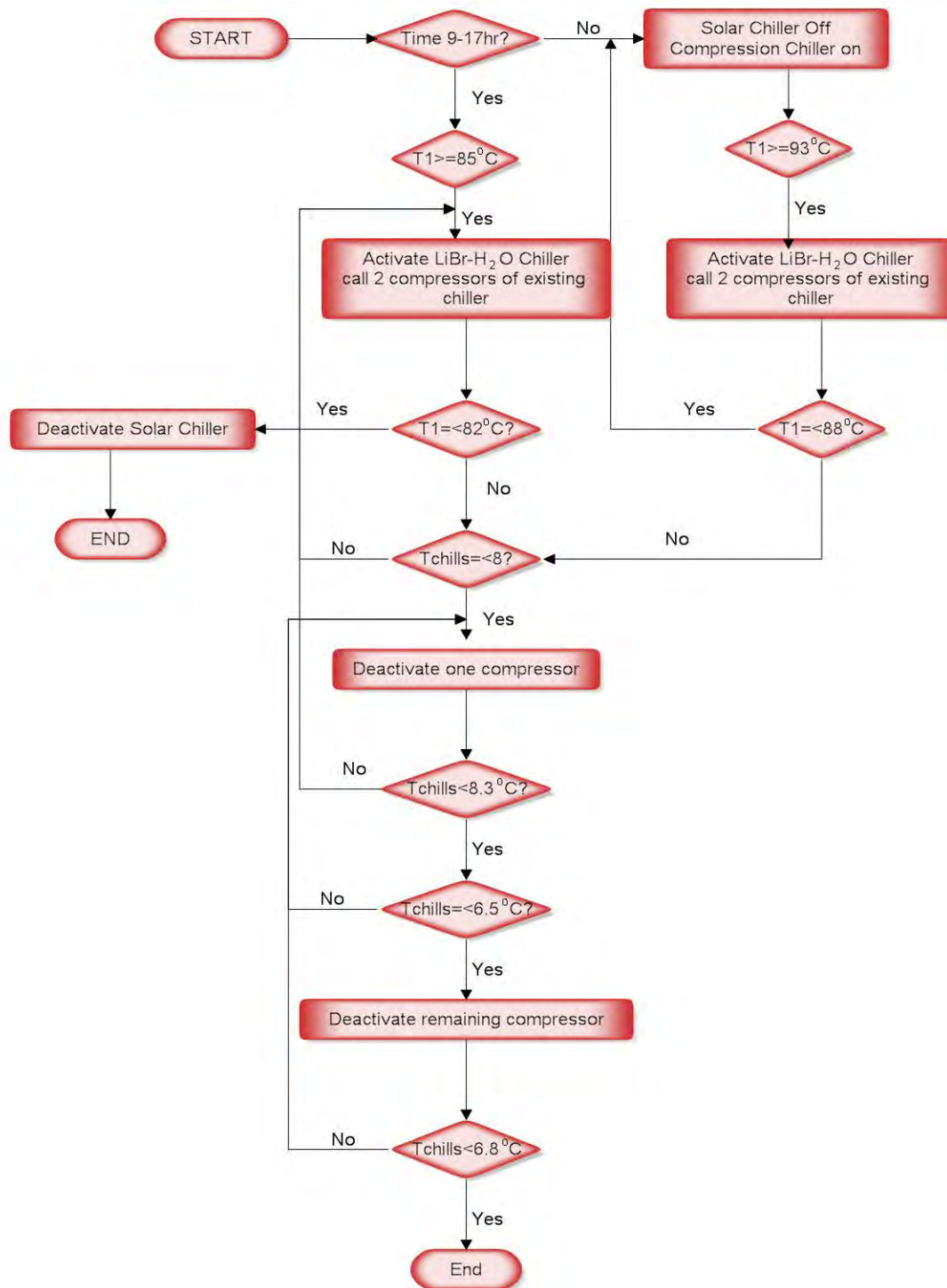


Figure 5.9: Chiller Control Logic

#### 5.3.3.4 Cooling Tower Fan and Cooling Tower Valve

A three way valve is used to bypass the cooling tower, if the cooling tower supply temperature is under 28°C, the valve is closed and the water coming out of the chiller directly goes back into it. At 28°C, the valve starts to open up and fully open at 30°C. The opening of the cooling tower valve can be represented by the following equation:

$$CT = 0.5(T_{CTS} - 28) \quad (5.7)$$

Where:

$CT$  Percentage of cooling tower valve open

$T_{CTS}$  Cooling tower return temperature

Equation 5.7 is valid for the following conditions:  $28^{\circ}\text{C} \leq T_{CTS} \leq 30^{\circ}\text{C}$

In order to improve the cooling of the water, a fan starts when the cooling tower return temperature reaches 31°C and reaches its highest speed when the cooling tower return temperature reaches 33°C.

### 5.4 Vodafone Site Solutions Innovation Center (Vodafone SSIC)

The second case study is the Vodafone Site Solution Innovation Center (SSIC), located at the Vodacom Campus in Midrand and is the first 6 Green Star SA accredited building in South Africa. The Green Building Council of South Africa (GBCSA) defines a green building as a building that is energy and resource efficient and incorporates practices in design, construction and operation that are designed to achieve a significant reduction or elimination of negative impacts on the occupants and the environment. In this building, use is made of two types of solar technologies: a photovoltaic (PV) electricity generation and a solar thermal heating and cooling through a solar absorption system. This study focuses on the solar powered absorption system. This is a solar autonomous thermal heating and cooling system to maintain room temperature at comfort level throughout the year. Two rock storages are located under the building: one pre-cools the supply air to the building so that the cooling load is reduced and the other pre-cool the supply air to the dry cooler at ambient air temperature to facilitate heat rejection.

The maximum cooling demand is around 20kW, the maximum heating load is 22.5kW. The annual cooling load demand is 18.4MWh and the heating demand is 3.2MWh. The system is made up of:

- 116m<sup>2</sup> evacuated tube collector array.

- 6.5m<sup>3</sup> hot water storage.
- Yazaki WFC10 absorption chiller with a dry cooler for heat rejection.
- 1m<sup>3</sup> cold storage tank.

#### 5.4.1 Solar Collector Array

The solar collector array is made up of 116m<sup>2</sup> of Linuo U-pipe collectors horizontally mounted on top of the building as shown in Figure 5.10. There are six parallel sections made of four sections with ten collectors in series and two sections with nine collectors. The collector array flow rate varies from 1740l/hr to 3480l/hr. There are security pressure release valves, air release valves and non return valves to prevent backward flow during the night. The collectors are filled with a solution of 20% glycol and 80% water. The parameters of the collectors are presented in the Table 5.3 below:

**Table 5.3: Linuo LN58/1800-20 U-pipe collector parameters**

Parameter	Value
Intercept efficiency	0.681
First order efficiency coefficient	1.6W/m <sup>2</sup> .K
Second Order efficiency Coefficient	0.006W/m <sup>2</sup> .K <sup>2</sup>
Aperture Area	2.03m <sup>2</sup>



**Figure 5.10: Photo of the Solar Collector Array at Vodafone SSIC**

### 5.4.2 Heat Exchanger

A counter-flow heat exchanger with an overall heat transfer coefficient of 10kW/K is situated between the collector field and the hot water storage tank. It prevents the mixing of the glycol water-mixture in the collectors with the water in the storage tank. It is also included to avoid completely filling the storage tank with anti-freeze mixture which would have increased the investment costs (73).

### 5.4.3 Thermal Energy Storage Tanks

The excess heat energy produced by the collector is stored in a 7000litres partitioned tank with a 1000litre cold water storage tank. The hot water tank is divided into two 3500litre tanks by high density rock wool and has 200mm rock wool insulation. This partitioning enables the tank to operate with the top half in the morning when there is reduced solar irradiation available and consequently allows the system to start operating much earlier in the day. The chilled water storage tank has 50mm thick Armaflex insulation.

### 5.4.4 Air Handling Unit

There is a Viking AH-H-5 air handling unit, with an air supply quantity of 2.5m<sup>3</sup>/s, total cooling capacity of 25kW and a total heating capacity of 27kW at 50% of the design airflow. The Air Handling Unit specifications are presented in Table 5.4:

**Table 5.4: Air Handling Unit Specifications**

	<b>Chilled water Coil</b>	<b>Hot Water Coil</b>
Total Airflow	2.5m <sup>3</sup> /s	2.5m <sup>3</sup> /s
Total Capacity	25kW	27kW@50% airflow
Air On(DB/WB)	26/19°C	4°C
Air side/Water side Pressure drop	61Pa/29.6kPa	5.7Pa/13.56kPa @50% airflow

### 5.4.5 Thermally Active Slab

Concrete Core Tempering also known as Thermally Activated Building Systems (TABS) is a method of introducing heating or cooling into a concrete structure by means of embedding a series of pipes in the concrete floor or cooling slab (74). The cooling energy produced is used to substitute the heating or cooling energy generated by a central air-conditioning system. In this project, a thermally active slab was installed to reduce the cooling loads and building loads that the absorption chiller has to provide. A photograph of the TABS is shown whilst still under construction in Figure 5.11. It consists of 2x9 port manifolds, generating an estimated  $24.3\text{kW/m}^2$  of cooling energy and  $63\text{kW/m}^2$  of heating energy. It is made up of approximately 2 500m of 20x2mm PE-Xa pipes. The TABS lowers the air temperature when the air comes in contact with the cooled slab hence condensation of water vapor takes place on the floor. To solve this problem, the system is integrated with a dehumidification system.



**Figure 5.11: Photograph of the thermally active slab under construction**

### 5.4.6 Rock storage for the building air supply

Fresh air is cooled in a rock store below the building before it is released into the office space through the perimeter floor vents. The rock storage has a width of 3.1m, a height of 1.1m and a depth in the direction of air flow of 1.5m. The pebbles have a minimum size of 80mm, heat capacity of  $840\text{J/kg.K}$  and a bulk density of  $1000\text{kg/m}^3$ . The effective thermal conductivity of the air pebble mixture is  $0.1\text{W/m.K}$ . When



there is cooling demand and free cooling is possible, with an ambient temperature above 21°C and the outlet temperature of the rock storage is 2K below ambient temperature then pre-cooling of air takes place in the rock storage. An airflow of 1250l/s which is half of the design airflow of the Air Handling Unit is used.

The rock storage is regenerated when there is no cooling demand and the outlet temperature from the rock storage is above 18°C so as to prevent excessive regeneration in times of little or no cooling demand. Reduction of electricity consumption is achieved during regeneration by using an airflow rate of 625l/s. The pre-cooling of the building supply air reduces the maximum cooling load from 20.3kW to 19.5kW. The rock storage reaches a maximum cooling of 10.3kW and on average it reduces the cooling load after free cooling by 36%. The relevant rock store cooling outputs are shown in Figure 5.12.

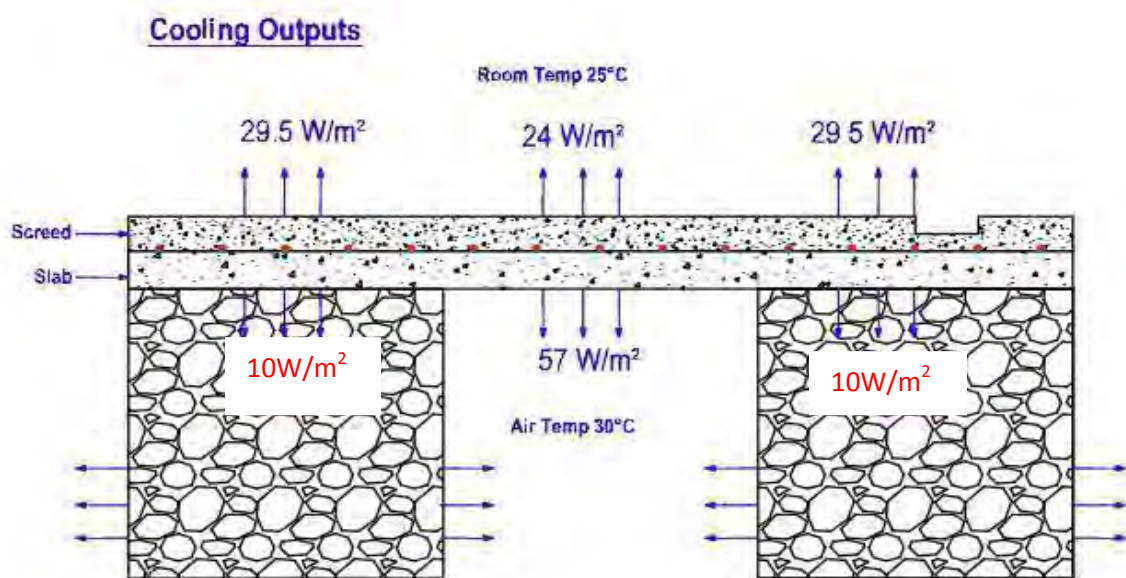


**Figure 5.12: Schematic diagram showing the rock store and the cooling outputs as a result of pre-cooling and the TAS. Courtesy of Voltas Technologies**

#### 5.4.7 Rock storage for the supply air to the dry cooler

This rock storage is activated by motorized dampers to pre-cool the supply air to the dry cooler. It has dimensions of a total width of 33.2m, height of 1.1m and a depth in the direction of flow of 1m. Pre-cooling of air in this rock storage occurs when there is demand for active cooling, the ambient temperature is above 26°C and the temperature of the rock storage is 1K below ambient temperature. Regeneration of the rock storage happens when there is no demand for active cooling and temperature at

the inlet of the rock storage is above 16°C and temperature of the inlet of the rock storage is 4K below ambient temperature. During regeneration, airflow is half of the air flow during operation of the cooling system. The pre-cooling of the supply air to the dry cooler is an efficient measure to reduce the cooling water temperature during hot days. On very hot days, the capacity of the rock storage is not sufficient to provide the necessary pre-cooling. This problem is overcome by use of a temperature controlled motorized damper. A part of the supply air to the dry cooler is cooled in the rock storage whenever the ambient temperature exceeds 28°C; this extends the capacity of the rock storage. One advantage of doing this is that the pressure drop and consequently the electricity consumption of the fan are reduced in comparison to the cooling of the entire supply air.

#### 5.4.8 Dry Cooler

The heat of condensation and absorption is removed from the absorption chiller through use of a dry cooler. The dry cooler is designed to reach temperatures 5K above ambient. The main dry cooler parameters are given in the Table 5.5.

**Table 5.5: Dry cooler parameters**

<b>FLUID</b>	<b>AIR</b>	<b>WATER</b>
Entering Temperature	26.00°C	35.00°C
Exit Temperature	33.68°C	30.91°C
Mass flow	10.92kg/s	5.07kg/s
Volume flow	11.47m <sup>3</sup> /s	5.10l/s
Pressure drop	95.42Pa	39.99kPa
Face velocity	2.58m/s	Heat Rejection: 86.68kW

#### 5.4.9 Vodafone Control System

To ensure efficient operation of the system, a control system focusing on the chiller, pumps, dry cooler and the solar and water valves is implemented. This control strategy is presented here.

### 5.4.9.1 Absorption Chiller

The chiller is enabled throughout the day, but on the following conditions:

- If within time schedule i.e. between 9:00hrs and 17:00hrs and the hot water tank temperature,  $T1 > 80^{\circ}\text{C}$
- If out of schedule and the hot water tank temperature,  $T1 > 93^{\circ}\text{C}$
- If there is no need for cooling the chiller will stop. If the primary chilled water supply temperature is less than  $7^{\circ}\text{C}$  and if the temperature difference between the primary chilled water supply and return temperatures is equal or less than  $1^{\circ}\text{C}$ , then the chiller is deactivated.

The control logic is presented in Figure 5.13.

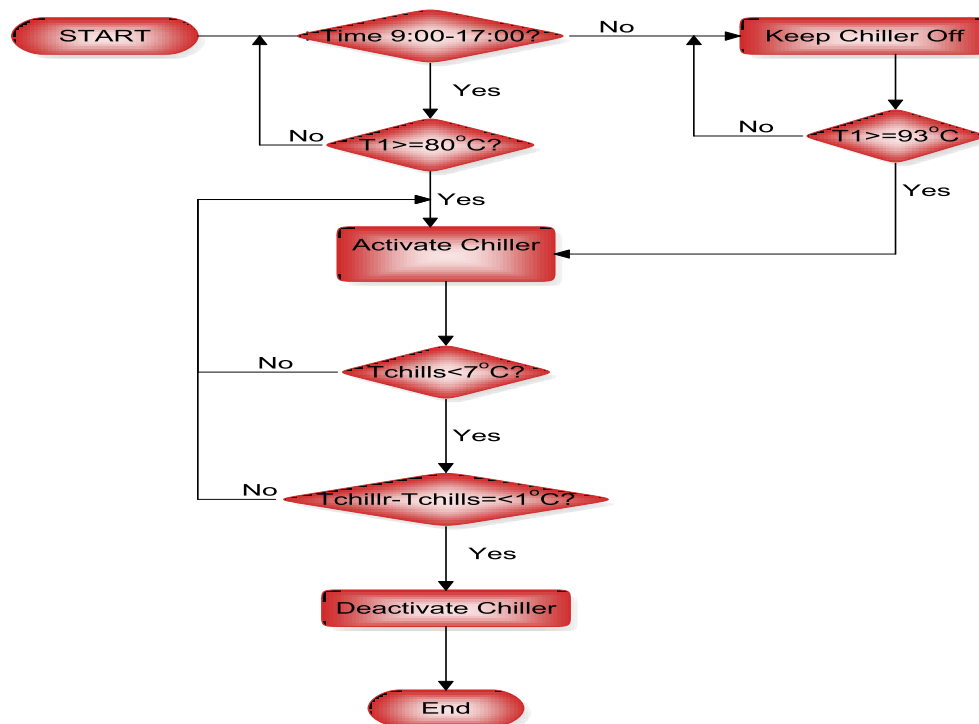


Figure 5.13: Vodafone Absorption Chiller Control Logic



### 5.4.9.2 Solar, Chilled and Hot water Pumps

The solar primary pumps are run in a duty /stand by manner and are only enabled once the average of the solar return temperature ( $T_{SR}$ ) is greater than  $80^{\circ}\text{C}$  and if the solar return temperature is at least  $6^{\circ}\text{C}$  greater than the hot water tank temperature  $T1$ . The pumps are switched off if the temperature difference between the solar return temperature and the hot water temperature  $T1$  is less than  $2^{\circ}\text{C}$ . The primary and secondary solar water pump has a high water temperature shut off mechanism. If at any time the hot water tank temperature  $T1$  is greater than  $96^{\circ}\text{C}$ , then the pumps are turned off. They are only switched back on when  $T1$  falls below  $95^{\circ}\text{C}$ . The control logic for the solar primary water pump control logic is shown in Figure 5.14.

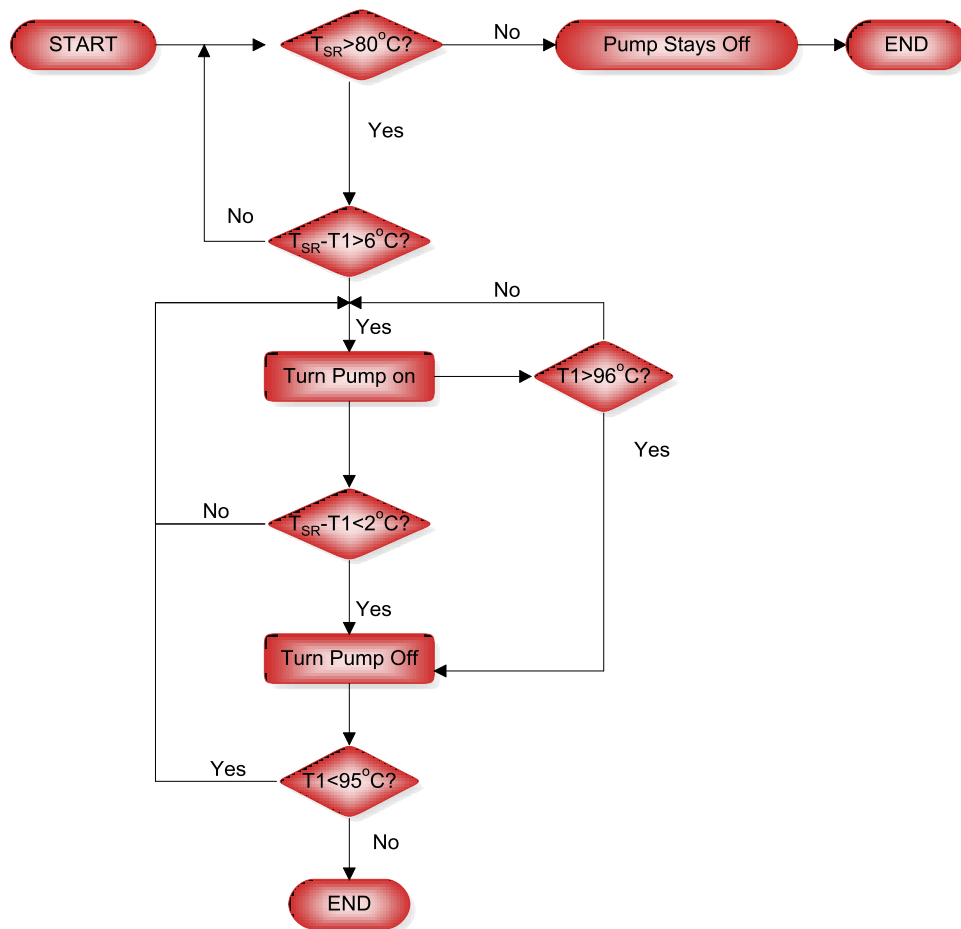
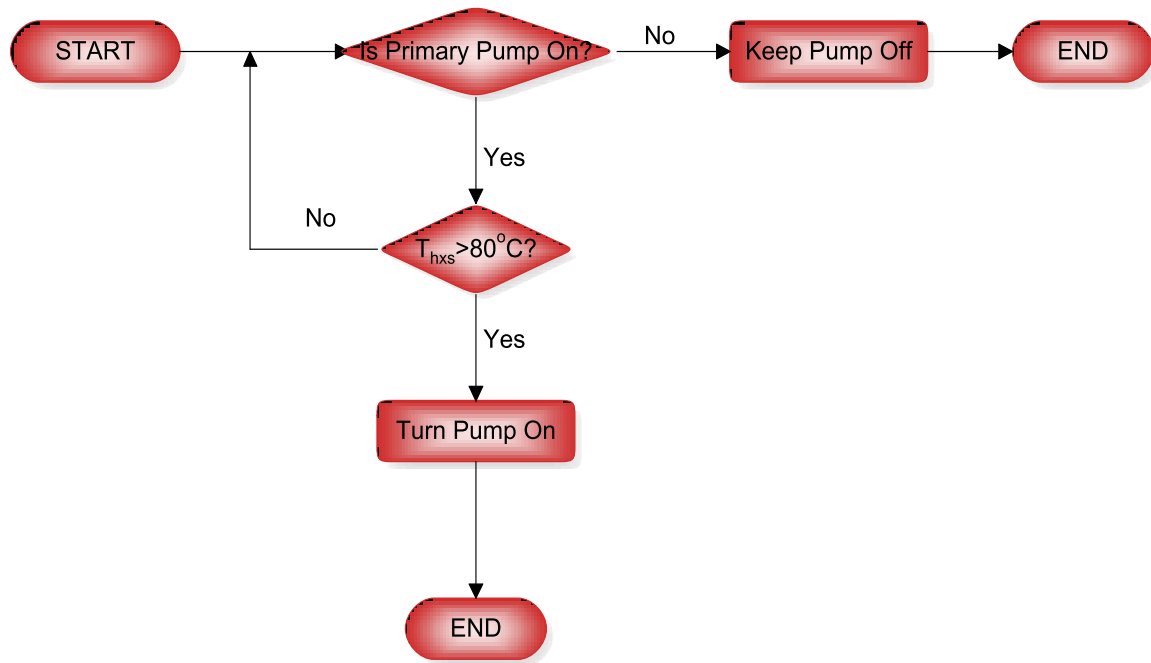


Figure 5.14: Solar Primary Water Pump Control Logic

There are two secondary solar pumps in the system and both are enabled if the solar primary pumps are running and if the solar heat exchanger supply temperature, ( $T_{hxs}$ ) is greater than  $80^{\circ}\text{C}$  as indicated in Figure 5.15.



**Figure 5.15: Secondary Solar Water Pump Control Logic**

All the other pumps are enabled through the chiller i.e. when the chiller is activated then the pumps are also switched on. The primary hot water pump and the secondary chilled water pump are only enabled when either the thermally active slab or the air handling unit require heating and cooling respectively.

#### 5.4.9.3 Solar and Hot Water Valves

The two solar valves, SV1 and SV2 (MV1 and MV2) are controlled via the hot water tank T1 temperature and start to modulate closed from  $88^{\circ}\text{C}$  to  $90^{\circ}\text{C}$ . There is a minimum closed position of 15% for the valves so they will never be fully closed. When the hot water tank temperature, T1 is greater than  $92^{\circ}\text{C}$ , then SV1 starts closing. When hot water tank temperature, T3 is greater than  $92^{\circ}\text{C}$  then SV2 starts closing and the bottom half of the tank starts charging. The hot water valve, HV1 (MV3) is normally open, but will start to modulate closed from  $88^{\circ}\text{C}$  to  $93^{\circ}\text{C}$  via the chiller hot water supply temperature. The other two valves HV2 and HV3 (MV4 and MV5) are seasonally controlled and are only in operation in winter.

#### **5.4.9.4 Dry Cooler**

The dry cooler pumps are run on a standby mode and are enabled via the chiller. The dry cooler fan is enabled via the chiller and is controlled through the dry cooler return temperature to maintain a temperature of 25°C. The fan speed is controlled by the dry cooler return temperature and the fan has a night time schedule to flush the rock store with cold air. If the ambient temperature is less than the basement temperature then the dry cooler damper is opened. The dry cooler valve is controlled through the dry cooler return temperature to prevent water temperature below 24°C.

#### **5.4.9.5 Air Handling Unit (AHU)**

Two time schedules are used to control the air handling unit (AHU):

- i. A control schedule between 6:00 and 18:00.
- ii. A night flush schedule, between 3:00 and 5:00 which is only active in summer and only the fan will run.

Once the AHU is enabled, the fan will run at a constant speed of 70% of the rated speed. If the ambient temperature is greater than 24°C and the enthalpy is greater than 65J/kg, then the ambient damper is open otherwise the rock storage is the one that is open. The cooling pump is enabled if the building temperature is greater than 22°C and the ambient temperature is greater than 24°C and enthalpy is greater than 65J/kg. The cooling valve is maintained through the AHU chilled water return temperature to maintain a temperature of 14°C. The heating mode of the AHU is only enabled in winter and the hot water pump is enabled when the average building temperature is less than 20°C. The hot water valve is controlled through the AHU hot water return temperature to maintain a temperature of 47°C.

#### **5.4.9.6 Thermally Active Slab**

The slab is enabled through a time schedule between 6:00 and 17:00. The two thermally activated slab pumps are run together and are enabled if the average slab temperature is greater than 20°C and for heating if the average slab temperature is less than 18°C. In summer, the valve is controlled via the supply water temperature to maintain a set point of 20°C, where as in winter a set point of 40°C is maintained. The system has a seasonal valve that is 100% open in summer and closed in winter.

### 5.4.9.7 Dehumidification Fins

The dehumidification fins are enabled through a time schedule between 8:00 and 17:00. The pump is only enabled in summer or when the slab is in cooling mode. The bypass valve is controlled through the fins return water temperature to maintain a set point of 5°C.

## 5.5 Data Monitoring System

The two solar powered absorption systems are monitored and their data is recorded by a Carel BMS system called Plant VisorPro shown in Figure 5.16. It is a monitoring and management system for complete control and optimization of refrigeration and HVAC systems. This system ensures remote access to all devices in the system. There is complete control of the system at all stages of operation. It provides centralized configuration of all parameters, system interface, data logging, activity scheduling and alarm management with all automatic signals and actions. Temperature sensors and flow meters are located at appropriate positions to collect all the relevant temperatures and flow rates, respectively.

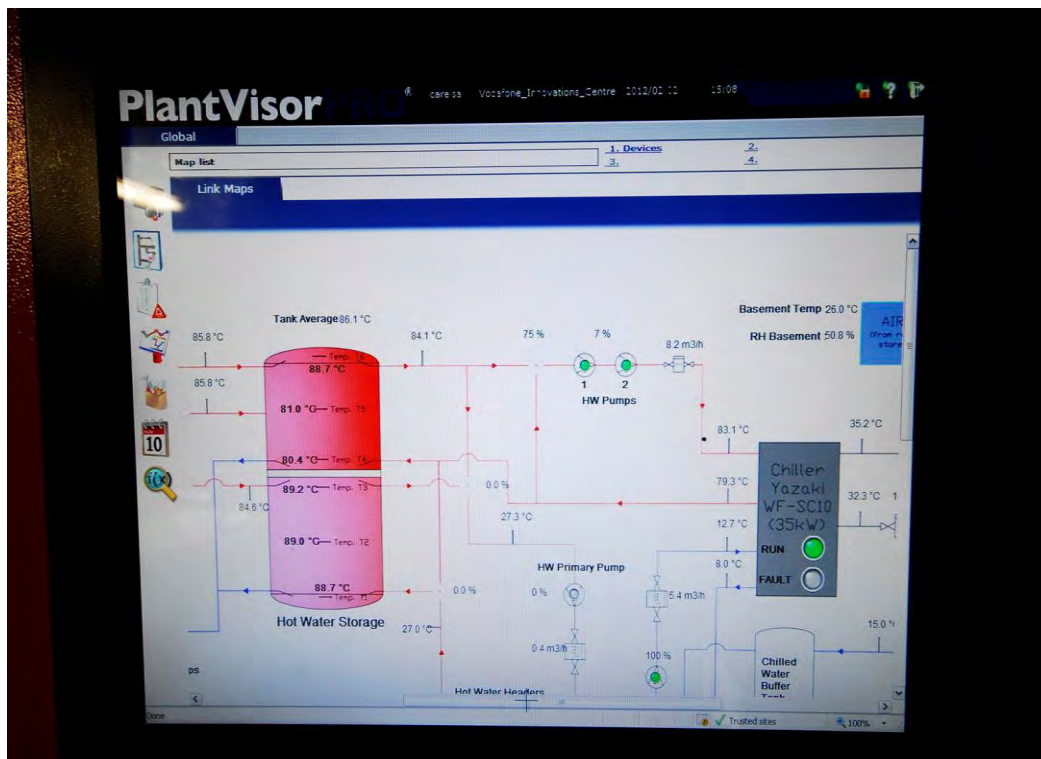


Figure 5.16: Photo of the Plant VisorPro screen

## 5.6 Circulation Pumps

The Vodafone Site Solution Innovation Center has several circulation pumps installed. Table 5.5 presents their technical specifications along with their electrical energy consumption.

**Table 5.5: Circulation Pumps Specifications**

<b>Item description</b>	<b>Flow / Head</b>	<b>Pump type</b>	<b>Number of pumps</b>	<b>Power consumption(kW)</b>	<b>VSD (%)</b>
Solar primary	4.00m <sup>3</sup> /h @ 22.30m	CRE 5-5 AN-FGJ-A-E-HQQE	1 standby, 1 duty	0.63	90
Solar Secondary	8.64m <sup>3</sup> /h @ 11.1m	TPE 32-120/2-A-F-A-BAQE	2 in series	0.644	89
Hot water Tank / chiller	8.64m <sup>3</sup> /h @ 16.41m	TPE 32-120/4-A-F-A-BAQE	2 in series	1.188	90
Hot water Primary	9.1m <sup>3</sup> /h @ 7.5m	TPE 32-120/4-A-F-A-BAQE	1	0.577	88
Dry cooler	18.4m <sup>3</sup> /h @ 17.5m	TPE 40-240/2-A-F-B-BAQE	1 duty, 1 standby	1.87	93
Chilled water Primary	5.5m <sup>3</sup> /h @ 10.5m	TPE 32-120/4-A-F-A-BAQE	1	0.559	95
Chilled water Secondary	5.5m <sup>3</sup> /h @ 5.24me	TPE 32-120/2-A-F-A-BAQE	1	0.215	77
Cold AHU	4.32m <sup>3</sup> /h @ 8.624m	TPE 32-120/2-A-F-A-BAQE	1 + 1 spare	0.294	96
Cold Fins	1.91m <sup>3</sup> /h @ 5.02m	UPS32-70 180	1 + 1 spare	0.111	
Hot AHU	5.04m <sup>3</sup> /h @ 10.48m	TPE 32-120/4-A-F-A-BAQE	1 + 1 spare	0.553	96
TAS	4.04m <sup>3</sup> /h @ 5.1m	UPS32-70 180	2 in parallel	0.222	
Power consumption				6.863	

## CHAPTER SIX

---

### 6 SYSTEM SIMULATIONS USING TRNSYS

#### 6.1 Overview

A solar cooling system is made up of various components, the proper sizing of which is a complex problem. In order to obtain the integrated performance over extended periods and information on process dynamics, numerical simulations are required. Reliable simulation is a must when dealing with solar cooling systems as there is no standard layout for this application and there is a lack of dependable experimental cooling facilities with accurate data (52). Simulations are quick and inexpensive and can produce information on the effect of design variable changes on system performance. They are uniquely suited to parametric studies and thus offer the design engineer the capability to explore the effects of design variables on long term system performance. In this chapter the two case studies i.e. the Netcare Moot Hospital system and the Vodafone Site Solutions Innovation Center system are simulated using the TRNSYS simulation software and their predicted behaviors presented. Parametric studies are also conducted for the Moot Hospital system.

#### 6.2 TRNSYS interface

TRNSYS was originally designed for solar energy applications and is now used for simulation of a wide variety of thermal processes. It is a simulation environment for transient simulation which employs an open modular structure that allows the user to build a representative model of a physical system. It allows evaluating the behavior of a solar application in a quasi-steady state analysis improving the accuracy in describing applications that are characterized by the intermittent behavior of solar energy.

#### 6.3 Netcare Moot Hospital System

This case study is solar powered cooling system that is used in conjunction with an existing conventional vapor compression system at Netcare Moot Hospital in Pretoria. It has a solar thermal collector array made up of 58 evacuated tube collectors, two hot storage tanks with a volume of 600 liters each, a Yazaki WFC10 absorption chiller, with a capacity of 35kW, and a wet cooling tower for the rejection of the heat

of condensation and absorption from the chiller. The project location is Pretoria, with the following characteristics:

- Coordinates: 25°42'49"S, 28°13'5"
- Average annual global irradiation: 1961 kWh/m<sup>2</sup>
- Height above sea level: 1350m

The Netcare Moot Hospital system is simulated and the expected results for 4 December presented. The TRNSYS configuration for the system is shown in Figure 6.1.

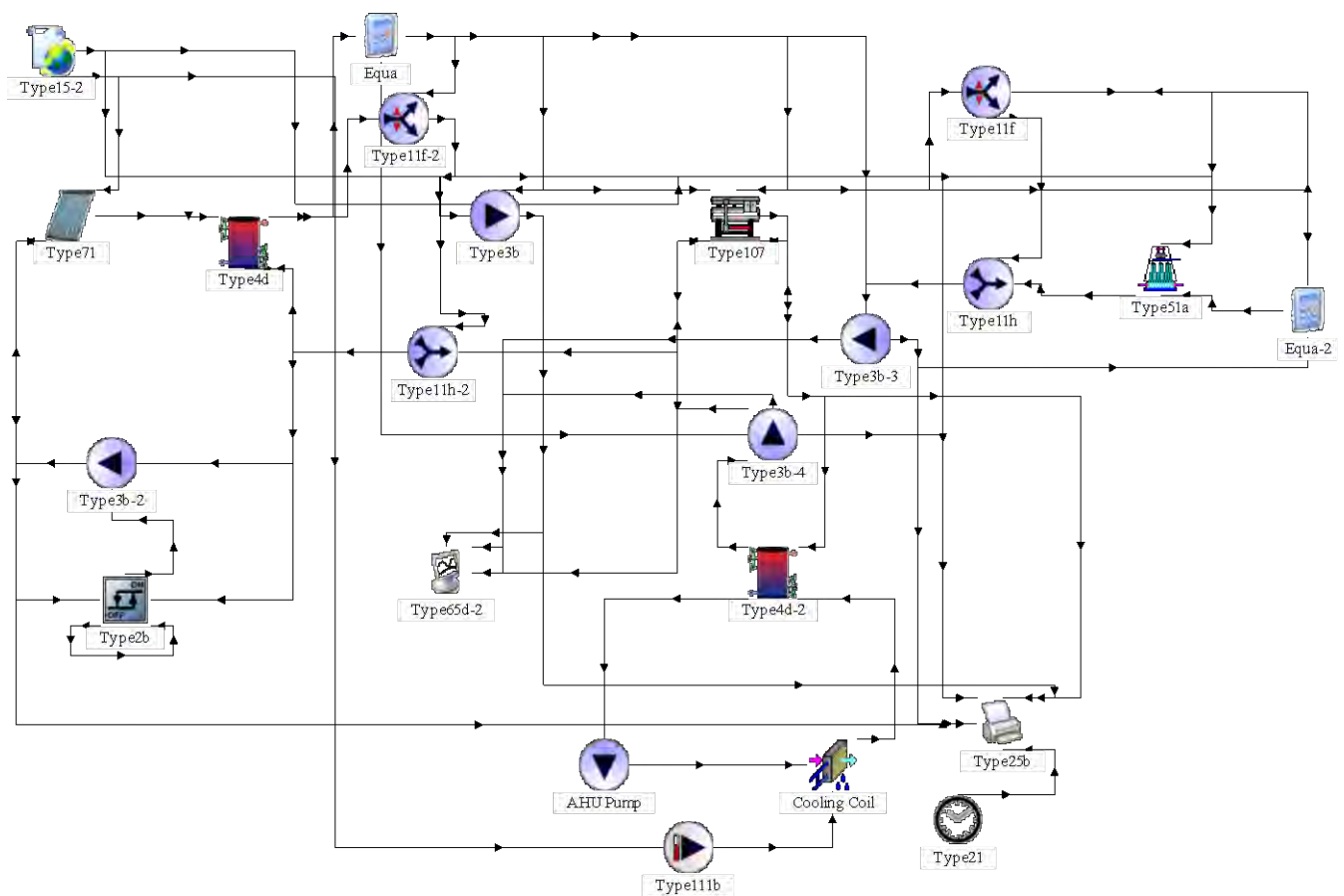


**Figure 6.1: Configuration of the Moot Hospital system using TRNSYS**

### 6.3.1 Solar Thermal Collector Performance

On December 4 it is predicted that a total of 9 780kW of solar energy is incident on the collector array and of this 1 548.8kW is converted into useful energy output. The distribution of incident solar energy,

collector useful energy output and the collector thermal efficiency are shown in Figure 6.2. The average incident solar energy is 177.8.kW and the maximum is 331.2kW. The average useful energy output and the maximum useful energy output are 48.4kW and 56.1kW, respectively. The collector efficiency has an average value of 20%. The incident solar energy increases steadily from around 5:30 and reaches its peak around midday and starts decreasing at a steady rate until sunset. The solar collector pump switches on when the difference between the collector outlet temperature and the temperature at the top of the storage tank becomes greater than 6°C, only after this does the collector start producing useful energy output. When the sun rises it starts heating the collector until around 7:00, when the set temperature difference for the pump to operate is attained and the collector starts producing useful energy output. The collector energy output gradually rises and reaches a peak of 56.1kW around 12:00, and then stays approximately constant until later in the afternoon around 15:00, then gradually decreases and stopping to operate around 17:00 as the amount of incident solar energy decreases.

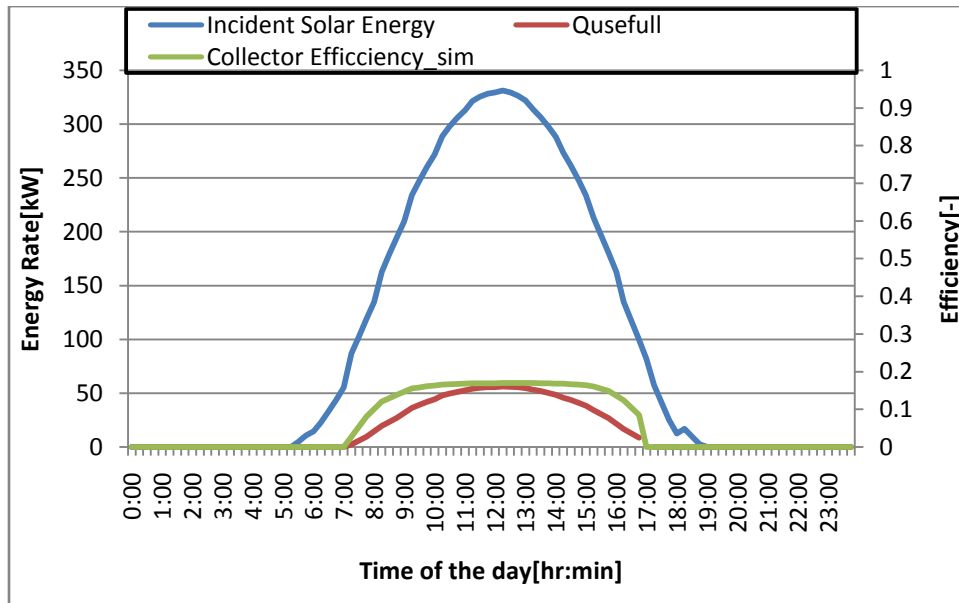


**Figure 6.2: Distributions of the collector useful energy output, incident solar energy and the collector thermal efficiency on December 4**

### 6.3.2 Absorption Chiller Performance

The temperature distributions for the chiller water streams are shown in Figure 6.3. The chiller is energized by water temperature between 70°C and 95°C, but the system control strategy is that the chiller



will only start producing cooling energy if the hot water temperature that is being inputted into the generator exceeds  $81^{\circ}\text{C}$ . The simulation was done with a simulation time step of 15 minutes and there are 96 data points for December 4. Of those 96 data points, 28 of them are above the chiller switch on temperature of  $81^{\circ}\text{C}$  for the generator inlet temperature representing 29.2% of the time. This temperature decreases slightly around 9:00 when the chiller starts drawing hot water from the storage tank. The chilled water return temperature starts to gradually decrease when the chiller is switched on, and then evens out as the day progresses. This is different from the chilled water supply temperature whose distribution is a function of the system control system. The system control strategy requires that the chiller switches off if the chilled water supply temperature falls below  $7^{\circ}\text{C}$ , and switches on again when it exceeds  $8^{\circ}\text{C}$ , and this starts happening around 11:00 hence the observed displayed distribution.

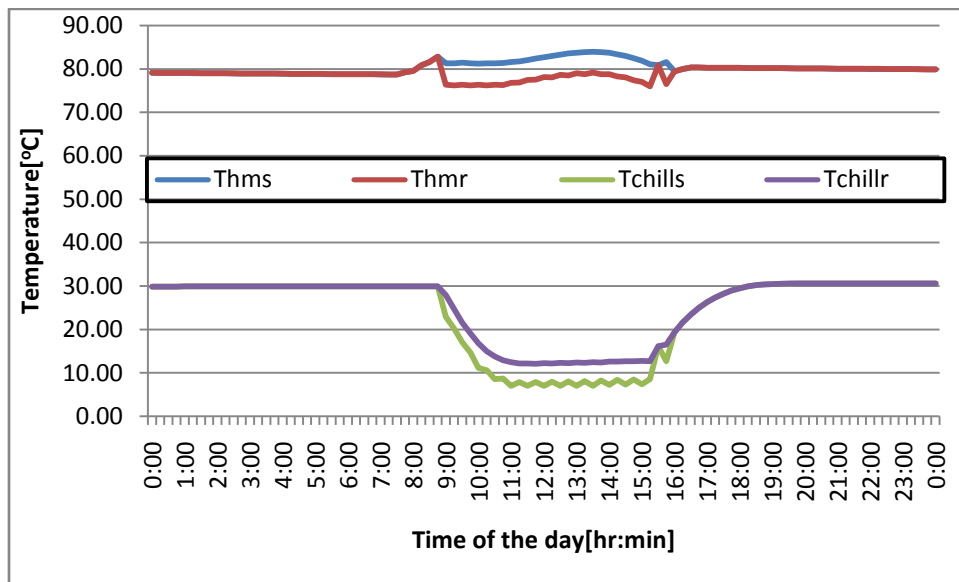


**Figure 6.3: Temperature distributions of the chiller water streams on December 4**

The distribution of the chilled water supply temperature also affects the amount of chilled water energy produced by the chiller, and the distribution of this energy closely resembles that of the chilled water temperature. Figure 6.4 shows that the amount of chilled water energy produced by the chiller and the heat energy supplied to the chiller steadily increase from 9:00 when the chiller is switched on and then oscillates throughout the around an average of 29.1kW. The zero value indicated in the energy distribution occurs when the generator inlet temperature falls below  $81^{\circ}\text{C}$  and the chiller temporarily stops. The chiller receives a total of 1330kW of energy from the tank at an average of 47.5kW, with a

maximum of 50.8kW. Of this heat energy, 813.4kW is converted into cooling energy an average of 29.1kW with a maximum of 36.1kW.

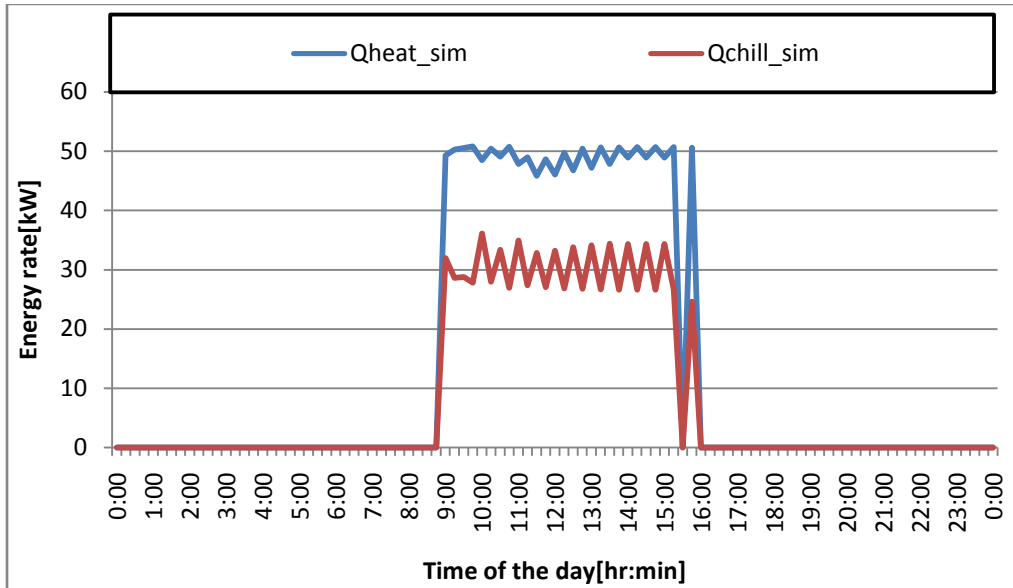


**Figure 6.4: Chiller heat energy input and cold energy output distributions on December 4**

The COP is given as the chilled water energy produced divided by the heat energy input into the generator. The heat energy input remains fairly constant throughout the day and consequently the COP distribution mirrors the chilled water energy distribution. The variation of the chiller COP is shown in Figure 6.5.

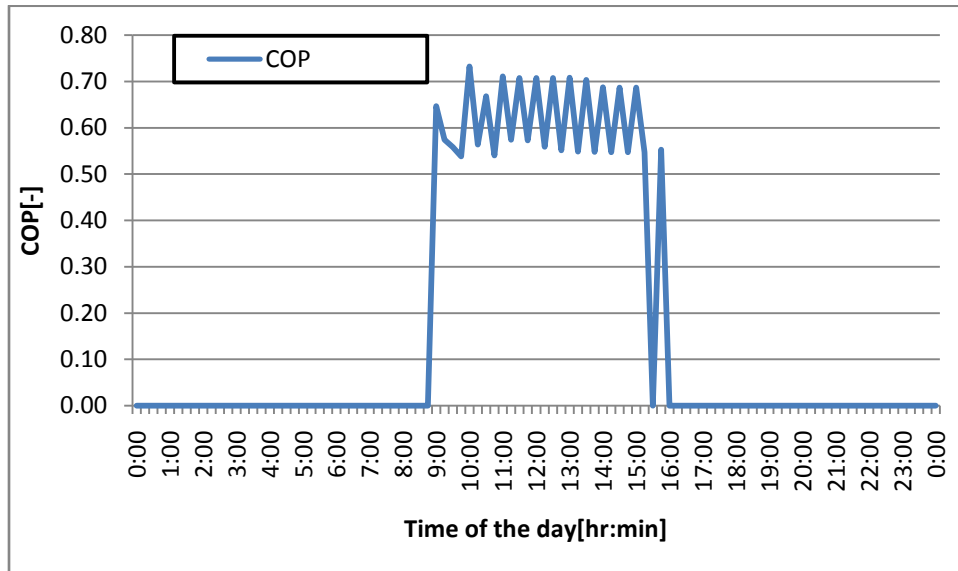


**Figure 6.5: Distributions of COP on December 4**

## 6.4 Vodafone SSIC System

This case study is an autonomous thermal heating and cooling system for an office building to maintain room temperatures at comfort conditions around the year. The need for active cooling is reduced by constructing a rock bed storage that will precool the building supply air. The functionality of the solar cooling and heating systems, the rock bed storage are analyzed.

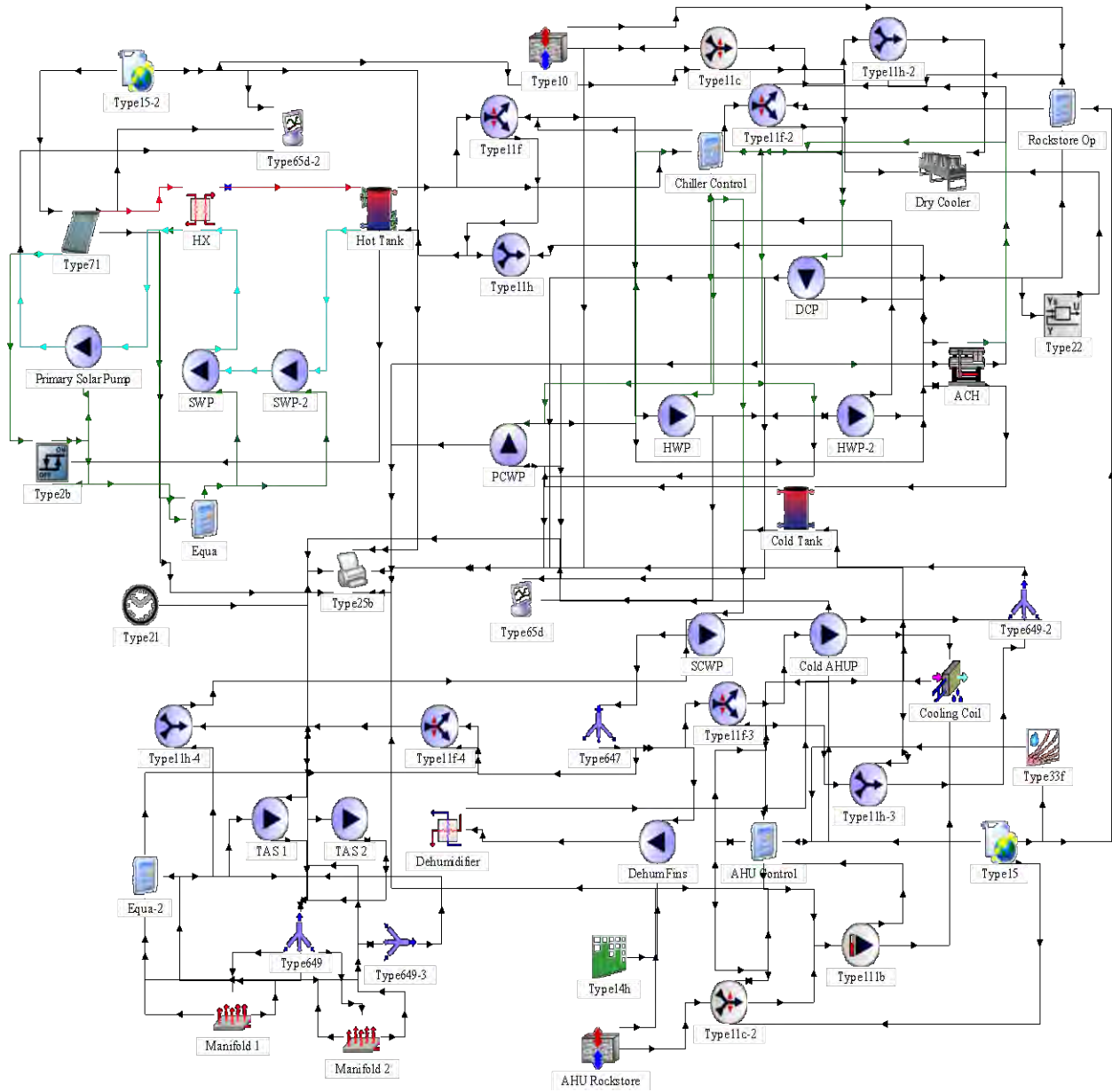


Figure 6.6: Configuration of the Vodafone SSIC system using TRNSYS

The project location is Johannesburg, with the following characteristics:

- Coordinates: 26°12'S, 28°4'O
- Average annual global irradiation: 2084kWh/m<sup>2</sup>
- Height above sea level: 1700m

The annual cooling demand is 18.4MWh with a maximum cooling load of around 20kW whilst the annual heating load is 3.2MWh with a maximum heating load of 22.5kW. The system was designed by Voltas Technologies and consisted of:

- 116m<sup>2</sup> vacuum tube collector array.
- 6.5m<sup>3</sup> hot water storage.
- Yazaki WFC10 absorption chiller with a dry cooler for heat rejection.
- 1m<sup>3</sup> cold storage tank.

In addition, two rock storages are located underneath the building. The first one is used to pre-cool the supply air to the dry cooler at high ambient temperatures to facilitate the heat rejection, as the chiller only operates with cooling water temperatures below 35°C. The second one pre-cools the supply air to the building.

## 6.5 Collector Output

On January 31, the sun rises just before 6:00 and incident solar energy is recorded from this time steadily rising to 4.93kW around midday and steadily decreases to zero at sunset. The collector starts producing useful energy gain around 7:00, this lag in useful energy production from the incident solar energy can be attributed to the time it takes for the water that is in the collectors at the beginning of the day to be heated up sufficiently to produce the 6°C difference that is required for the solar primary pump to be activated. The solar collector efficiency rises sharply for the first two hours of collector useful energy production then remains fairly constant during a significant length of the day and then sharply decreases towards sunset. The simulation predicts that on January 31 a total of 15 518kW of solar energy is incident on the collector array and of this 2 329kW is converted into useful energy output. The average incident solar energy is 298.4kW and the maximum is 493.4kW. The average useful energy output and the maximum useful energy out are 52.9kW and 77.2kW respectively. The collector efficiency has an average value of 13.8%.

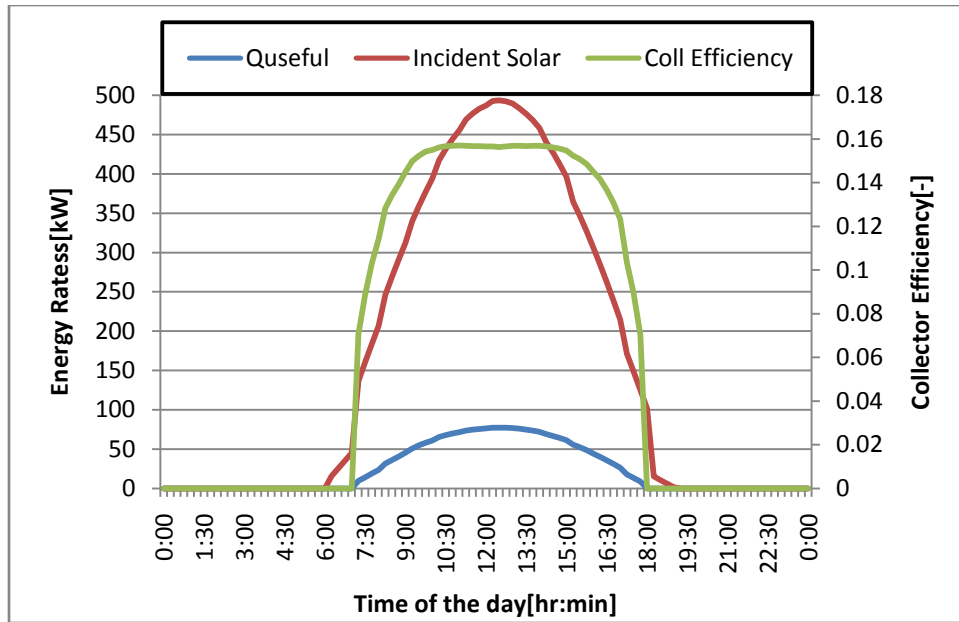


Figure 6.7: Distributions of the collector useful energy output, incident solar energy and the collector thermal efficiency January 31

## 6.6 Absorption Chiller Performance

The chiller is energized by water temperature between 70°C and 95°C, but the system control strategy is that the chiller will only start producing cooling energy if the hot water temperature that being inputted into the generator exceeds 80°C. The simulated variation of the chiller water streams is shown in Figure 6.8.

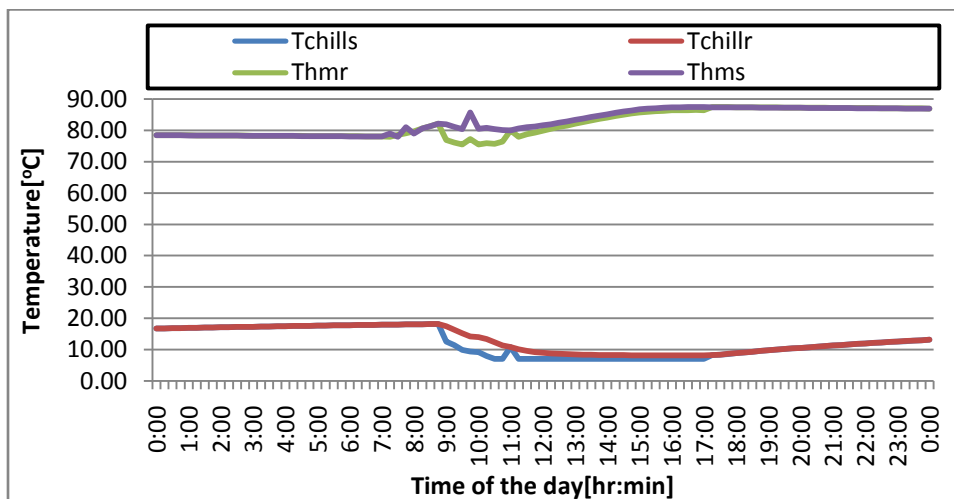
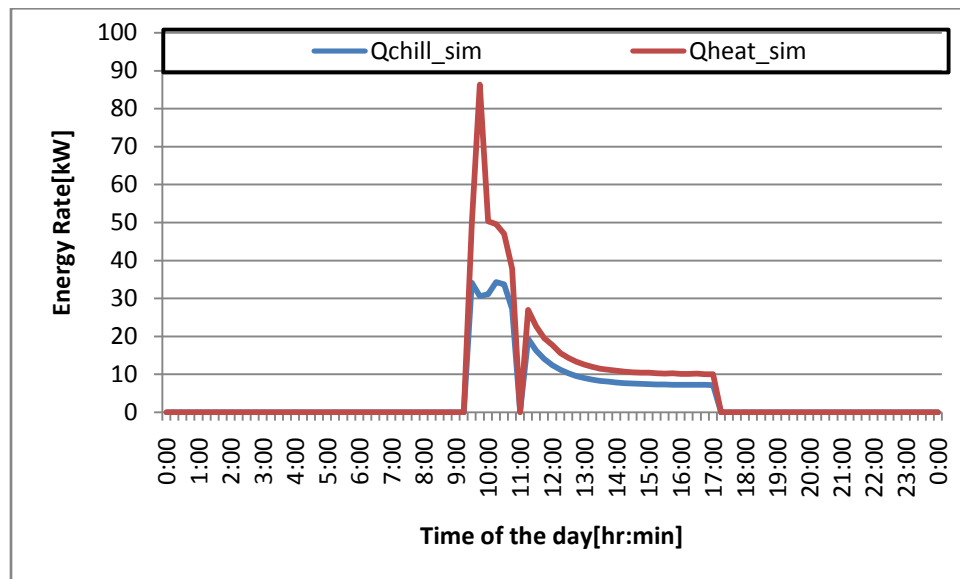


Figure 6.8: Temperature distributions of the chiller water streams on January 31

The simulation was done with a simulation time step of 15 minutes and there are 96 data points for January 31. Sixty three of those data points are above 80°C, thus for 65.6% of the time, the generator inlet temperature exceeds the set point for the chiller to be activated. This temperature decreases a bit around 9:00 when the chiller starts drawing hot water from the storage tank. The chilled water return temperature starts decreasing gradually when the chiller is switched on, and then evens out as the day progresses.

Figure 6.9 shows the amount cooling energy produced by the chiller and the heat energy supplied to the chiller steadily increases from 9:00 when the chiller is switched on and then becomes zero at 11:00 when the chiller temporarily stops producing or drawing any energy from the hot water storage tank. This is because around this time the heat medium stream temperatures will be equal and also the chilled water stream temperature will be equal. As a result the temperature differences of the chiller water streams being zero, no energy is produced. After this the energy distributions mirror the distribution of the temperature streams with both the heat medium energy and chilled water energy varying in an almost quadratic fashion. The chiller receives a total of 632kW of energy form the tank at an average of 20.4kW, with a maximum of 86.2kW. Of this energy, 414.7kW of cold are produced at an average of 13.4kW with a maximum of 34.3 kW.



**Figure 6.9: Chiller energy distributions on January 31**

The solar COP is calculated as the chilled water energy produced divided by the collector useful energy output. The useful collector energy output increases steadily from around 6:30 in the morning reaching its maximum value around midday, it then starts decreasing steadily reaching zero around 18:00. The

chilled water energy as shown in Figure 6.9 can be split into two distinct periods i.e. time before 11:00 and time after 11:00. When the chiller is switched on at 9:00, the chilled water output has an average of about 30kW, and then at 11:00 it decreases sharply to zero due to the chilled water supply and return temperatures being equal. After 11:00 the distribution of the chilled water energy is approximately parabolic until around 13:00, when it becomes fairly constant. This leads to the distribution of solar COP observed in Figure 6.10 with a fairly constant distribution before 11:00 and an approximate parabola facing upwards for the rest of the day. The heat energy input to the generator distribution shown in Figure 6:10 shows three distinct periods i.e. from 9:00 to around 10:00, from 10:00 to around 11:00 and after 11:00 to 17:00 when the chiller is switched off. In the first hour the energy supplied to the chiller generator decrease sharply and then in the second hour it is still decreasing but at a slower rate. After 11:00 the heat energy input to the generator varies in an approximate parabolic fashion until 13:00 then remains fairly constant until end of day. This variation of heat energy input and that of the chilled water energy result in the observed COP variation. The COP is almost constant and the SCOP remains almost constant after 11:00 due to the uniform distributions of the chilled water and heat medium energy rates and this is shown in Figure 6.10.

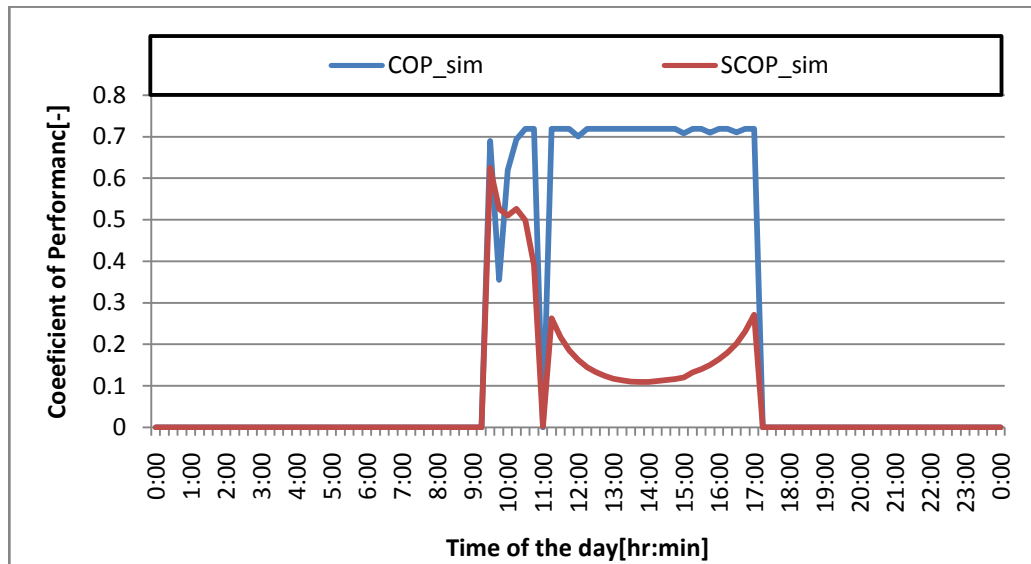


**Figure 6.10: Distributions of COP and SCOP on January 31**

### 6.7 Effect of the rock storages

On January 31, the ambient temperature in the supplied file lies above 26°C during 8.25 hours and above 29°C during 4.25 hours. The average temperature between 6:00 and 18:00 is 25.4°C and the maximum is

30.19°C. If the rock storage is used to pre-cool the supply air to the dry cooler, the supply air to the dry cooler follows the distribution shown in Figure 6.11. The dry cooler pump is activated according to the chiller schedule so it is switched on at 9:00. At this time, the ambient temperature is still below the maximum permissible dry cooler air supply temperature of 26°C, so the dry cooler will be operating using ambient air. It continues using ambient air until the ambient temperature exceeds 24, then the rock store damper is opened, and pre-cooling starts and so that when the ambient temperature is around 30°C the temperature of air going into the dry cooler is only about 20°C. This continues up to 17:00 when the ambient temperature is once again below 24°C. Evidently, the cooling of the supply air to the dry cooler is an efficient measure of reducing the cooling water temperature during hot days. An improvement that can be done is to start cooling a part of the supply air in the rock storage at 24°C then increase this fraction until the entire supply is sent via the rock store when the ambient temperature exceeds 26°C. The pressure drop and thus electricity consumption of the fan will be reduced as opposed to cooling the entire supply air when the temperature reaches 24°C.

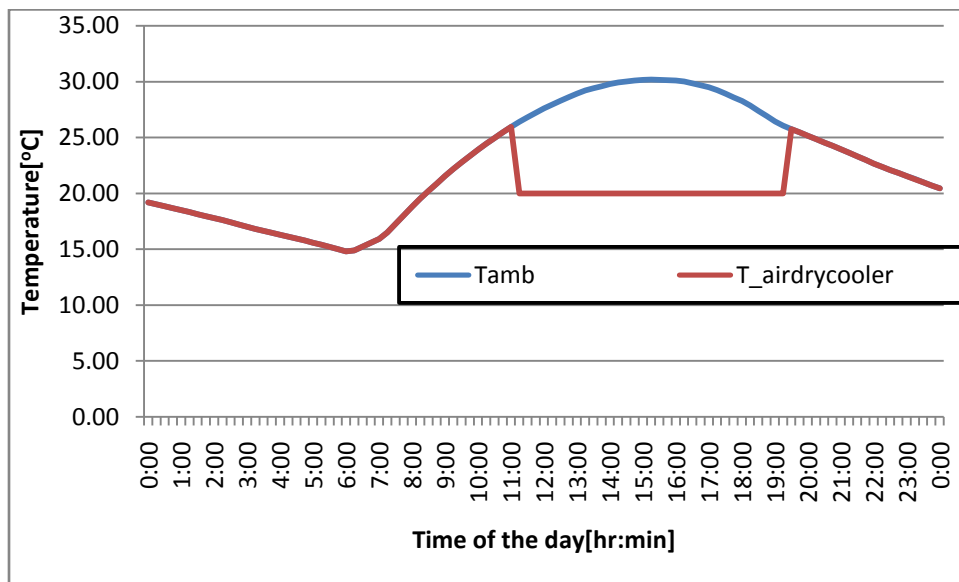


**Figure 6.11: Distributions of the ambient temperature and the dry cooler supply air temperature on January 31**



## CHAPTER SEVEN

---

### 7 CASE STUDIES: SYSTEM PERFORMANCE ANALYSIS

#### 7.1 Overview

The two case studies i.e. Case Study 1: the Moot Hospital System and Case Study 2: Vodafone Site Solutions Innovation Center (SSIC), both have a Carel VisorPro Building Management System installed to monitor and record key system performance parameters. They also have a robust network of sensors installed throughout the systems and the buildings, so as to enable thorough monitoring for both system performance control and problem diagnosis. In the case of the Moot system data was collected from October 2009 to October 2011, whereas for the Vodafone SSIC system data was collected from November 2011 up to the present day. This large amount of data recorded provides a strong basis for analysis and evaluation of the solar powered absorption systems. The individual components are analyzed separately and then the overall system performance discussed. In this chapter, the results of these monitored parameters and overall system performances for both case studies are presented and analyzed.

#### 7.2 Moot Hospital

Case Study 1 is located at Netcare Moot Hospital in Pretoria. The hospital is located at a latitude of 25°42'49"S and a longitude of 28°13'5". This area receives on average 3220 hours of sunshine a year. The key weather parameters for Pretoria are presented in Table 7.1

**Table 7.1: Climate Data for Pretoria (75)**

Variable	Jan	Feb	Mar	Apr	May	Jun	Jul	Aug	Sep	Oct	Nov	Dec
Insolation, kWh/m <sup>2</sup> /day	6.70	6.10	5.46	4.77	4.21	3.80	4.08	4.78	5.69	5.98	6.29	6.62
Clearness Index	0.57	0.55	0.56	0.59	0.64	0.65	0.66	0.65	0.64	0.58	0.55	0.56
Temperature, °C	22.2	22.1	21.1	18.7	15.2	11.6	11.5	14.6	18.5	20.2	20.9	21.4

### 7.2.1 Solar Collector Performance

The period from November to February sees Pretoria receiving the most amounts of solar radiation with an average hourly radiation of  $276.9\text{kW/m}^2$  and an average maximum ambient temperature of  $32.38^\circ\text{C}$ . The values for these parameters start decreasing steadily in March and reach their lowest values in July and then start increasing again in August all the way up to the end of February. The yearly distribution of Hourly radiation mean daily temperature is shown in Figure 7.1.

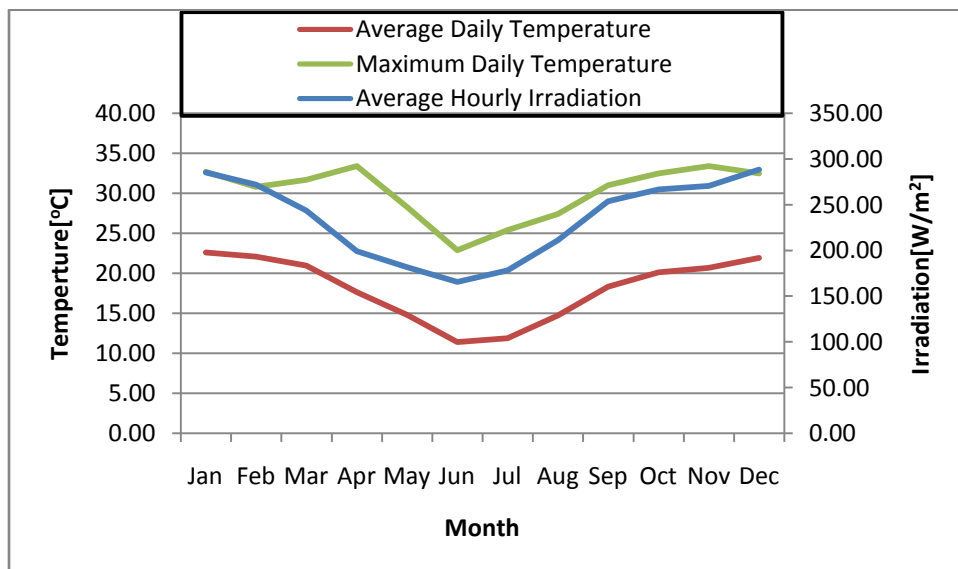
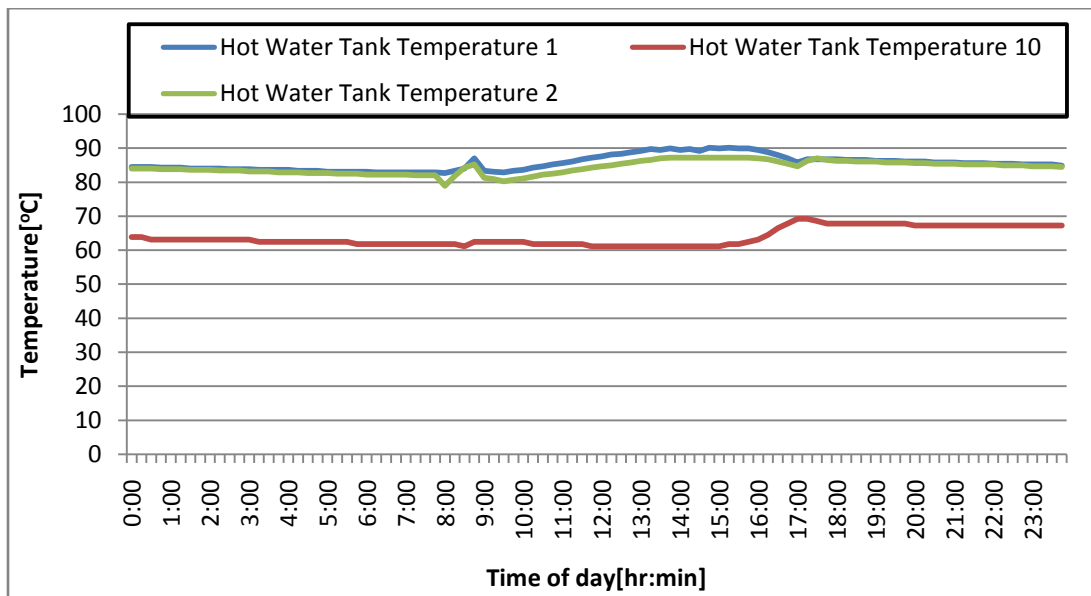


Figure 7.1: Distribution of Temperature and Irradiation for Pretoria

### 7.2.2 Thermal Energy Storage Tank Performance

The absorption chiller is driven by the hot water coming from the storage tank only. As a result, the performance of the storage tank is crucial for the operation of the system. The absorption chiller starts to produce cooling energy once the hot water outlet from the storage tank exceeds  $81^\circ\text{C}$  during the period between 9:00 and 17:00, and can also produce cooling energy out of schedule if the hot water outlet temperature from the tank exceeds  $93^\circ\text{C}$ . The temperature distribution in the hot water storage tank is shown in Fig 7.2. If either hot water temperature  $T1$  or  $T2$  is above  $81^\circ\text{C}$ , the chiller draws hot water at temperature  $T1$  and produces useful cooling energy. If this temperature exceeds  $95^\circ\text{C}$ , the chiller starts drawing hot water at temperature  $T2$ , provided this temperature is below  $95^\circ\text{C}$ . If both  $T1$  and  $T2$  are above  $95^\circ\text{C}$ , then the three-way valve closes and prevents the high temperature water from entering the

chiller. On December 4, 2010 as shown in Figure 7.2, the hot water temperature  $T1$  is above  $81^{\circ}\text{C}$  during the whole day. This means the storage tank is able to supply the required input energy into the chiller for the whole day. This temperature starts increasing steadily from 6:00 when the sun comes out and continues until it reaches  $87^{\circ}\text{C}$  at 8:45. At 9:00 the chiller is switched on and starts drawing water from the tank hence  $T1$  noticeably decreases for about an hour and then starts to increase at a steady rate as the available solar energy increases. This trend continues culminating in the highest temperature of  $90^{\circ}\text{C}$ , that is experienced at 14:45 and then starts to decrease and the amount of solar energy starts to decrease as well. At 17:00 the chiller is switched off, and since it is no longer drawing water from the tank, a temperature increase in the tank is observed. The bottom water temperature,  $T10$  remains at a more or less constant level throughout the day, or increasing slightly when the top water temperature is at its highest.



**Figure 7.2: Temperature Distributions in the Hot Water Storage Tank**

### 7.2.3 Absorption Chiller Performance

According to the design information provided by Voltas Technologies, this system was designed with the intention that it will provide the amount of cooling energy provided in Figure 7.3. The chiller was supposed to be switched on at 9:00 and provide an hourly average of 20% or 7kW of its nominal capacity; this would increase to 80% or 28kW at 10:00, and then reach 100% or 35kW at 12:00. It would continue providing 35kW of energy for five hours until 17:00, when 28kW for two hours until 19:00 when it would then provide 7kW for an hour before being switched off. The absorption chiller is considered as a black

box, a component that simply outputs chilled water when supplied with hot water. These design values were arbitrarily chosen, as the amount of the building cooling load that the absorption cooling system was supposed to cover.

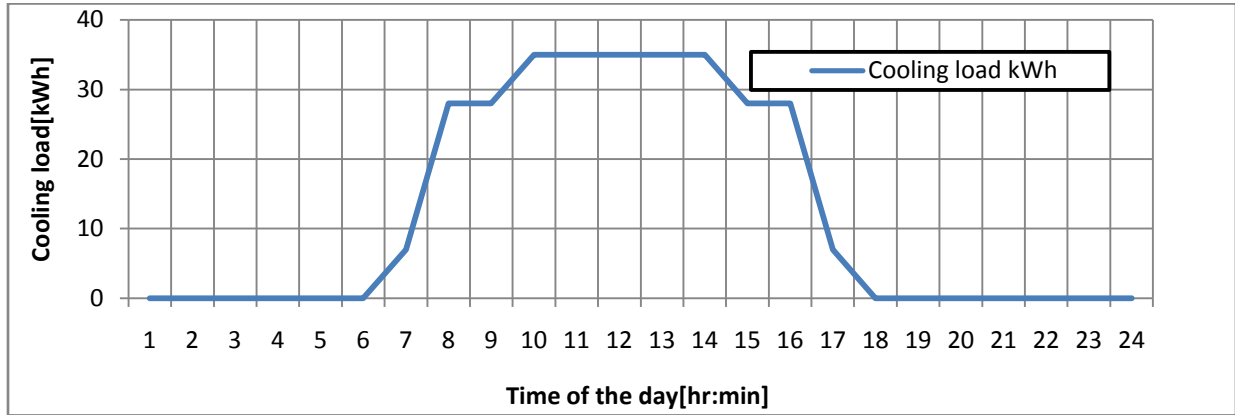


**Figure 7.3: Moot Hospital Cooling Load Distribution**

The chiller is energized by water temperature between 70°C and 95°C, but the system control strategy states that the chiller will only start producing cooling energy if the hot water temperature that is being fed into the generator exceeds 81°C. The system performance values were recorded at 15minute intervals and there are 3307 data points from 13:00 on November 1 to the end of day on December 4. Of these recorded values, 846 of them, representing 25.5% of the time were above 70°C, suggesting the chiller could have run for 25.5% of the time if required. The generator inlet temperature exceeds the threshold value of 81°C for 494times which represents 14.9% of the time. This results in part load behavior for the chiller and the amount of cooling energy produced is presented in the Table 7.2.

**Table 7.2: Summary of Energy Produced by the Chiller in November 2010**

Energy produced by YAZAKI chiller between 01/11/2010 and 4/12/2010	4.097 MWh
Extrapolated Energy for the year	43,983 MWh
Maximum power reached (kW)	31 kW
Average power	20.5 kW
Lowest chilled supplied temperature	6.6 °C
Average temperature of chilled supplied water	8.4 °C

Pretoria, experiences its greatest need for air-conditioning in the period from November to the end of February. The average insolation in this period is  $6.43\text{kWk/m}^2/\text{day}$ , the average highest temperature experienced is  $28^\circ\text{C}$  and the average daily mean temperature is  $21.64$ , therefore presented here are the results of the Netcare Moot Hospital system operation for this period.

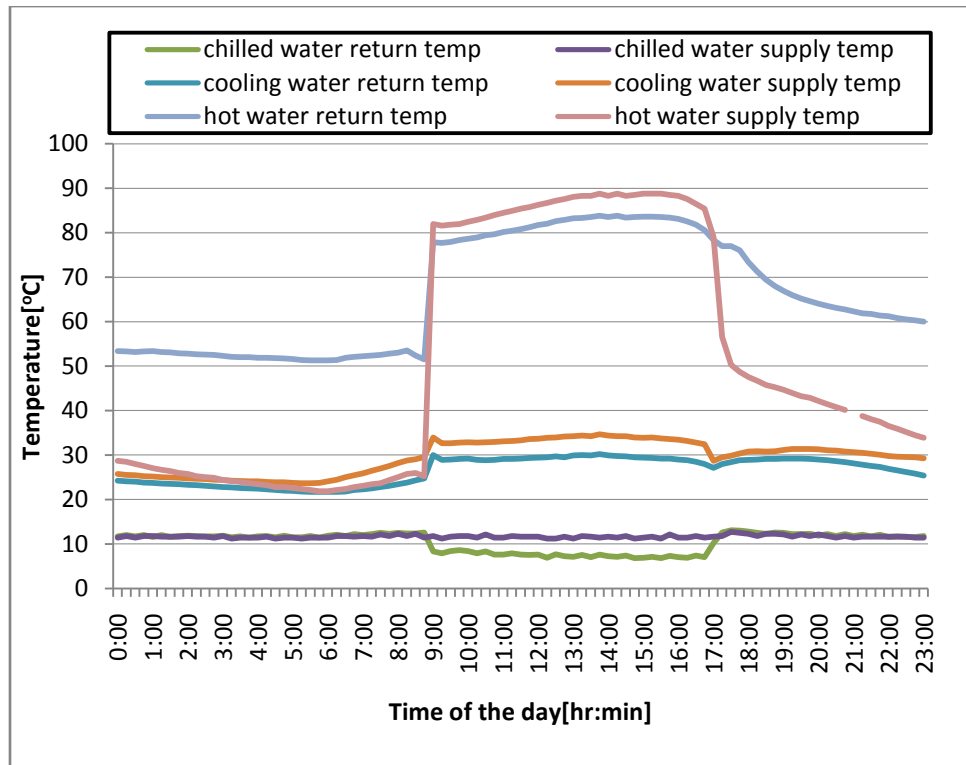


**Figure 7.4: Temperature distributions of the chiller water streams on December 4 2010.**

In this high air-conditioning energy demand period, from 9:00-17:00, the solar powered chiller is in priority mode. If the temperature at the top of the tank is higher than  $81^\circ\text{C}$ , the solar absorption chiller can operate in either of two modes. It either operates alone or in combination with one stage of the electric chiller if the chilled water temperature is above  $6.5^\circ\text{C}$ . If the chilled water temperature is above  $8^\circ\text{C}$ , then it operates with two stages of the electric chiller. For 17:00-9:00, the electric chiller has priority, but if the temperature at the top of the hot water storage tank is above  $93^\circ\text{C}$  then the solar absorption chiller will operate. A three way valve is used to bypass the cooling tower, if the cooling tower supply temperature is under  $28^\circ\text{C}$ , the valve is closed and the water coming out of the chiller directly goes back into it. When the temperature reaches  $28^\circ\text{C}$ , the valve starts to open and reaches 100% when the temperature reaches  $30^\circ\text{C}$ . The temperature distributions for the input and output streams into the absorption chiller on December 4 2010 are shown in Figure 7.4.

The chiller is on a time schedule and switches on at 9:00, as a result, before 9:00 the recorded chiller hot water inlet temperature is about 25°C since the chiller will not be drawing any water from the hot storage tank. At 9:00, the chiller starts getting water from the tank, so the inlet water temperature rises from 25.1°C to 82°C. This rapid rise at the chiller inlet and outlet is as a result of the three way valve opening to allow water into the chiller when the chiller is switched on. This temperature gradually increases to a maximum of 88.8°C at 15:00 as incident solar energy increases. The cooling effect starts to be produced at 9:00 when the chiller is switched on hence the marked decrease in the chilled water temperature from 12.5°C to 8.4°C. This temperature eventually stabilizes and reaches a lowest temperature of 6.8°C at 13:45 as seen by the almost flat line on the graph between 9:00 and 17:00.

The distribution for energy produced is shown in fig 7.5. The system starts producing cooling energy at 9:00 when it is switched on since the hot water supply temperature is 82°C at that time. It produces 22.2kW from 35.2kW of heat supplied to the hot water, giving a COP of 0.63. This COP value remains almost constant throughout the day, indicating a steady supply of hot water from the storage tank. The maximum values of cooling energy produced and heat energy supplied are 28.6kW and 45.7kW, respectively.

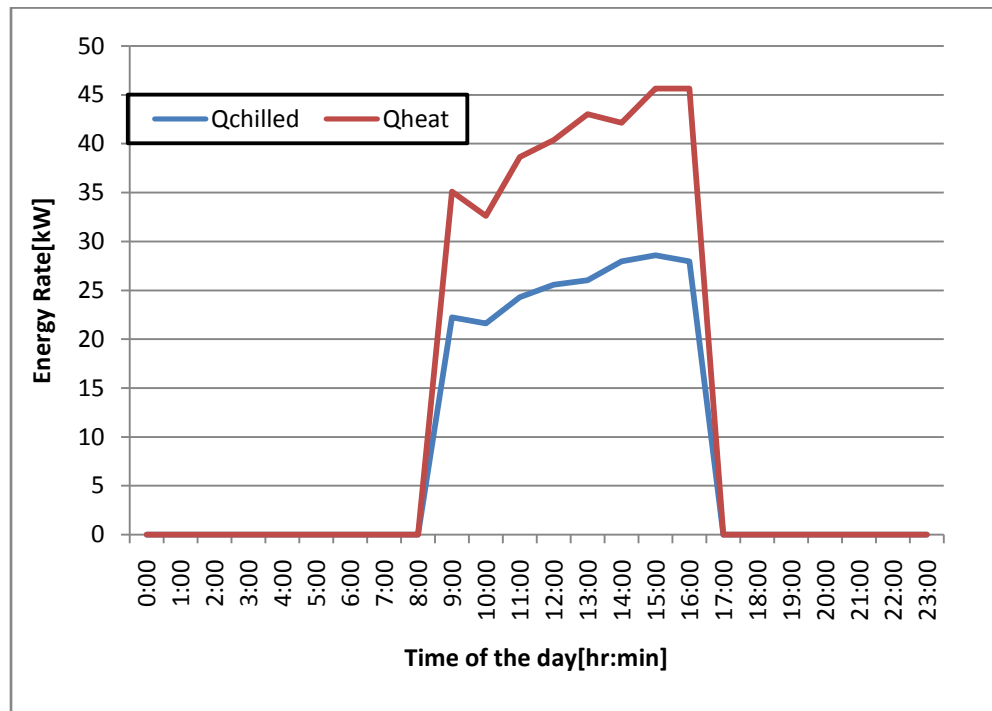


**Figure 7.5: Chiller energy distributions on December 4 2010**

The distribution of the COP of the chiller is shown in Figure 7.6. The coefficient of performance (COP) for the chiller is given as:

$$COP = \frac{Q_{chill}}{Q_{heat}} \quad 7.1.$$

Where:

$Q_{chill}$  Evaporator heat output

$Q_{heat}$  Generator heat input

The solar coefficient of performance ( $SCOP$  or  $COP_{sol}$ ) is given as:

$$SCOP = \frac{Q_{chill}}{Q_{solar}} \quad 7.2.$$

Where:

$Q_{solar}$  Collector solar energy output

Using equations (7.1) and (7.2) and the energy distributions shown in Figure 7.5, we get the distribution shown in Figure 7.6. The COP of the chiller has an average value of 0.63, which is comparable to the manufacturer's value of 0.7. The solar coefficient of performance has an average value of 0.11.

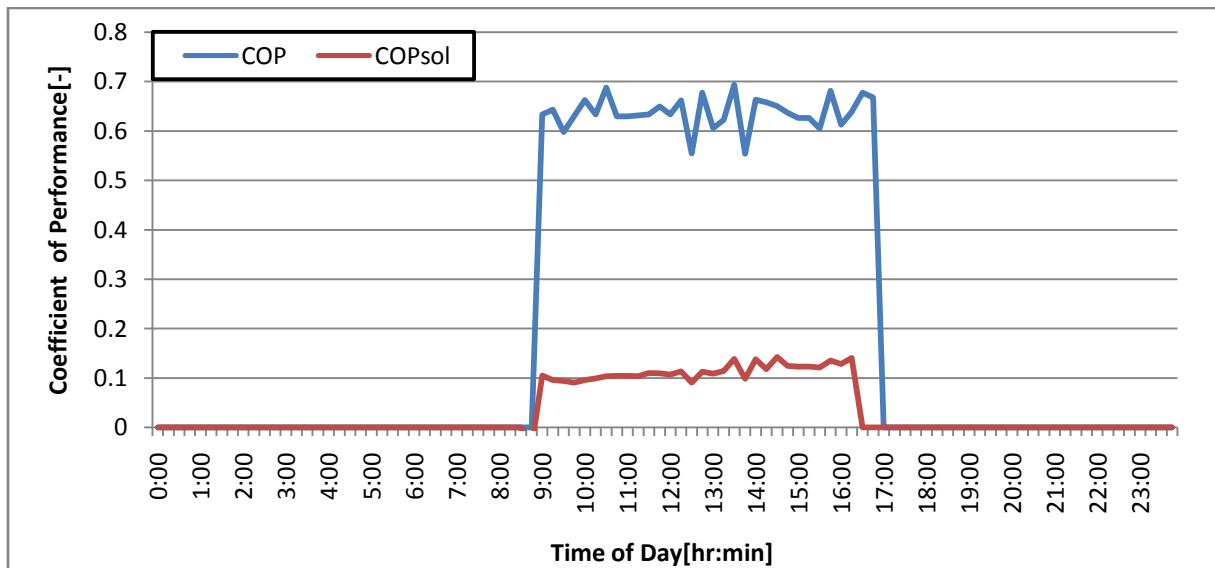


Figure 7.6: Distributions of the Chiller and Solar COP on December 4 2010

### 7.3 Vodafone Site Solutions Innovation Center

The second case study is located at the Vodacom Campus in Midrand. This is an autonomous solar thermal heating and cooling system to maintain room temperature at comfort level around the year. The Vodacom Campus is located at a latitude of 25°58'14''S and a longitude of 28°7'37''. This area receives on average 3128.3 hours of sunshine a year. The key weather parameters for Johannesburg are presented in Table 7.3.

**Table 7.3: Johannesburg Climatic Data (75)**

Variable	Jan	Feb	Mar	Apr	May	Jun	Jul	Aug	Sep	Oct	Nov	Dec
Insolation, kWh/m <sup>2</sup> /day	6.70	6.10	5.46	4.77	4.21	3.80	4.08	4.78	5.69	5.98	6.29	6.62
Clearness Index	0.57	0.55	0.56	0.59	0.64	0.65	0.66	0.65	0.64	0.58	0.55	0.56
Temperature °C	22.23	22.11	21.1	18.66	15.3	11.6	11.5	14.61	18.5	20.20	20.9	21.4
Wind speed, m/s	3.62	3.50	3.37	3.54	3.74	4.04	4.18	4.74	4.95	4.73	4.31	3.77

#### 7.3.1 Building Loads

In Midrand the average ambient temperatures are highest in the period from November to April and the cooling requirements follow the same pattern. During this period the temperatures fall to about 15°C after midnight and these low temperatures are the ones that are responsible for the observed low heating requirements. The outside ambient temperatures start falling below 10°C in April and hence the heating loads for the building start steadily increasing reaching its peak in July. The load profile for the office building is shown in the Figure7:7. The maximum cooling load is around 20kW and is experienced the period from November to February whereas the maximum heating load is 22.5kW and is recorded in July. The annual cooling demand is 18.4MW and the annual heating demand is 3.2MW.



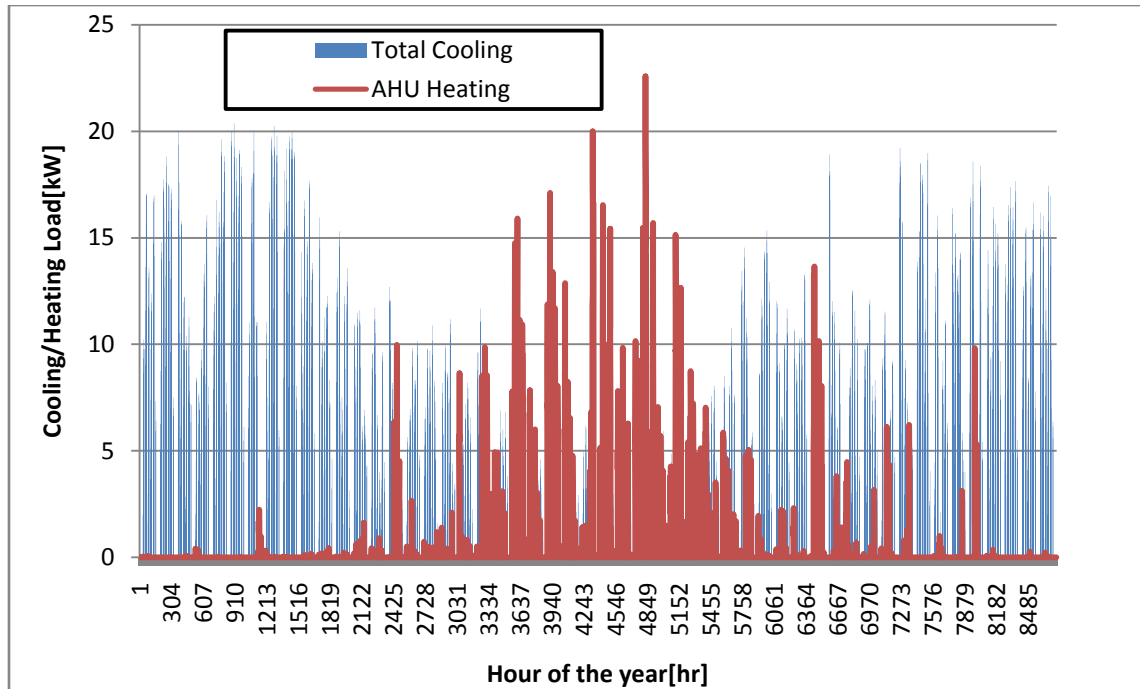


**Figure 7.7: Load Profile for the building**

The peak sizing for the cooling system was performed using January 15 2002. The cooling for the building increases steadily from morning as the ambient temperature and incident solar irradiation increases. The peak cooling load does not occur around midday, when the solar energy is at its maximum but occurs later in the day. This can be explained by the delay due to conduction of the incident solar energy by the walls, roof and windows of the building, this heat energy is later transferred to the cooling space by convection, and hence the demand for cooling energy due to this absorbed heat is experienced a few hours after it has been absorbed. The peak load is 24.87kW and occurs at 16:30, the average load is 8.86kW. This particular day experiences an average dry bulb temperature of 24.4°C, with the maximum of 30°C being recorded at 15:00. The distribution of the cooling for this day is shown in the Figure 7.8.

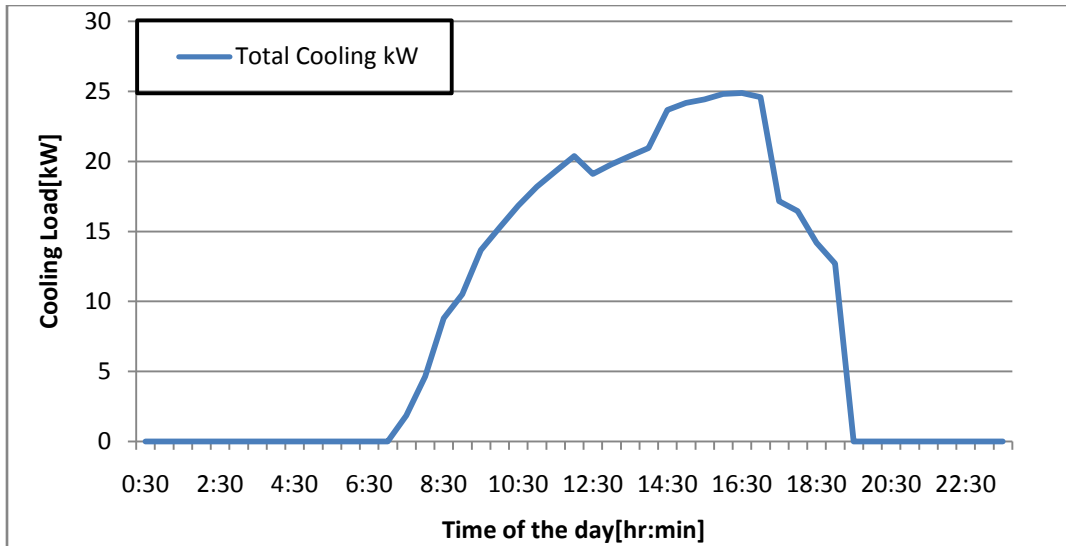


**Figure 7.8: Distribution of the cooling load for January 15**

In winter the system provides heating for the building. In this process the absorption chiller is not involved, a three-way valve is used to bypass the chiller in winter so that hot water can be delivered from the hot water storage tank directly to the air handling unit and the thermally active slab. The heating energy demand quickly rises in the morning, and reaches its peak before midday. The high demand in the morning can be attributed to lower temperatures and incident solar irradiation in the morning, so as the day progresses and the ambient temperature and incident solar radiation increase the building energy demand steadily decreases. The day that experiences the highest heating energy demand is July 21 2002, with a maximum heating load of 22.5kW and an average of 6.64kW.

The distribution of the heating load on this day is shown in the Figure 7.9.

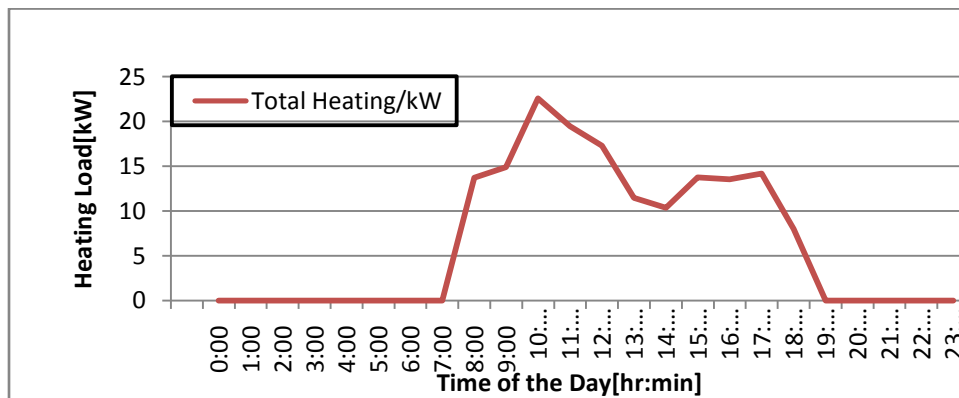


**Figure 7.9: Distribution of heating load distribution on July 21**

### 7.3.2 Solar Array Performance

The collector produces a total of 3048.8kW of energy, at an average of 31.43kW, with a maximum value of 143.7kW on January 31, 2012 refer to Figure 7.10. There is a rapid rise in both the collector outlet and inlet temperatures at 7:45, because that is the time when the primary solar pump is switched on and starts to circulate water in the collectors that have already been warmed up by the early morning sun. The collector inlet is slightly greater than the outlet at the beginning that is why no useful energy is produced by the collector. Once the outlet temperature becomes greater than the inlet then useful energy starts being produced. The useful energy produced increases rapidly in the first hour and then stays approximately constant throughout the day. However, an inexplicable jump in the solar primary rise and fall occurs in the solar primary pump flow rate, hence the very high value of 143.7kW is recorded at 13:45. The graph shows that there is a fairly constant change in these parameters throughout the day.

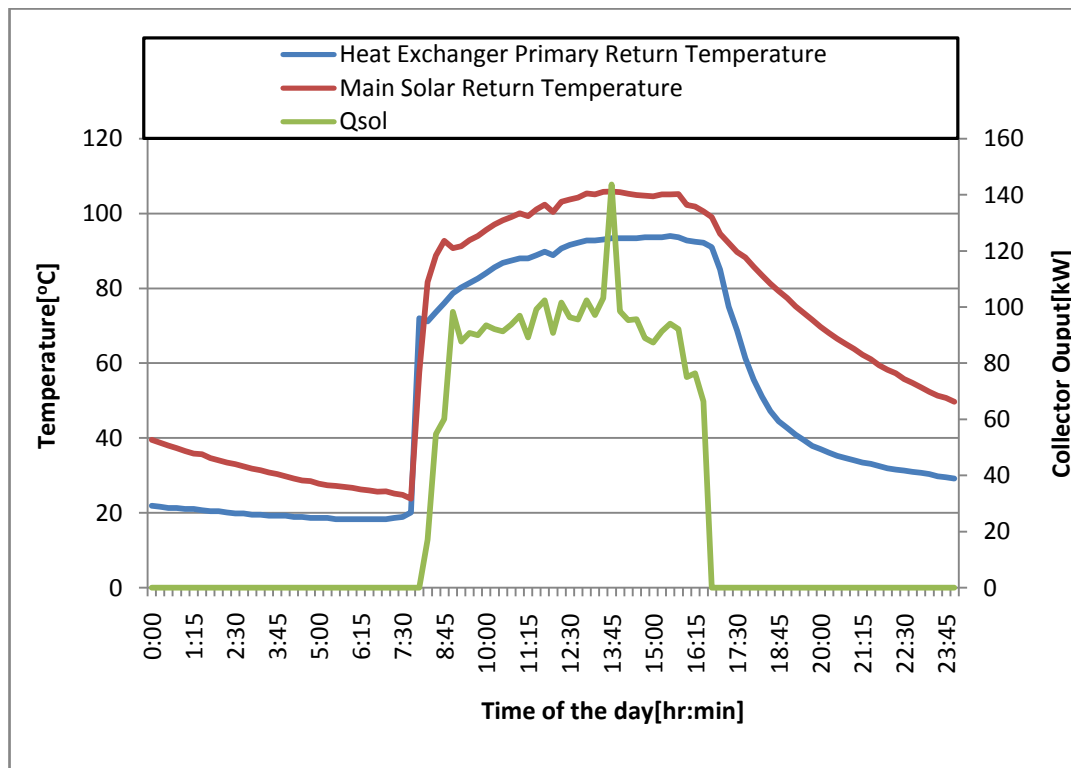


**Figure 7.10: Distributions of collector energy output, inlet and outlet temperature on January 31, 2012**

The total amount of solar irradiation on the collector array is  $33914\text{W/m}^2$ , and multiplying this with the array area of  $116\text{m}^2$  we get the total amount of incident solar energy being equal to  $3.934\text{MW}$ , with an

average of 40.57kW and a maximum of 138.9kW recorded at 12:15. The evacuated tube collectors that are used in this system are defined by the following equation:

$$\eta = 0.745 - 2.007 \left( \frac{T_m - T_a}{G_t} \right) - 0.005 \left[ \frac{(T_m - T_a)^2}{G_t} \right] \quad 7.3.$$

$T_m$  Collector average temperature

$G_t$  Incident solar energy

$T_a$  Ambient temperature

The third term on the right hand side of equation (7.3) can be neglected without any significant effect on the collector efficiency. In the morning, the collector average temperature is approximately equal to the ambient temperature so the collector efficiency is equal to the nominal efficiency of 0.745. There is a rapid increase in the difference between the average collector temperature and the ambient temperature and hence the sharp decrease in the collector efficiency. As the incident solar energy increases, the efficiency starts increasing with a distribution similar in shape to the solar energy distribution and reaches its peak around mid day. The incident solar radiation then steadily decreases after mid day and consequently the collector efficiency does the same. The distribution of the collector efficiency given by the above equation is shown in the Figure 7.11.

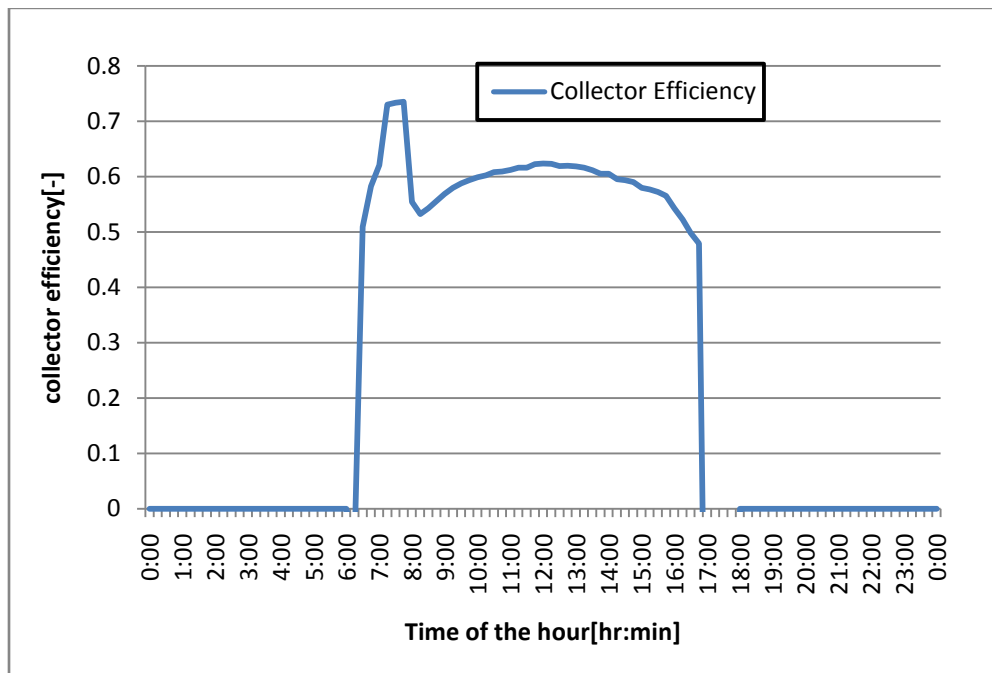
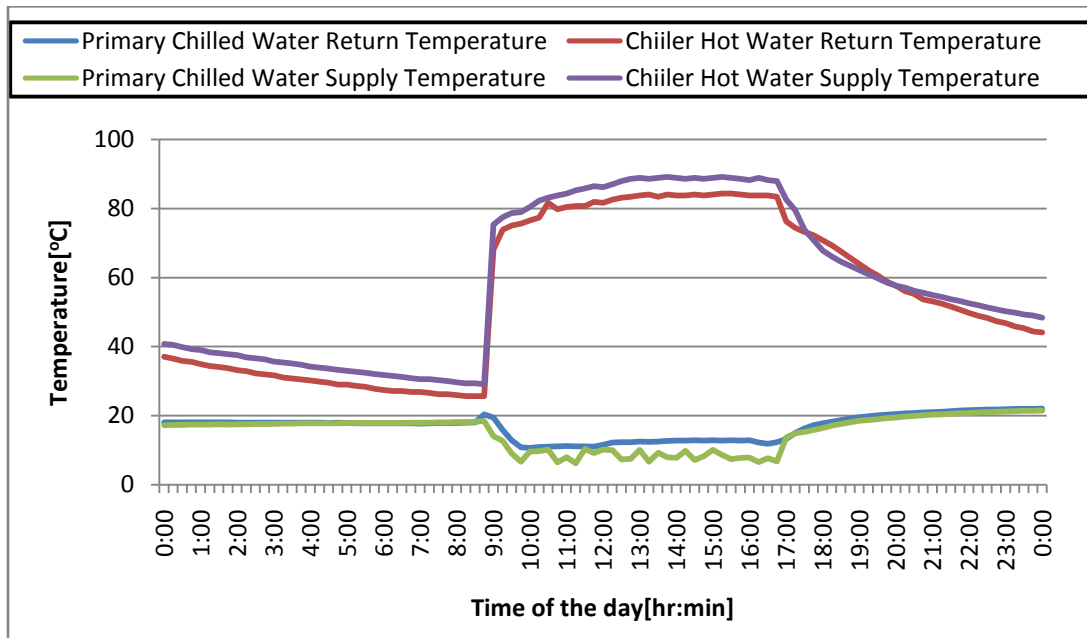


Figure 7.11: Distribution of collector efficiency on January 31, 2012

### 7.3.3 Absorption Chiller Performance

The distribution of the temperature streams going in and out of the chiller is presented in Figure 7.12. The chiller is energized by water temperature between 70°C and 95°C, but the system control strategy states that the chiller will only start producing cooling energy if the hot water temperature that is being inputted into the generator exceeds 80°C. The system performance values were recorded at 15minute intervals and there are 96 data points on January 31, 2012. Of these recorded values, 35 of them, representing 36.5% of the time were above 70°C, meaning the chiller could have run for 36.5% of the time if required. The generator inlet temperature exceeds the threshold value of 80°C for 28 of these recorded values representing 29.2% of the time.



**Figure 7.12: Temperature distributions of the chiller water streams on January 31, 2012**

It can be seen that the hot water stream temperatures rise sharply when the chiller is switched on at 9:00 then they become fairly constant before gradually falling after the chiller is switched off at 17:00. The chilled water return temperature starts decreasing gradually at chiller switch on, and then evens out as the day progresses. This is different from the chilled water supply temperature which shows an up and down trend. This is because the system control strategy requires that the chiller switches off if the chilled water supply temperature falls below 7°C, so each time the temperature falls below 7°C the chiller temporarily stops hence the displayed distribution. This is also seen in the variation of the chiller COP and solar COP as seen in Figure 7.13 below.

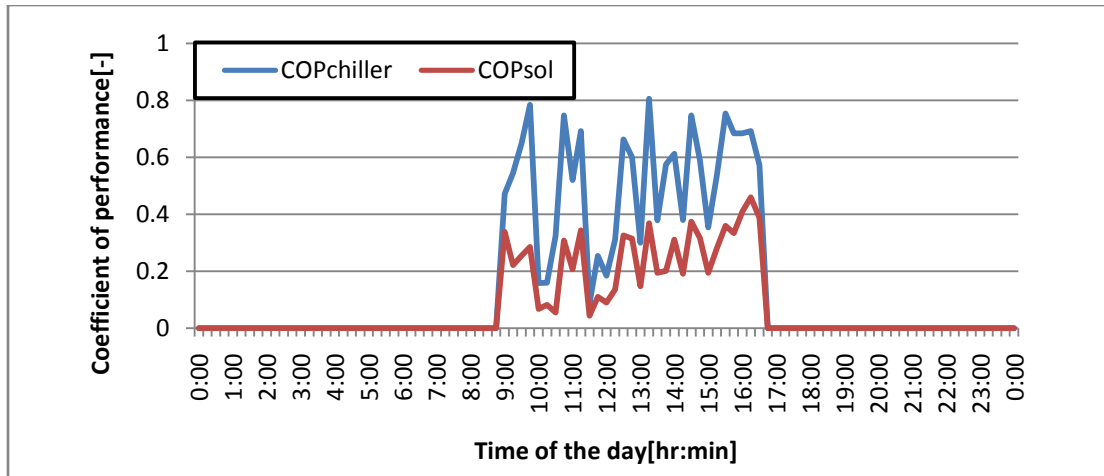


**Figure 7.13: Distributions of COP and SCOP on January 31 2012**

### 7.3.4 Air Handling Unit (AHU)

The air handling unit is in operation between 6:00 and 18:00 and its pump will be switched on if the average building space temperature exceeds 22°C. The average building space temperature reaches 22°C at 10:15 and the air handling unit pump is switched on. The difference between the air handling unit return and supply water streams decreases at the moment the pump is switched on hence the sharp decrease in the cooling energy produced that is observed. The average building space temperature continues increasing until it reaches a peak of 24.9°C, then it starts decreasing. The building space temperature does not surpass the set temperature of 25°C, during this period, showing that the air handling unit is able to maintain the building space conditions at the desired levels. The air handling unit only starts to produce cooling energy when the pump is turned on. It produces a total of 384kW at an average of 3.96kW with a maximum of 24.28kW. The distribution of the inlet and outlet water temperatures and the cooling energy are shown in Figure 7.14. The air handling unit produces energy at a fairly constant rate throughout the day.

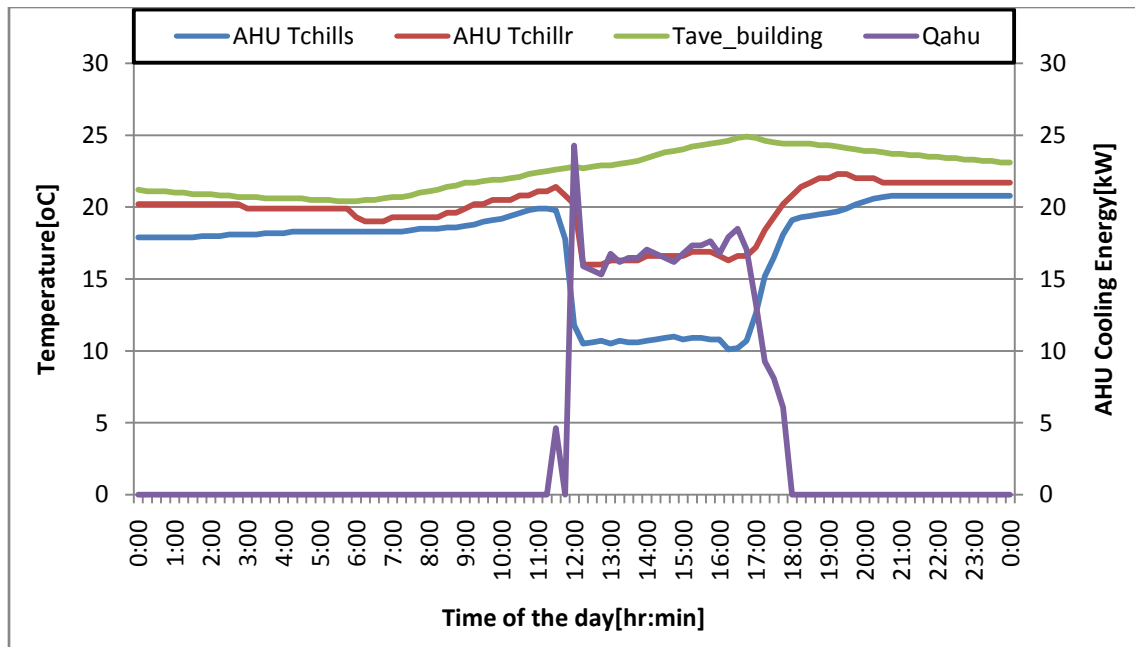


**Figure 7.14: Distributions of the AHU temperatures of the water streams and cooling energy on January 31, 2012**

### 7.3.5 Thermally Activated Slab (TAS)

The Thermally Activated Slab (TAS) acts by reducing the building cooling load through radiant and convective cooling as the cold water travels in the embedded pipes underneath the floor. On January 30, 2012 the TAS produced 1527kW of energy at an average of 15.74kW with a maximum of 45.52kW. These large amounts of cooling energy produced are the ones that resulted in the AHU producing an average of 3.96kW, which represents about 15.3% of its total cooling capacity. The TAS satisfies the bulk of the cooling demand. The energy is produced from the moment that the slab pumps are switched on and the energy production proceeds at a rate that is approximately constant. The input and outlet temperatures of the TAS are also fairly even throughout the day. The variations of these temperatures and the cooling energy produced are shown in Figure 7.15.

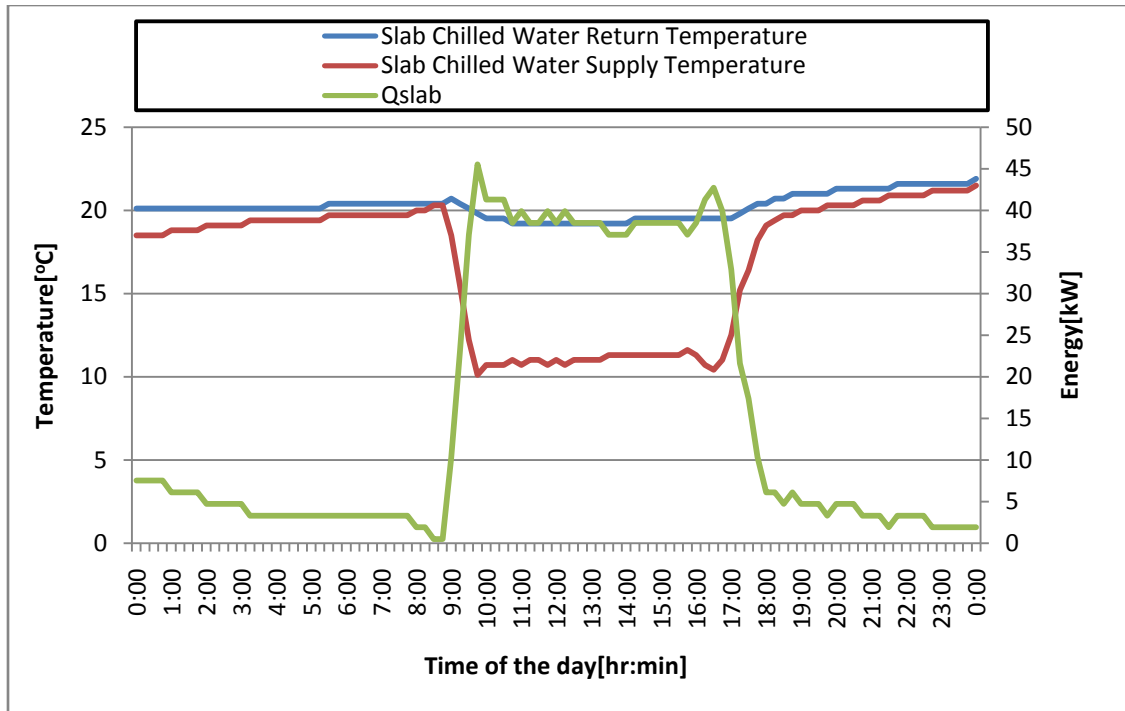


**Figure 7.15: Distributions of the TAS water stream temperatures and the cooling energy on January 31, 2012**

### 7.3.6 Dehumidification Fins

The thermally active slab uses radiant cooling so the water vapor that is in the air condenses as the room air temperature decreases. To take care of these increases in humidity dehumidification fins are always installed together with the thermally active slab. The dehumidification fins are controlled by a time schedule between 8:00 and 17:00. The system is supposed to maintain the building humidity in the range 50-60%, and when the dehumidification fins starts operating at full capacity to reduce the humidity and maintain it in the desired range. As observed for the temperatures of the supply and return water stream temperatures, the dehumidification fins operate at fairly constant rate until 17:00 when they are automatically switched off. These fins not only reduce the air humidity but also do some cooling of their own. The fins produced 253kW of cooling energy at an average of 2.6kW with a maximum of 11.1kW. The Figure 7.16 shows these variations.



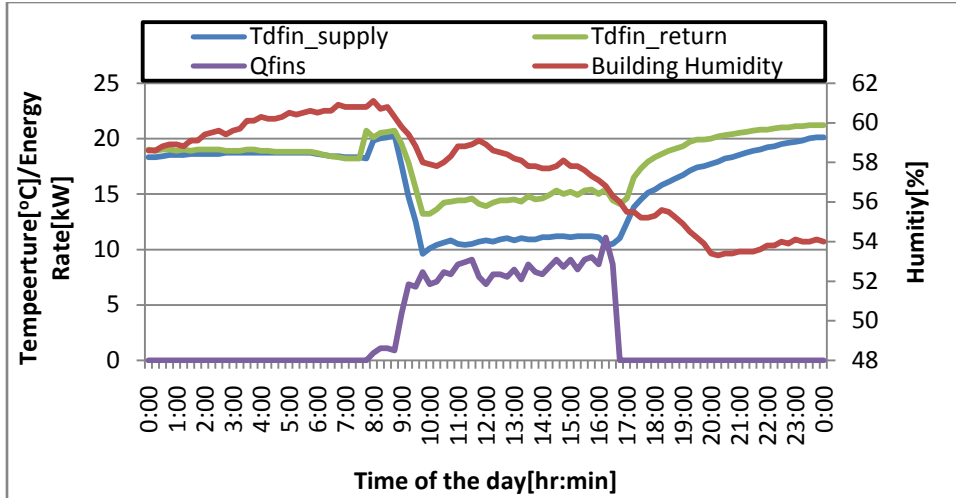


Figure 7.16: Distributions of the inlet and outlet water temperatures and the dehumidification fins cooling energy on January 31, 2012

### 7.3.7 Dry Cooler

The heat of condensation and absorption is removed from the absorption chiller through use of a dry cooler. The sensor from the dry cooler pump flow recorded a strange value for the first 15mins after switching on hence the calculated value for the cooling energy produced is way above the 86.68kW which is the maximum duty that the dry cooler can provide. Ignoring that strange value, it is observed that the dry cooler produced a total of 1741kW at an average of 56.2kW with a maximum of 70.45kW.

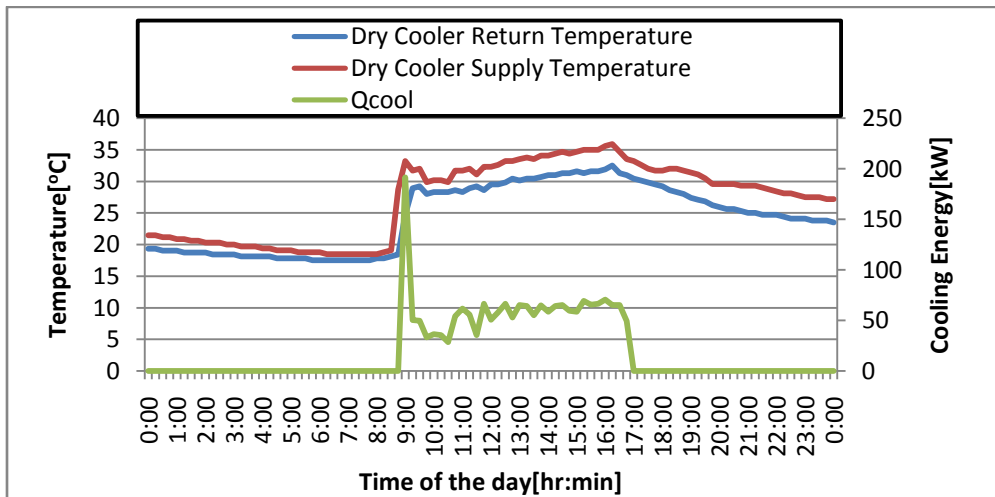
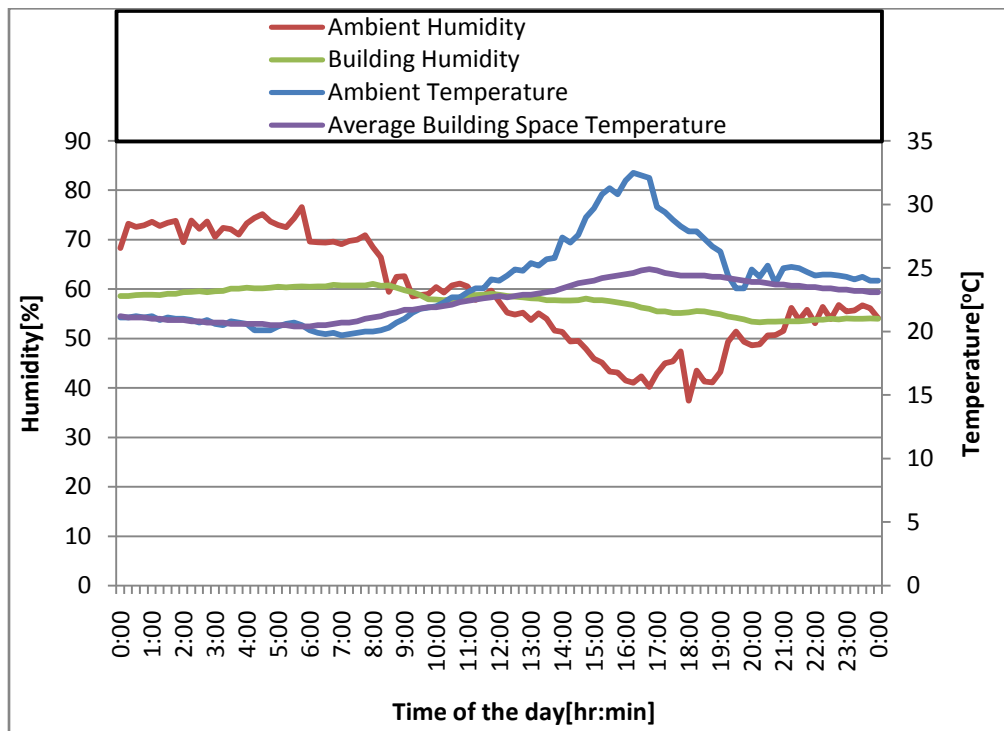


Figure 7.17: Distributions of the inlet and outlet water temperatures and the dehumidification fins cooling energy on January 31, 2012

### 7.3.8 Building environment

The system was designed to keep the building space temperature between 20 and 25°C, and the humidity between 50 and 60%. The ambient conditions determine the amount of work that the system has to perform for these desired conditions to be maintained. On 31 January 2012, there was an average ambient temperature of 23.82°C, with a maximum temperature of 32.5°C, whilst the ambient humidity had an average of 58.82% and a maximum of 76.6%. The solar cooling system was able to maintain the temperature within the desired limits throughout the day, with the average building temperature having a mean value of 22.47°C and a maximum of 24.9°C and a minimum of 20.4°C. The humidity had an average value of 57.6% with maximum and minimum values of 61.15 and 53.3% respectively.



**Figure 7.18: Distributions of the ambient and building humidity and temperatures on January 31, 2012**

## 7.4 Vodafone SSIC Economic Analysis

The costs of a solar powered cooling system can be broken down into capital costs, operating costs and costs for energy. In this case, the system is wholly dependent on solar energy so the costs of energy can

be neglected without any significant loss of accuracy. The capital costs for the Vodafone SSIC system are shown in Table 7.4.

**Table 7.4: Vodafone SSIC System Capital Costs**

Item	Costs[R]
Air Conditioning Equipment	1, 918,544.00
Solar Equipment	559,422.89
De-humidification Fins	270,000.00
Thermally Activated Slab	118,350.00
Total Installation Value	2,866,436.89

To measure economic performance we use the total cost of the cooling system. We will make use of the annuity method, where all cash flows are connected into a series of annual payments of equal amounts. The annuity is found by first calculating the net present value (NPV) of all costs occurring at different times during the project, i.e. by discounting all costs to the time when the investment takes place. The NPV is the total present worth of the gains from the solar system compared to the electricity only system. The initial investment costs as well as further investments for component exchange in further years result in a capital value of the investment, which is calculated using the rate of inflation and the basic interest rate ( $d$ ). The capital value is given as:

$$CV = \sum P(t) \frac{(1+f)^t}{(1+d)^t} \quad 7.4.$$

Where:

$CV$  Capital value

$P(t)$  Investment at time  $t$

$t$  Time

$d$  Basic interest rate

$f$  Inflation rate

The prime interest rate given by the South African Reserve Bank as of May 2012 is 5.75% and the inflation rate is 9% (76). With these values the CV is found as R1 934 844.90.

Annual expenses for maintenance and plant operation, which occur regularly during the life of the plant, are discounted to the present value by multiplication of the expenses with the present value factor (PVF). The PVF is given by the following equation:

$$PVF(N, f, d) = \frac{1 + f}{d - f} \left[ 1 - \left( \frac{1 + f}{1 + d} \right)^N \right] \quad 7.5.$$

Where:

$PVF(N, f, d)$	The present value factor
$N$	Life time of the plan
$f$	5.75
$d$	9
$N$	The PVF is calculated to be 2.08

In the case of solar cooling plants, no annual income is generated (70), so that the NPV is simply obtained from the sum of discounted investment costs and the discounted annual expenses. It is here defined with a positive sign to obtain annuity values:

$$NPV = CV + EX \cdot PVF(N, f, d) \quad 7.6.$$

Where:  $EX$  Annual expenses

The annual expenses include maintenance costs, energy and water costs. The maintenance costs over the lifetime of the system are taken as 2% of the initial capital investment and the average life of the system is taken as 20 years (70). The annual expenses ( $EX$ ) are found to be R57328.74. This consequently results in the NPV for the system being equal to R2, 054,088.64

To obtain the annuity, the NPV is multiplied by a recovery factor,  $r_f$  which is calculated from the discount rate and the life time of the plant.

$$a = NPV \cdot r_f(N, d) \quad 7.7.$$

Where:

$r_f$  Recovery factor and is given as:

$$r_f = \frac{d(1+d)^N}{(1+d)^N - 1} \quad 7.8.$$

The recovery factor,  $r_f$  is calculated and found to be 0.11. The annuity for the system is R225, 949.75

The cost per kWh of cooling energy produced is the ratio of the annuity divided by the annual cooling energy produced (70). The cost per kWh is R28.88. This is very high compared to the current prevailing tariffs which are shown in Table 7.5. One possible reason for such a high cost per kWh is the fact that this particular system is an autonomous solar system hence it is oversized to cater for times of low solar energy.

**Table 7.5: Commercial power tariffs from 1 April 2012 (77)**

	Service charge [R/day]	Network Charge [R/day]	Energy Rate [c/kWh]	Environmental levy Charge[c/kWh]	
				Apr to Jun	Jul to Mar
Business rate 1	12.95	15.05	83.23	Apr to Jun	Jul to Mar
Business rate 2	12.95	25.37	83.28	2.28	3.99
Business rate 3		43.83	83.28	2.28	3.99
Business rate 4			211.86	2.28	3.99

NB: all rates are Vat Inclusive

## CHAPTER EIGHT

---

### **8 COMPARISON OF SIMULATION AND SYSTEM PERFORMANCE RESULTS**

#### **8.1 Overview**

In this chapter the results of the case study performance analysis and the simulations are compared and any discrepancies noted and explained. The TRNSYS simulation results show good agreement with the recorded system performance results. Possible sources of the differences include the weather conditions, thermal losses from the transportation pipes and simulation software limitations.

#### **8.2 Moot Hospital System**

This case study was installed in combination with the existing vapor compression air conditioning system with the aim of demonstrating the operating and economic characteristics under South African climatic conditions. The initial design included two storage tanks with a volume of 600 liters each, one was to store hot water while it was intended that the other one would contain phase change materials (PCM). This plan was later abandoned due to the prohibitive costs of the PCM, but only after the system had already been constructed. As a result the system cost much more than anticipated and was a bit over designed and hence no accurate economic data can be deduced from it. It was also envisaged that the system capacity was going to be increased from 35kW to 200kW but those plans were later abandoned and the system has since then been decommissioned. Having said that, the Moot Hospital cooling system still provides a good idea as to the technical effectiveness of solar powered absorption systems and here a comparison is made between the experimental/recorded performance data and the results of the TRNSYS simulation.

##### **8.2.1 Solar Thermal Collector Performance**

When this system was installed there were a lot of oversights and as a result there is no accurate data available detailing the solar irradiation that was incident on the solar collector array. By the time we participated in the project, it had already been decided that the project was not going to be extended into the next phase and the level of maintenance of the data collection system in particular had gone down and

even some of the sensors that had been initially installed were no longer being serviced when they broke down. This made comparing the simulation collector performance and the actual collector thermal performance difficult. Fortunately, the temperature sensor for the collector outlet temperature was still working and a comparison of the collector outlet temperatures is presented in Figure 8.1 below. The recorded outlet temperature is about 6% higher than the simulated outlet temperature; this can be attributed to differences in the actual weather on the day and the weather data used for the simulation.

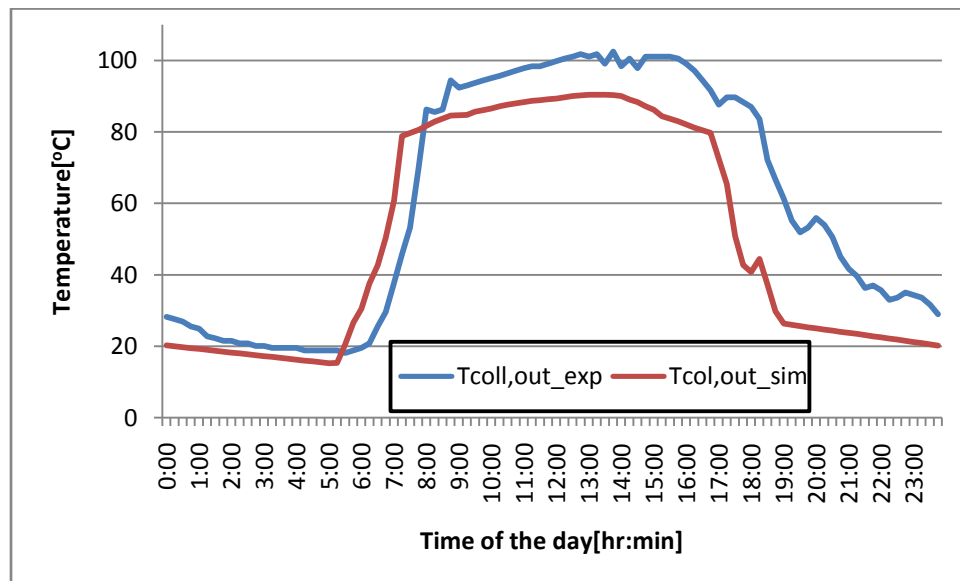


**Figure 8.1: Collector outlet temperature distributions for December 4**

### 8.2.2 Absorption Chiller Performance

The chiller water stream temperature distributions are compared in Figure 8.2; the recorded values for the hot water streams are slightly higher than those for the simulated values. The major observable difference is that the recorded temperatures start and end with much lower values. They closely follow the distribution of the incident solar radiation. On the other hand the simulated values are maintained at a more or less constant value throughout the day. The possible reasons for these differences are wind speed effects, thermal losses from the tank, cloud cover and thermal losses from the distribution pipes. All these losses are difficult to account for in the TRNSYS simulation environment hence the hot water temperature distributions do not go down during the time when the chiller is switched off. The simulation results also show a relatively higher temperature difference between the inlet and outlet streams hence the

amount of heat energy supplied to the chiller and the cooling energy produced are higher for the simulation than what was recorded. This is seen in the energy rates distributions in Figure 8.3.

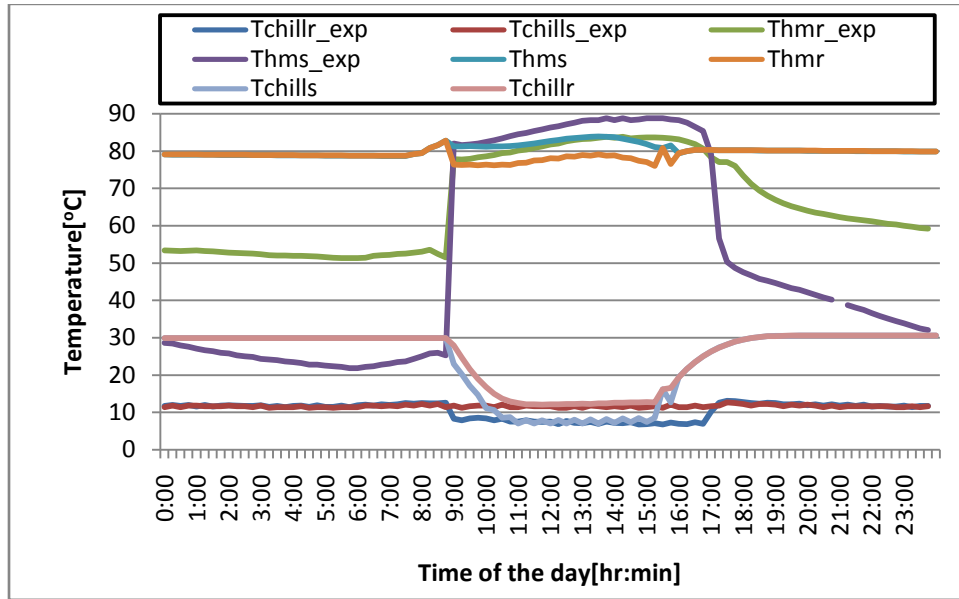


**Figure 8.2: Comparison of the chiller water stream temperature distributions for December 4**

The energy rates distributions also follow the same trend as the temperatures with the recorded values increasing for the time the chiller is switched on and reaching a maximum towards the end of the day, whereas the simulated values are fairly even throughout the day.

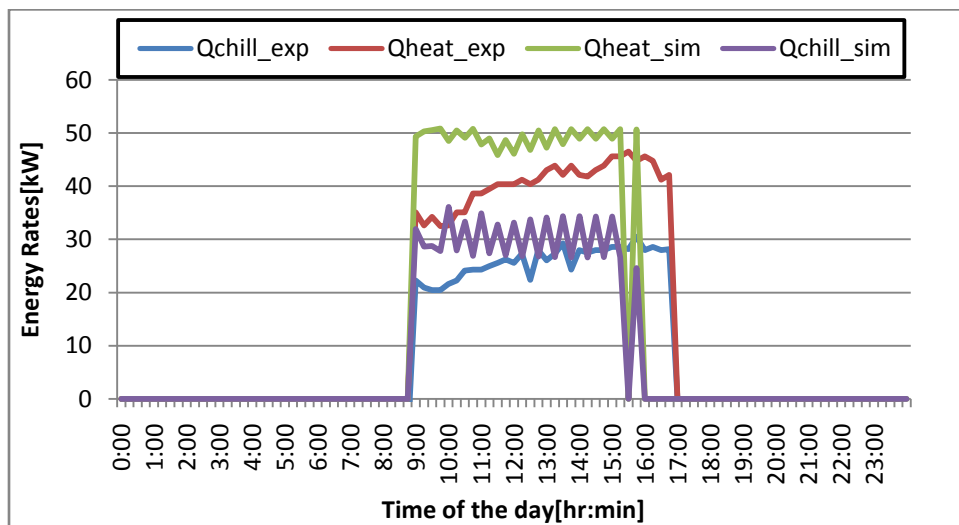


**Figure 8.3: Comparison of the heat medium energy and the cooling energy for December 4**



The simulated average values are higher than the recorded values but the total amounts of energy are comparable and are shown in Table 8.1 below.

**Table 6: Summary of the simulated and recorded chiller energy rates**

	Recorded, Qchill_exp	Simulated, Qchill_sim	Difference (%)	Recorded, Qheat_exp	Simulated, Qheat_sim	Difference (%)
Sum/kW	827.4	813.4	1.69	1298.2	1330	2.39
Average/kW	25.9	29.1	10.9	40.6	47.5	14.5
Maximum/kW	30.5	36.1	15.5	46.5	50.8	8.46

For the simulation system performance results, the heat energy input into the generator is fairly even through the day, whereas the chilled water energy produced oscillates with an average of 29kW, and hence the distribution closely resembles the chilled water distribution. The COP for the simulation has an average value of 0.61 whereas for the recorded system performance results have an average of 0.63. The chiller COPs are shown in Figure 8.4.

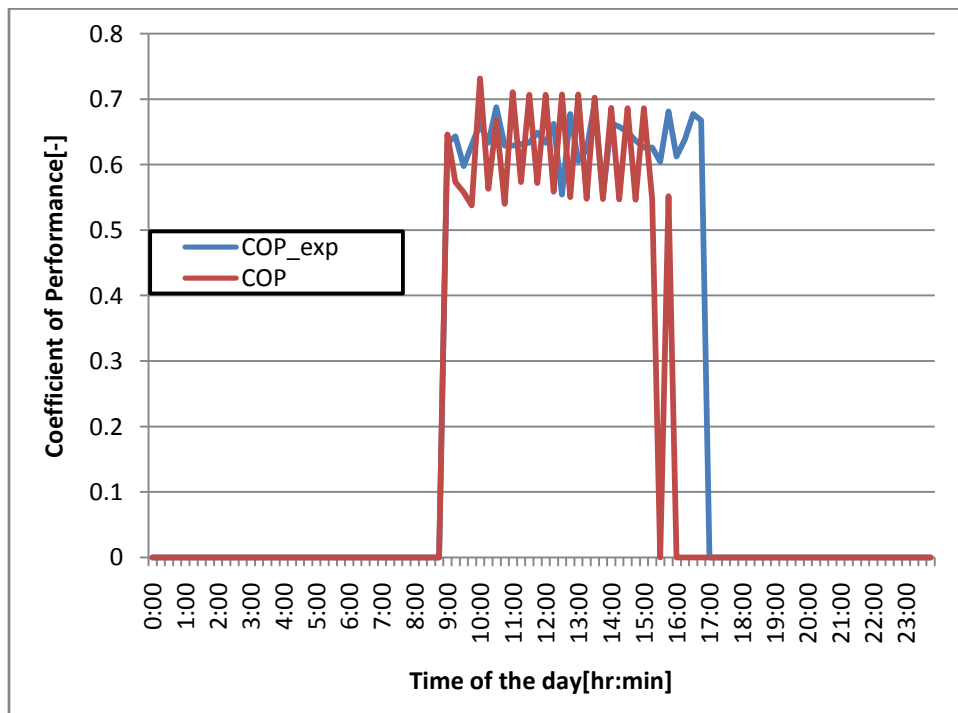


**Figure 8.4: Comparison of the recorded and simulated COPs on December 4**

### 8.3 Vodafone Site Solutions Innovation Center (Vodafone SSIC)

This case study is located at the Vodacom Campus in Midrand and is an autonomous solar heating and cooling system designed to keep conditions in an office building at comfort levels. There are some observed differences between the simulation results and the recorded system performance results. The ambient temperature and all other system performance parameters were measured at 15min intervals, whereas the simulation weather data is presented for every hour. As a result the simulation weather produces a smooth curve and the recorded weather has a curve that shows data points at 15 minute intervals. The major cause of the observed differences is the weather data. The TRNSYS simulation software has weather data that is in the Typical Meteorological Year 2 (TMY2) format. A typical meteorological year (TMY) is a collation of selected weather data for a specific location, generated from a data bank much longer than a year in duration (78). The TMY consists of months selected from different years combined to form a complete year. This is the weather data that is used in the simulation whereas recorded data can vary significantly from year to year. An example of these weather differences is shown in the distributions of ambient temperature shown in Figure 8.5.

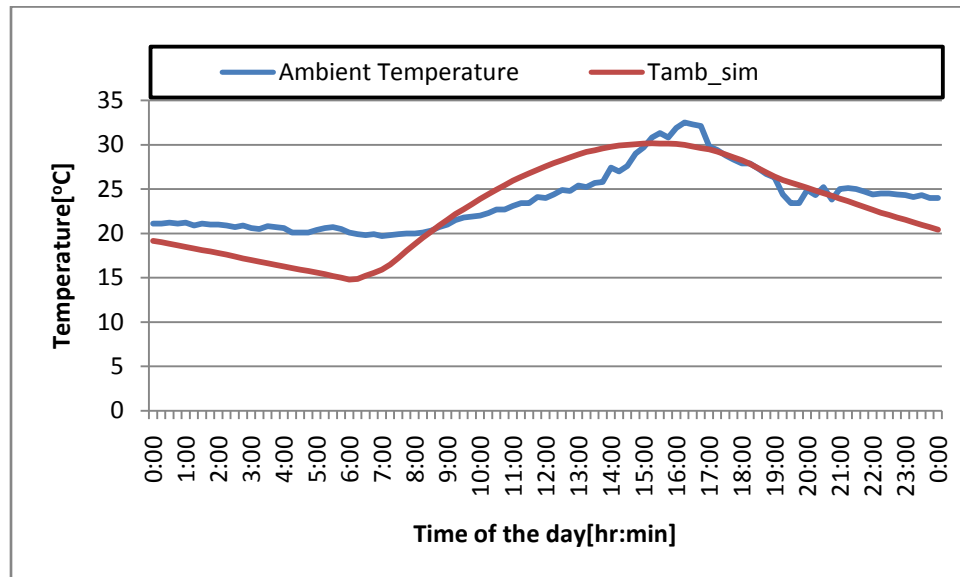


Figure 8.5: Distributions of ambient temperatures on January 31

### 8.3.1 Collector Thermal Performance

The simulation collector model does not include the effects of cloud cover and wind velocity. The variations seen on the experimental curve can be explained by these two phenomena. Also the exact amount of heat loss cannot be measured in the simulation model and hence the simulation model produces a smooth curve whilst the one for the experimental results is not due to the above stated effects. The collector useful energy output distributions on January 31 are shown in Figure 8.6. The recorded values are about 12% higher throughout the day.

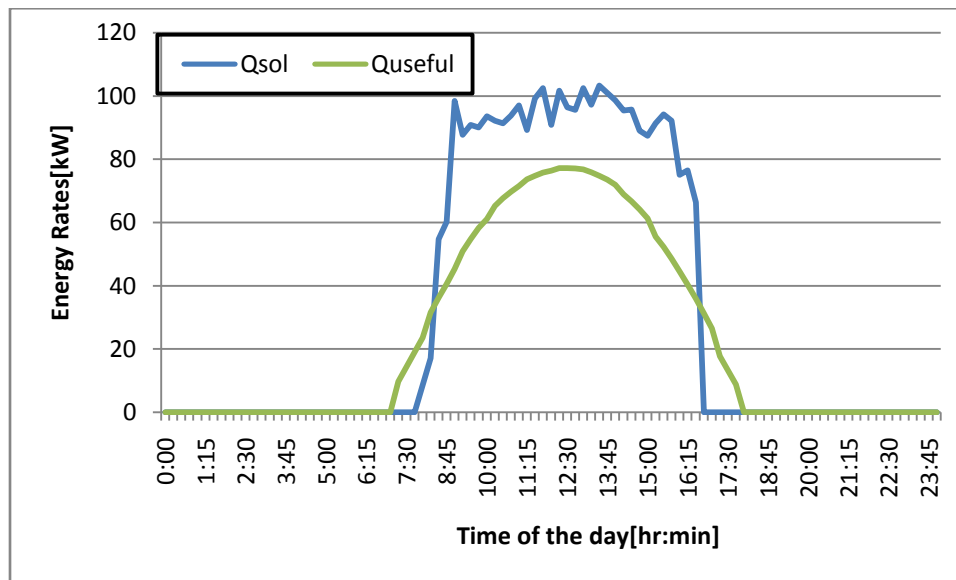
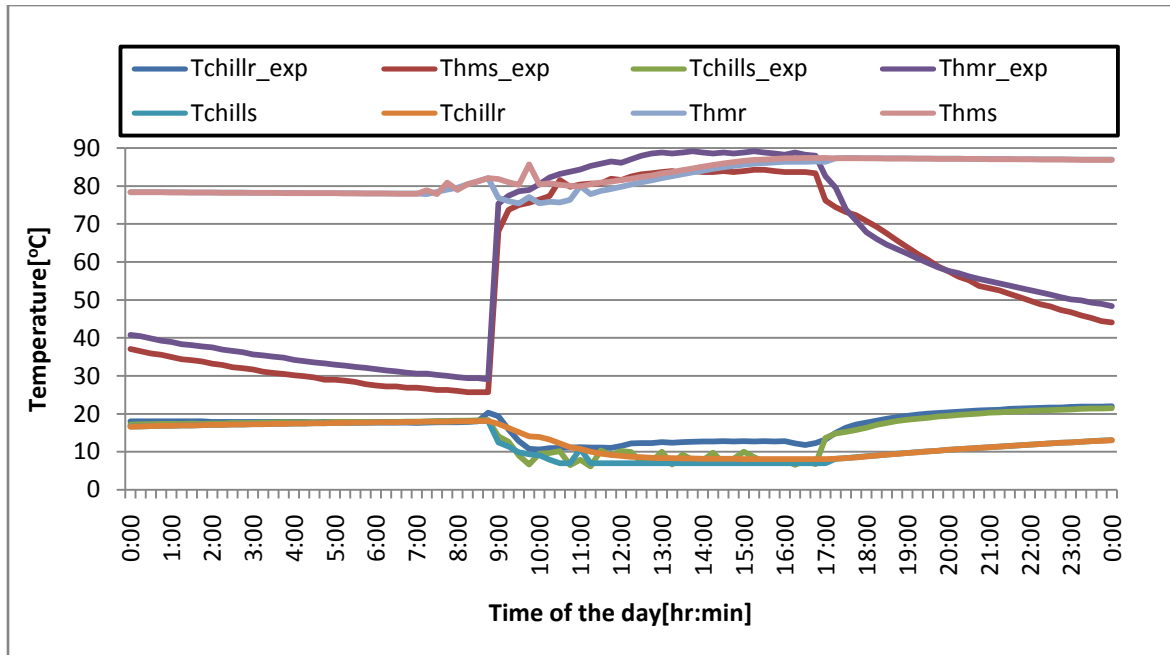


Figure 8.6: Comparison of collector useful energy output on January 31

### 8.3.2 Absorption Chiller Performance

The temperature distributions for the chiller water streams are shown in Figure 8.7. The differences are minimal and can be attributed to the difference in real and simulated weather conditions. The simulation does not simulate heat losses in the distribution pipes and the thermal loss to the environment for the tank, but most significantly there is no component in TRNSYS that simulates a partitioned storage tank as is used in this case study. The simulated hot water stream temperatures remain high throughout, the simulation does not indicate when the chiller has switched off, and it still records water temperature value even though no water will be flowing into the chiller. There is an average of 2°C difference between the simulated and recorded values.



**Figure 8.7: Comparison of the chiller water stream temperature distributions for December 4**

Figure 8.8 shows the distributions of the energy rates on January 31. The energy rates depend on the temperature differences between the inlet and outlet water streams and the water flow rates of these streams. In the case of the simulated results the chiller temporarily stops producing energy around 11:00 due to the temperature differences being equal to zero as indicated in Figure 8.8. Afterwards, the variation of the two energy streams is approximately quadratic. The recorded values oscillate closely resembling the chilled water and hot water supply temperatures.

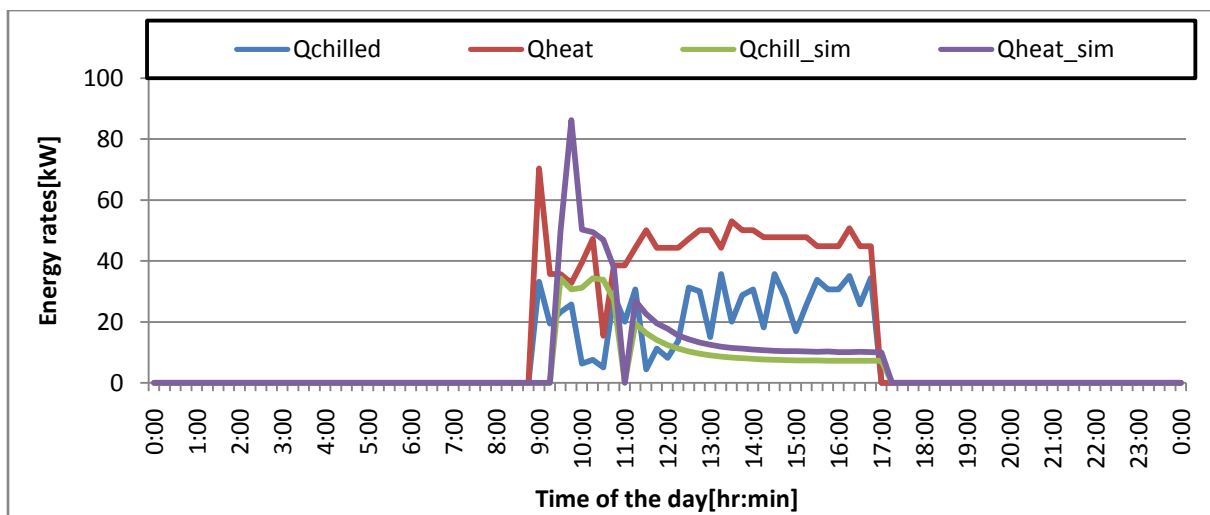


**Figure 8.8: Distributions of the heat medium and chilled water energy rates on January 31**

The COP distributions are shown in Figure 8.9 below. The COP for the simulation is fairly constant because of the uniform variation of the energy rates, whereas that for the recorded system results mirror the distribution of the recorded system performance results. The highest COP obtained for both cases is slightly higher than the manufacturers stated value of 0.7.

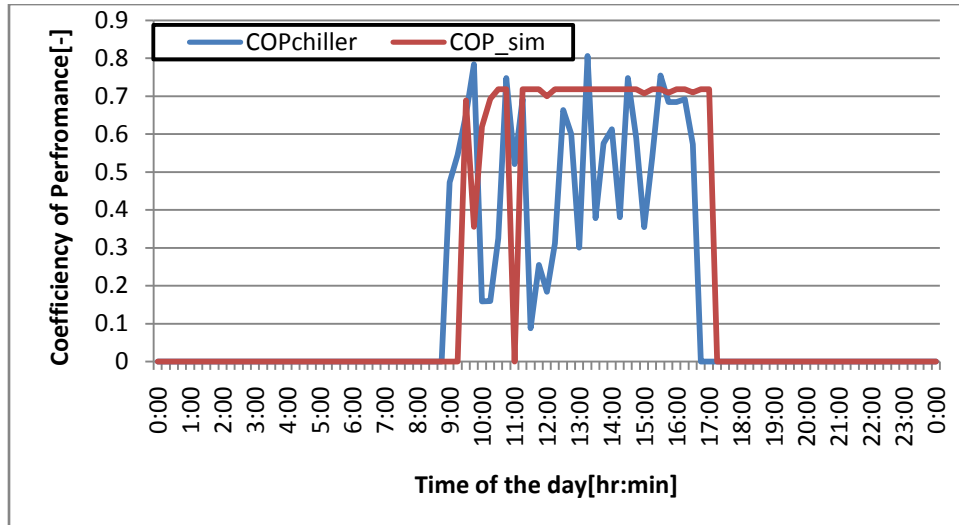


Figure 8.9: The distributions for the simulated and recorded COP on January 31

## CHAPTER NINE

---

### 9 CONCLUSIONS AND RECOMMENDATIONS

#### 9.1 Conclusions and Recommendations

The earth has been experiencing an increase in annual mean temperatures and these have led to an increase in the use of air-conditioning in the hot/humid climates and consequently a significant increase in the demand for primary energy during the summer months. Conventional air conditioning systems make use of the vapor compression cycle, but increased global warming and environmental effects of chlorofluorocarbons have stimulated interest in the development of absorption systems. The resulting electricity overloads have created a pressing need for the utilization of alternative energy for air-conditioning purposes. Solar energy is a very good candidate for utilization in air conditioning applications because peak cooling loads coincide with maximum available solar power.

This Master's thesis has presented an investigation of solar powered absorption systems for South Africa. Two case studies, one at Moot Hospital in Pretoria and another at the Vodafone Site Solutions Innovation Center in Midrand were simulated and had their system performance data recorded and analyzed. These two sets of results were also compared and the major conclusions drawn from the study are presented in this chapter.

The simulations were carried out using TRNSYS and the results showed good agreement with the recorded system performance results. There were some observed differences and these can be mostly attributed to weather data that is used in TRNSYS. The weather data in TRNSYS is in the form of a typical meteorological year which is a data set of meteorological elements which consist of months selected from different years combined to form a complete year. This is in contrast with the recorded data that can vary greatly from year to year. In addition, the solar thermal losses in the distribution pipes cannot be adequately catered for in the simulation.

The main objectives of this study were to show the technical effectiveness of solar power cooling systems and to obtain an idea of the costs involved. Reliable solar system design can only be done through detailed dynamic systems simulations which consider the operating conditions and system configuration of the chiller and cooling load distribution of the conditioned space. The Netcare Moot Hospital plant in particular showed the importance of proper design for such infrastructures. Given the major capital outlays required unnecessary costs can be incurred with slight miscalculations in the design of the system.

The Netcare Moot Hospital system ended up with two hot water storage tanks of 600 litres each, when only one was needed to carry out the cooling operation. For new buildings, to reduce the overall strain on the system, pre-cooling of the supply air to the conditioned space is an effective way to reduce the cooling load as illustrated by the rock storage that was installed in the Vodafone SSIC system. It is important to factor in the air-conditioning system when the initial design of the building is done.

It is more cost effective to utilize solar powered cooling system in combination with a conventional vapor compression system, as autonomous solar operation leads to an oversized system to cater for the periods with low or no incident solar energy. The control system is also a very important part of the system and has a decisive influence on the overall efficiency of the solar powered cooling system. For high solar system efficiency, an early start up of the system is required and this can be achieved by use of a partitioned tank. Standard chiller start-up temperatures are around 80°C and if we have a tank that is partitioned, these temperatures can easily be reached by heating a reduced volume of water and the system can start well before the average time of 11:00.

## **9.2 Recommendations for Future Work**

The Netcare Moot Hospital system was installed with the intention of demonstrating solar powered absorption cooling and to give an indication of the costs. Unfortunately the system was inadequately designed and did not act as an accurate measure of both the technical and financial performance, so there is need to properly design and install a system and get a more accurate reflection of solar powered absorption cooling. Additional work needs to be done regarding the cooling of absorption chillers, because currently this can only be achieved through use of a wet or dry cooling tower. The space requirements for this cooling system make it impossible to think of solar powered absorption cooling as an alternative way of achieving domestic air-conditioning. There is also a shortage of small unit absorption chillers that are fit for residential applications. Given the high levels of solar radiation available in South Africa, there is need to assess the effectiveness of the utilization of flat plate collectors as opposed to evacuated tube collectors will affect system performance. This has the potential of reducing the initial system costs since flat plate collectors are on average cheaper than evacuated tube collectors. Another way to reduce the costs will be to include provision of hot water as part of the design brief for the solar powered absorption system. There is also need to accurately predict the electrical consumption of the system components to get an accurate idea of the energy savings. The system control strategies should also take into consideration the building occupancy patterns, so that the system can feed the cold water produced into the storage tank during periods of lower occupancy.

Finally having proven the immense potential of solar powered absorption systems, there is need to lobby the government to put in place incentives for people to use the technology. Legislation that for example compels people to install solar cooling systems in all new commercial and industrial buildings exceeding a certain size can be enacted. ESKOM can also help in this by coming up with a rebate for such systems.



## 10 References

1. **IEA SHC Task 38.** *Solar Air-conditioning and Refrigeration Position Paper*. October 2011.
2. **Tsoutsos T, Aloumpi E, Gkouskos Z, Karagiorgas M:** *Design of a Solar Absorption Cooling System in a Greek Hospital*: Energy and Buildings, 2009 pages 265-272, Vol. 42.
3. **Haw M and Hughes A:** *Clean Energy and Development for South Africa: Background Data*. 2007.
4. **Weiss W and Mauthener F:** *Solar Heat Worldwide: Markets and Contribution to the Energy Supply 2008; Solar Heating and Cooling* : International Energy Agency, 2011.
5. **Henning M:** *Solar Air Conditioning of Buildings-An Overview*. 2005.
6. **Hang Y, Qu M and Zhao F:** *Economical and Environmental Assessment of an Optimized Solar Cooling System for a Medium-Sized Benchmark Office Building in Los Angeles, California* : Renewable Energy, 2011pages 648-658, Vol. 36.
7. **Florides GA, Kalogirou SA, Tassou SA, Wrobel LC:** *Design and Construction of a LiBr-Water Absorption Machine*: Energy Conversion and Management, 2003, pages 2483-2508, Vol. 44.
8. **Mittal V, Kasana KS, Thakur NS:** *The Study of Solar Absorption Air Conditioning Systems*: Journal of Energy in Southern Africa, 2005, pages 59-66, Vol. 16.
9. **Eicker U and Pietruschka :** *Design and Performance of Solar Powered Absorption Cooling Systems in Office Buildings*: Energy and Buildings, 2009, pages 81-91, Vol. 41.
10. **Kalogirou S. A:** *Recent: Patents in Absorption Cooling*: Recent Patents on Mechanical Engineering, 2008, pages 58-68, Vol. 1.
11. **Agyenim F, Knight I, Rhodes M:** *Design and Experimental Testing of the Performance of an Outdoor LiBr-Water Solar Thermal Absorption Cooling System with a Cold Store*: Solar Energy, 2010, pages 635-744, Vol. 83.
12. **Casals X. G:** *Solar Absorption Cooling in Spain: Perspectives and Outcomes from the Simulation of Recent Installations*: Renewable Energy , 2006, Vol. 31.
13. **Calise F, Palombo A, Vanoli L:** *Maximization of Primary Energy Savings of Solar Heating and cooling Systems by Transient Simulations and Computer Design of Experiments*: Applied Energy, 2010, pages 524-540, Vol. 87.
14. **Ghaddar N K, Shihab M and Bdeir F:** *Modeling and Simulation of Solar Absorption System Performance in Beirut*: Renewable Energy, 1997, pages 539-558, Vol. 10.
15. **van der Merwe C:** *Solar -Powered Air-Conditioning Tested at Pretoria Hopsital*. Engineering News. 23 October 2009.
16. **International Energy Agency Solar Heating and Cooling Programme:** *International Energy Agency Solar Heating and Cooling Programme*. [Online] [Cited: 1 12, 2011.] [www.iea-shc.org](http://www.iea-shc.org).

17. **Qu M, Yin H, Archer D. H:** *A Solar Thermal Cooling and Heating System for a Building: Experimental and Model Based Performance Analysis and Design*: Solar Energy, 2010, pages 166-182, Vol. 83.
18. **Ali A. H. H, Noeres P, Pollebeg C:** *Performance Assessment of an Integrated Free Cooling and Solar Powered Single-Effect LiBr-Water Absorption Chiller*: Solar Energy, 2008, pages 1021-1030, Vol. 82.
19. **Vidal H, Escobar R, Colle S:** *Simulation and Optimization of a Solar Driven Air Conditioning System for a House in Chile*: Proceedings of the ISES World Congress , 2001.
20. **Mittal V, Kasana KS, Thakur NS:** *Modeling and Simulation of a Solar Absorption Cooling System for India*: Journal of Energy in Southern Africa, 2006, Vol. 17.
21. **Marc O, Lucas F, Sinama F, Monceyron:** *Experimental Investigation of a Solar Cooling Absorption System Operating without a Backup System Under Tropical Climate*: Energy and Buildings, 2010, pages 774-782, Vol. 42.
22. **Gabsi S and Cahouchi B:** *Design and Simulation of a Absorption Diffusion Solar Refrigeration Unit*: American Journal of Applied Sciences, 2007, pages 85-88, Vol. 4.
23. **Florides G. A, Kalogirou S. A, Tassou SA, Wrobel LC:** *Modeling and Simulation of an absorption Solar Cooling System for Cyprus*: Solar Energy, 2002, pages 43-51, Vol. 72.
24. **Zhai XQ and Wang R. Z:** *A review for Absorption and Adsorption Solar Cooling Systems in China* : Renewable Energy, 2009, pages 1523-1531, Vol. 13.
25. **Florides G and Kalogirou S.A:** *Simulation of LiBr Absorption Solar Cooling System and Global Warming Impact* : World Renewable Energy Congress V11, 2002.
26. **Balaras C. A, Grossman G, Henning H. M, Infante-Ferreira C. A, Podesser E, Wang L, Wiemlun E:** *Solar Air Conditioning in Europe- an Overview* : Renewable and Sustainable Energy Reviews, 2007, pages 299-314, Vol. 11.
27. **Balghouthi M, Chabhani M. H, Guizan A:** *Investigation of a Solar Cooling Installation in Tunisia* : Applied Energy, 2012.
28. **Al-Alili A, Hwang Y, Radermacher R, Kubo I:** *Optimisation of a Solar Powered Absorption Cycle Under Abu Dhabi's Weather Conditions*: Solar Energy, 2010, pages 2034-2040, Vol. 84.
29. **Jia Q, Jian L, GuangMing C and RuXu D:** Chinese Science Bulletin, 2009, pages 504-515, Vol. 54.
30. **Moorthy M:** *Performance of Solar Airconditioning System using Heat Pipe Evacuated Tube Collectors* Pekan, Malaysia : National Conference in Mechanical Engineering Research and Postgraduate Studies, 2010, pages 564-572.
31. **Ortiz M, Barsun H, Vorobieff P, He H and Mammoli A:** *Modelling of a Solar-Assisted HAVC System with Thermal Storage* : Energy and Buildings, 2010, pages 500-509, Vol. 42.

32. **Palacin F, Monne C and Alonso S:** *Improvement of an Existing Solar Powered Absorption Cooling System by Means of Dynamical Simulation and Experimental Diagnosis.*: Energy, 2011, pages 4109-4118, Vol. 36.
33. **Assilzadeh F, Kalogirou S. A, Ali Y, Sopian K:** *Simulation and Optimisation of a Libr Solar Absorption System with Evacuated Tube Collectors:* Renewable Energy, 2005, pages 1143-1159, Vol. 30.
34. **Darkwa J, Fraser S and Chow D H C:** *Theoretical and Practical Analysis of an Intergrated Solar Hot Water-Powered Absorption Cooling System.*: Energy, 2012, pages 392-402, Vol. 39.
35. **Posiek S and Batlles F. J:** *Intergration of Solar Thermal Energy in Construction: Analysis of the Solar-Assisted Air Conditioning System Installed in the CIESOL Building:* Renewable Energy, 2009, pages 1423-1431, Vol. 34.
36. **Bernejo P, Pino F. J and Rosa F:** *Solar Absorption Cooling Plant in Seville:* Solar Energy, 2010, page 1503-1512, Vol. 84.
37. **Papadopoulos A. M, Oxizidis S and Kyriakos N:** *Perspectives of Solar Cooling in View of Developments in the Air Conditioning Sector.*: Renewable and Sustainable, 2003, page 419-438, Vol. 7.
38. **Internal Energy Agency, Solar Heat and Cooling(IEA-SHC) Task 38:** *Solar Air Conditioning and Refrigeration Position Paper:* IEA, 2001.
39. **Grossman G:** *Solar Powered Systems for Cooling, Dehumidification and Air Conditioning:* Solar Energy, 2002, pages 53-62, Vol. 72.
40. **Pesaran A. A, Penney T. R and Czanderna A. W:** *Desiccant Cooling State of the-Art Assessment:* National Renewable Energy Laboratory, 1992.
41. **Wang RZ, Ge TS, Chen C J, Ma Q, and Xiong Z Q:** *Solar Sorption Cooling Systems for Residential Applications: Options and Guidelines:* International Journal of Refrigeration, 2009, pages 638-660, Vol. 32.
42. **Mahesh A and Kuashik S.C:** *Solar Adsorption Cooling System: An Overview:* Journal of Renewable Energy, 2012, Vol. 4.
43. **Fan Y, Luo L and Souyin B:** *Review of Solar Sorption Refrigeration Technologies: Development and Applications :* Renewable and Sustainable Energy Reviews, 2007, Vol. 11.
44. **Kim D. S and Infante Ferreira C. A:** *Solar Refrigeration Options- a State of the Art Review :* International Journal of Refrigeration, 2008, pages 3-15, Vol. 31.
45. **Nurzia G:** *Design and Simulation of Solar Absorption Cooling Systems. PhD Thesis:* University of Bergamo, 2008.
46. **Bakhtiari B, Fradette L, Legros R and Paris J:** *A Model for Analysis and Design of LiBr-Water Absorption Heat Pumps:* Energy Conversion and Management, 2011, pages 149-1448, Vol. 52.

47. **Mazloumi A, Naghashzadegar M, and Javahedeh K:** *Simulation of a Solar Absorption System with Parabolic Trough Collector for Sunshine Hours.*: Energy Conversion and Management, October 2008, 2820-2832, Vol. 48.
48. **Khan J and Zubair S.M:** *An Improved Design and Rating Analyses of Counter Flow Wet Cooling Towers*: American Society of Mechanical Engineers, August 2001, Vol. 123.
49. **Milosavljevic N and Heikkila P:** *A Comprehensive Approach to Cooling Tower Design*: Applied Thermal Engineering, 2001, pages 899-915, Vol. 21.
50. **Solar Energy Lab:** *TRYSYS 17: A TRaNsient System Simulation Program: Volume 1: Getting Started* : University of Wisconsin-Madison, 2010.
51. **Duffie J. A and Beckman W.A:** *Solar Engineering of Thermal Processes, Third Edition*. New York : John Wiley, 2006.
52. **Salgado R. A:** *Optimized Solar Cooling Facility Configurations for the Mediterranean Warm Climate. PhD Thesis*. Madrid : Universidad Carlos 3 de Madrid, December 2008.
53. **Home Energy Metering:** *Measuring Solar Thermal Energy*: Home Energy Metering, 2011.
54. **Kalogirou S. A:** *Solar Thermal Collectors and Applications: Progress in Energy and Combustion Science* 2004, pages 231-295, Vol. 30.
55. **Singh H, Saini R. P and Saini J. S:** *A Review on Packed Bed Solar Energy Storage Systems. s.l. : Renewable and Sustainable Energy Reviews, 2010*, pages 1059-1069. Vol. 14.
56. **Morrison G L, Anderson T and Behnia M:** *Seasonal Performance Rating of Heat Pump Water Heaters: Solar Energy, 2004*, pages 147-152, Vol. 76.
57. **Solar, Fred.** *Solar Thermal 101:Evacuated Tube Collectors*: Free Hot Water Thermal Systems, 2010.
58. **Rabl A:** *Active Solar Collectors and Their Applications* : Oxford University Press, 1985.
59. **Karwa R, Karwa N, Misra R and Argawal P. C:** *Effect of flow Maldistribution on Thermal Performance of a Solar air Heater Array with Sub Collectors in Parallel*: Energy, 2007, pages 1260-1270, Vol. 32.
60. **Mammoli A, Vorobieff P, Barsun H, Burnett R and Fisher D:** *Energetic, Economic and Environmental Performance of a Solar-Thermal-Assisted HVAC System.*: Energy and Buildings, 2010, pages 1524-1535, Vol. 42.
61. **Li Z. F and Sumathy K:** *Simulation of a Solar Absorption Air Conditioning System*: Energy Conversion and Management, 2001, pages 1207-1216, Vol. 42.
62. **Martinez A. R:** *Solar Cooling and Dehumidifying*: Pergamon Press, 1981.
63. **Ataer O. E:** *Storage of Thermal Energy*. UNESCO- Encyclopedia of Life Support Systems(EOLSS. Oxford , UK : UNESCO, 2006.

64. **Macki E and Reeves G.** *Stratified Chilled Water Storage: Final Report*: EPRI, 1988.
65. **K, Li ZF and Sumathy:** *Performance Study of a Partitioned Thermally Stratified Storage Tank in a Solar powered Absorption Air Conditioning System*: Applied Thermal Engineering, 2002, page 313-327, Vol. 22.
66. **Kleinbach E. M:** *Performance Study of One-Dimensional Models for Stratified Thermal Storage Tank*. MSc Thesis. Madison : University of Wisconsin-Madison, 1990.
67. **Sakellari D:** *Modeling the Dynamics of Domestic Low Temperature Heat Pump Heating Systems for Improved Performance and Thermal Comfort-A Systems Approach*. Ph.D Thesis: Royal Institute of Technology, Sweden, 2005.
68. **Lazzarin R:** *Solar Cooling Plants:How to Arrange Solar Collectors, Absorption Chillers and Load*. Perugia : ATI National Congress, International Session, 2006.
69. **Crawley D. B, Hand J. W, Kummert M and Griffith B.T.** *Contrasting the Capabilities of Building Energy Performance Simulation Programs*: U.S. Department of Energy, Energy Efficiency and Renewable Energy, Building Energy Software Tools Directory, July 2005.
70. **Pietruschka D:** *Model Based Control Optimisation of Renewable Energy Based HVAC Systems:Solar Driven Absorption and Open Dessicant Evaporative Cooling*. Ph.D Thesis: De Montfort University and University of Applied Sciences Stuttgart, 2010.
71. **Edwards C:** *Performance Assessment of Solar Absorption Cooling for Ontario Housing*, MASC Thesis. Ottawa, Ontario, Canada : Carleton University, August 2011.
72. **Yazaki Cooperation:** *WFC-SC(H) 10,20 & 30 Version 9-1:Specifications*.
73. **Kohlenback P:** *Solar Cooling with Absorption Chillers: Control Strategies and Transient Chiller Performance*. Ph.D Thesis. Berlin : Technical University of Berlin, 2006.
74. **REHAU Polymer Limited.** *REHAU Polymer Ltd.* [Online] [Cited: May 30, 2012.] [http://www.rehau.co.za/094B4D9CA7EFB95BC12579590058BFFE\\_33BE485874AD15A0C12570EB002C8401.shtml](http://www.rehau.co.za/094B4D9CA7EFB95BC12579590058BFFE_33BE485874AD15A0C12570EB002C8401.shtml).
75. **New M, Lister, D, Hulme M. and Makin, I.** *A High-Resolution Data set of Surface Climate over Global Land Areas*. *Climate Research 21*: NASA Langley Research Center Atmospheric Science Data Center, 2002.
76. **South African Reserve Bank.** *South African Reserve Bank*. [Online] 05 2012. [Cited: 06 1, 2012.] [www.resbank.co.za](http://www.resbank.co.za).
77. **ESKOM.** *ESKOM*. [Online] April 2012. [Cited: June 27, 2012.] <http://www.eskom.co.za/c/53/tariffs-and-charges/>.
78. **Kalogirou S. A:** *Generation of Typical Meteorological Year(TMY-2) for Nicosia, Cyprus.:* Renewable Energy, 2003, pages 2317-2334, Vol. 28